The University of Manitoba

A Mass Spectrometric Study of Some Transition Metal Acetylacetonates

by

Charles Reichert

A Thesis

Submitted to

the Faculty of Graduate Studies and Research

In Partial Fulfillment

of the Requirements for the Degree

DOCTOR OF PHILOSOPHY

Winnipeg, Manitoba

May, 1969

ACKNOWLEDGEMENTS

I would like to express my thanks and appreciation to Dr. J.B. Westmore for his encouragement and advice during the present work.

I wish to thank Dr. H. Gesser and Mr. K.L. Lee for supplying some of the compounds used in this study. I am also grateful to Dr. G.M. Bancroft for his suggestions and help. Thanks are also due to Denis C.K. Lin for writing a computer program for calculating the possible metastable peaks in the spectra and his help along with Danny K.C. Fung in operation of the mass spectrometer.

I am grateful to the staff of the technical shops for their help in repair and maintenance of the instrument, and also to the glass blowing shop for their frequent assistance in glass blowing.

Finally, I wish to thank the National Research Council for their financial support in this work.

To My Wife

ABSTRACT

A mass spectral study is carried out on β-diketonates of the divalent and trivalent metals of the first transition series. Fragmentation of the chelates is influenced by the odd- or even-electron character of the ion. Unit change of valency of the metal of an ion effects the subsequent fragmentation by changing the ion's odd- or even-electron character. Electron withdrawing or electron donating groups can affect fragmentation of a chelate by enhancing or retarding the valency change of a metal atom.

Comparison of the appearance potential results with theoretical calculations and electronic spectra lead to the suggestion that on ionization of the chelates, by electron impact, the electron is lost from a π molecular orbital having largely ligand character. The fact that the metal affects the appearance potentials of the molecular ions only very slightly while electron withdrawing groups and electron donating groups attached to the ring change the results considerably supports the suggestion that the electron is lost from an orbital localized mainly on the ligands.

TABLE OF CONTENTS

LIST OF FIGURES

LIST OF TABLES

I INTRODUCTION

Mass Spectrometry traces its beginnings back to 1886 when positively charged "rays" were discovered by Goldstein (1) and to the important discovery by W. Wien (2) that they could be deflected by a magnetic field. These principles led to the developement of the direction focusing mass spectrometer as it is known today.

The separation of ions by mass in a mass spectrometer depends upon the fact that ions moving through a magnetic field will be deflected in a circular path. Thus ions of charge e accelerated across a potential V will attain a kinetic energy

$$\frac{1}{2}mv^2 = eV \qquad (1)$$

Entering the magnetic field the ions will be acted on by a force $\frac{Hev}{c}$, where H is the magnetic field strength

e the charge of the ion

v the velocity of the ion

c the speed of light.

This force must be equal to the centrifugal force, mv^2/r where r is the radius of curvature of the ion path.

Combining $$mv^2/r = \frac{Hev}{c} \qquad (2)$$

with equation (1) gives the basic equation of mass spectrometry.

$$\frac{m}{e} = \frac{r^2 H^2}{2Vc} \qquad (3)$$

If r, and V are kept constant we see that $\frac{m}{e}$ will depend only upon H, the magnetic field. By varying the magnetic field ions of different values of

m/e will thus be focused on the collector.

Even though the principle of mass spectrometry is old it was not until rather recently that mass spectrometry became a tool used in most chemical laboratories. It is now used extensively as a tool by organic and inorganic chemists to determine the molecular weight and structure of their compounds.

Since the introduction of the electron multiplier and electronic devices to greatly increase sensitivity, mass spectrometry has become widely used to study molecular ionization potentials and bond energies.

II TYPES OF IONS IN MASS SPECTRA

The ionization of the gaseous sample can be carried out in numerous ways such as electron impact, photo ionization, field ionization and thermal ionization, the most popular method being electron impact.

When an electron of sufficient energy i.e. $\sim$ 10 - 100 eV, strikes a molecule several reactions can occur.

(A) Parent Ions

Parent-molecule ions are formed by the removal of a single electron from the molecules admitted to the ion cource.

$$M + e \longrightarrow M^{+} + 2e \qquad (4)$$

The mass of M^{+} the parent ion is only very slightly less than the mass of the neutral molecule and thus the determination of the m/e value with the mass spectrometer gives the molecular weight of the sample.

(B) Multiply Charged Ions

If the energy of the electron beam is sufficiently high, two electrons can be removed from the molecule or atom.

$$M + e \longrightarrow M^{++} + 3e \qquad (5)$$

or

$$M^{+} + e \longrightarrow M^{++} + 2e \qquad (6)$$

The probability of the secondary ionization process is less, due to relatively low concentration of M^{+} ions in the ion source.

(C) Fragment Ions

The excess energy of the electrons used for ionization besides being dissipated as kinetic energy is absorbed into the vibrational modes of the molecule producing unimolecular dissociations. Various bond-

dissociation processes may take place during electron bombardment of the parent species.

$$ABC + e \longrightarrow AB^{+} + C + 2e \qquad (7)$$

$$ABC + e \longrightarrow BC^{+} + A + 2e \qquad (8)$$

Or if the ions simultaneously exhibit rearrangement of the atoms, the ion formed is termed a rearrangement ion.

$$ABC + e \longrightarrow AC^{+} + B + 2e \qquad (9)$$

(D) Metastable Ions

An ion formed in the ion source with sufficient excess energy in its vibrational modes will dissociate in the ion source. If it dissociates while in the field free region, that is, before it enters the accelerating region, the product ion will be focused in its "correct" m/e position in the mass spectrum. However if the rate of dissociation is slow so that the ion will spontaneously dissociate after it has been accelerated but before it has passed into the analyzing magnetic field the product ion will be diffusely focused at a non-integral mass number. These diffuse peaks are termed metastable peaks and will be found at an m/e value equal to

$$\frac{m^2}{m_o}$$

where m_o is the mass of the parent ion (3) and m is the mass of the new ion.

(E) Negative Ions

Negative ions may be formed in electron impact processes in two ways: 1) resonant electron capture

$$AB + e \longrightarrow AB^{-} \longrightarrow A + B^{-} \qquad (10)$$

2) ion pair production

$$AB + e \longrightarrow A^{+} + B^{-} + e \qquad (11)$$

(F) Rearrangement Ions

At the point of unimolecular dissociation of a parent ion, rearrangements of the atoms may take place. The ions produced in the mass spectrum cannot be accounted for by a simple mechanism involving cleavage of a single bond (see equation 9).

(G) Base Peak

By definition, the most intense peak in a spectrum is the base peak and is arbitrarily assigned an intensity of 100 units.

III THEORETICAL AND PRACTICAL CONSIDERATION OF ELECTRON IMPACT IONIZATION

A. Theory of Electron Impact

During a collision between an electron and an atom or molecule, energy can be transferred from the electron to the atomic system. According to the amount of energy transferred from the electron to the molecule, the latter may be brought into a neutral excited state or into an ionized state, excited or not. The excitation energy may be vibrational or electronic.

This interaction of electrons with matter and the consequent absorption of energy can be explained in terms of the Franck-Condon Principle. The fundamental assumption is that the time of interaction is so short (of the order of 10^{-15} sec. or less), compared to the time necessary for a vibration (10^{-12} - 10^{-13} sec), that nuclei may be considered as fixed at their equilibrium distances during the ionization process. Thus we see that the molecular ion immediately after electron impact has the same nuclear configuration that it has in the ground-state molecule (4).

Figure 1 shows the Morse electronic potential curves for a diatomic (or in general, for one of the possible modes of vibration of a polyatomic molecule) in the ground state AB and its excited states.

From the classical picture of vibrational motion, which does not differ greatly from simple harmonic motion, the molecule will spend the bulk of its time at one or other of the extremes of its vibrational

Figure 1

Possible Franck-Condon Transitions for the Diatomic Molecule Case as a result of Electron-Impact.

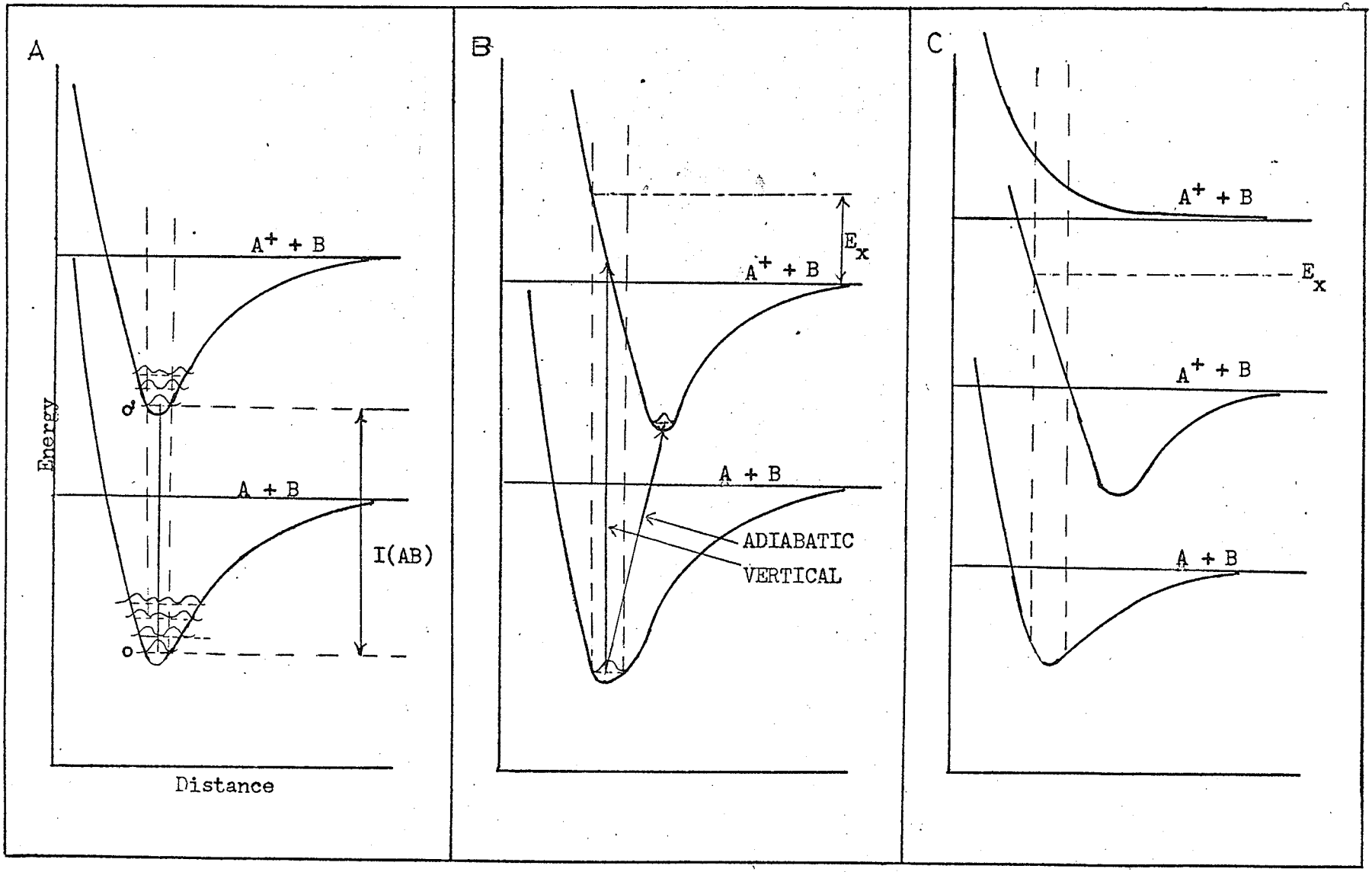
A
B
C
Energy
Distance
A+ + B
A + B
I(AB)
E_x
ADIABATIC
VERTICAL

motions. Solving the Schrodinger wave equation for ϕ, the wave function for the vibrational states, the probability of position of the nuclei is proportional to $|\phi|^2$ (5). Plotting $|\phi|^2$ for the first few vibrational levels, it is apparent that for the ground state the maximum probability occurs at the center of the potential energy curve, while for excited states, the maximum falls near the extremes of the classical limits as shown in Figure 1. As these are the most probable positions of the nuclei, it follows that the electronic transitions will most likely occur from these points on the potential curves.

Applying the Franck-Condon Principle to the transitions, two restrictions arise: 1) As the transition must take place such that the AB internuclear distance equals the AB^+ internuclear distance the transition must be represented by a vertical line.

2) Since the molecule must go to a point on the upper electronic state curve where the internal momentum is small or zero, i.e. point of maximum probability, the transition is most likely to end at either of the extremes of a vibrational level (or at the center of the lowest level).

According to the Franck-Condon Principle, electron impact ionization potentials are "vertical ionization potentials". Different types of ionization processes are therefore possible according to the shape and relative position of the potential energy curves or surfaces involved in the process as seen in Figure 1A,B,C.

When equilibrium distances are very much the same for the neutral

species and the ion, the vertical transition will occur with the highest probability to the lowest vibrational level of the ion. The resultant ionization potential will be very close to the "adiabatic" value (Fig. 1(A)) which is defined as the energy required to remove an electron from a molecule in its lowest vibrational level leaving the resultant ion in its lowest vibrational level.

In general the removal of an electron usually decreases the stability of the species, tending to increase the equilibrium distances (Fig. 1(B)). Vertical ionization in this case brings the ion into a vibrationally excited state.

Finally, as indicated in Fig. 3(C), the internuclear distance may be shifted so far in the AB^+ molecule that all transitions lie in the continuum. AB^+ is unstable and dissociates on the first vibration. When ionization potentials are measured by electron impact methods, the last detectable ions may be formed in excited vibrational states and an ionization potential greater than the adiabatic value may be obtained.

B. Ionization Efficiency Curves

The ionization efficiency curve of a particular ion under investigation is obtained by measuring the intensity of the ion beam, the ion current, while the energy of the ionizing electrons is changed. A graph of the type shown in Figure 2 is obtained on plotting the ion current versus the electron energy. Four sections encountered in a typical curve are: 1) a curved portion for the first volt or so above the threshold,

2) a linear portion for the next 10 to 20 v.,

Figure 2

A Typical Ionization Efficiency

Curve.

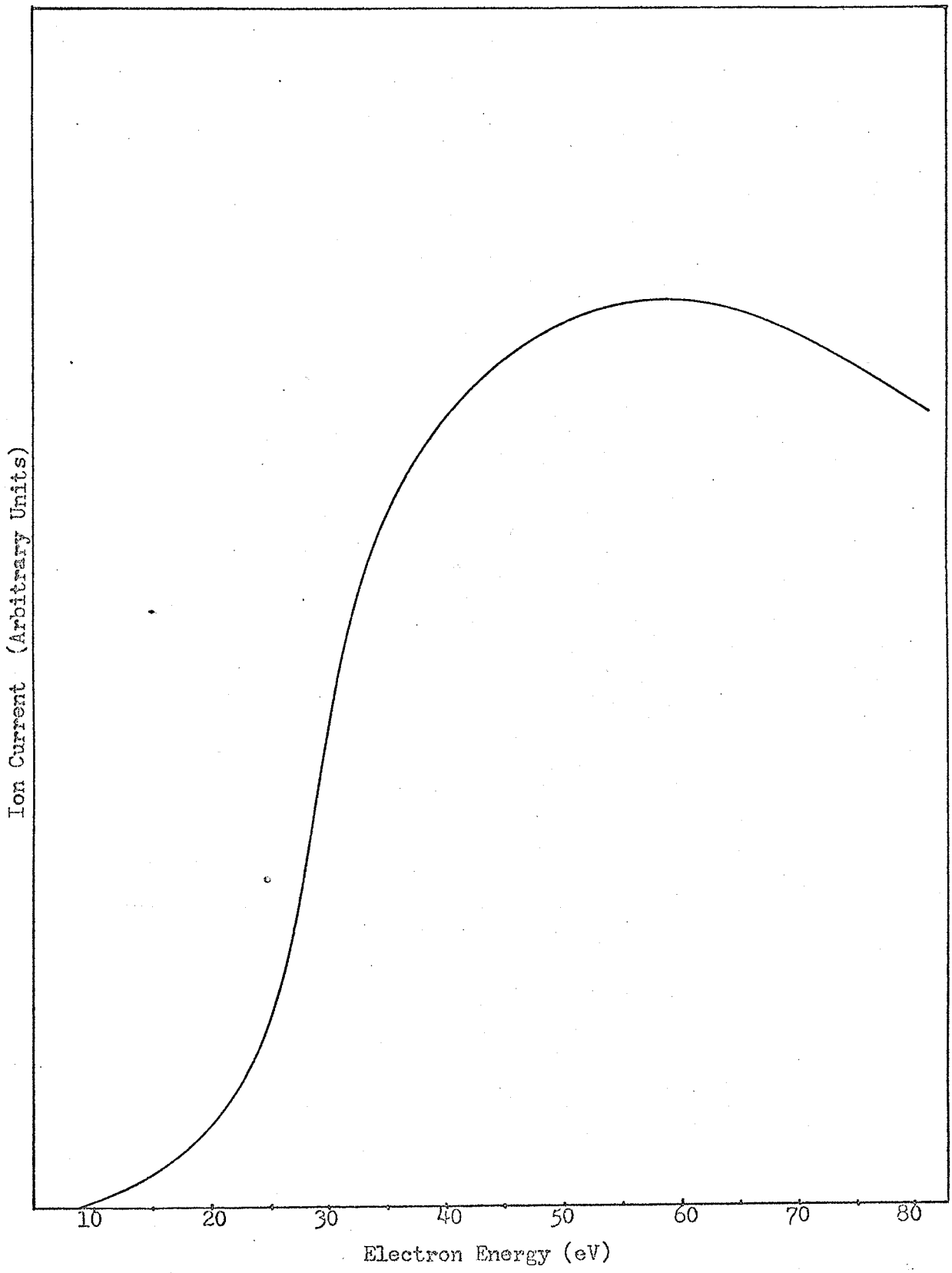
Ion Current (Arbitrary Units)
10
20
30
40
50
60
70
80
Electron Energy (eV)

3) a broad maximum between 50 and 100 v.,

and 4) a gradual, monotonic decrease as the voltage is further increased. The exact form of the curve depends to a considerable extent upon the nature of the ion.

The region of the very broad maximum with only small intensity changes with voltage is generally used for analytical purposes. Spectra found in the literature are therefore generally reported at 50 or 70 eV.

The first two sections of the curve, i.e. the initial curved portion and the linear portion up to approximately 20 volts, are used in determination of the appearance potential of an ion. The curved "foot" or "tail" is primarily caused by the inherent energy spread in the bombarding electrons, due to the Maxwellian distribution in the energy of electrons being emitted from the hot filament. The curvature due to this energy spread can be reduced by using a retarding potential on the electron beam (6) or by using an electron velocity analyzer apparatus (7).

A minor part of the "tail" is caused by excited vibrational states in the neutral molecule which are close in energy to the ground state. If these excited states are thermally populated, electronic transitions will take place from them at lower electron energies than for the ground state transitions. Generally at normal temperatures only the lowest vibrational level is occupied to any extent and the major part of the tail can be attributed to the energy spread of the bombarding electrons.

The presence of the "tail" in the ionization efficiency curve introduces problems in determining the minimum electron energy actually

required to ionize a particular molecule or atom. Several methods are used to determine the critical voltage and these will be discussed individually.

Whatever the method applied to the treatment of the ionization curve, it is always necessary to have a suitable calibration of the electron energy. The electron accelerating potential as measured by a voltmeter, is not representative of the actual energy of the electrons (8). There are contact and surface potentials, caused by molecules adsorbed on the different electrodes of the electron gun, which must be taken into account. Secondly due to the presence of a collimating magnet, collimating slits, repeller voltages, etc., the ionization chamber is not a field-free region. The ion accelerating system alters the potentials within the ionization chamber as well (9, 10). Thirdly, Waldron and Wood (8) found that a threshold voltage can alter by almost 0.5 eV by changing the pressure by a factor of 10 while a 100°C change in the filament temperature causes a change of 0.1 eV.

The simplest way to eliminate difficulties with regard to potentials is to use a reference standard calibrating gas, for which the ionization potential is accurately known. It is advantageous to choose as a calibrating gas one whose ionization potential is very nearly the same as for the ion being studied.

C. Conventional Methods of Determining Appearance Potentials

H.D. Smyth (11) in 1922 was first to propose and use the vanishing current method for the determination of appearance potentials.

This method assumes that the electron voltage at which the ion first appears is equivalent to the appearance potential. This problem of determining true onset of ionization from the ion current vs electron energy graph, which is approximately assymptotic to the abscissa, can be tackled in several ways, a number of the common methods will be discussed individually.

1. Linear Extrapolation

R.H. Vought (12) simply extrapolated the linear portion of the ionization efficiency curve back to zero ion current as shown in Figure (3A). The point of intersection of the energy axis was used as the ionization potential. Accuracy by this method is low and values of the ionization potential generally high. At best it can be used to determine an upper limit for the ionization potential.

2. Extrapolated Voltage Differences (Warren Method (13))

As in all the methods the ionization efficiency curves for the ion under investigation and reference gas are determined with both gases present in such proportions that the ion currents are very nearly the same. The ion current scale for either the sample ion or the calibrant ion is arbitrarily adjusted to make the linear portions of the ionization efficiency curves (between 10 - 30% of ion current at 50 eV) parallel (Figure 3B). The differences in the electron energy, ΔV, for corresponding points on the curves for the sample and reference gas for various values of the ion current, i, are measured, and a graph of ΔV versus i is drawn (Figure 3C). A straight line drawn through these points is extra-

Figure 3

The Determination of Appearance Potentials

A. Vought Linear Extrapolation Method

B,C. Warren Extrapolated Voltage Difference Method

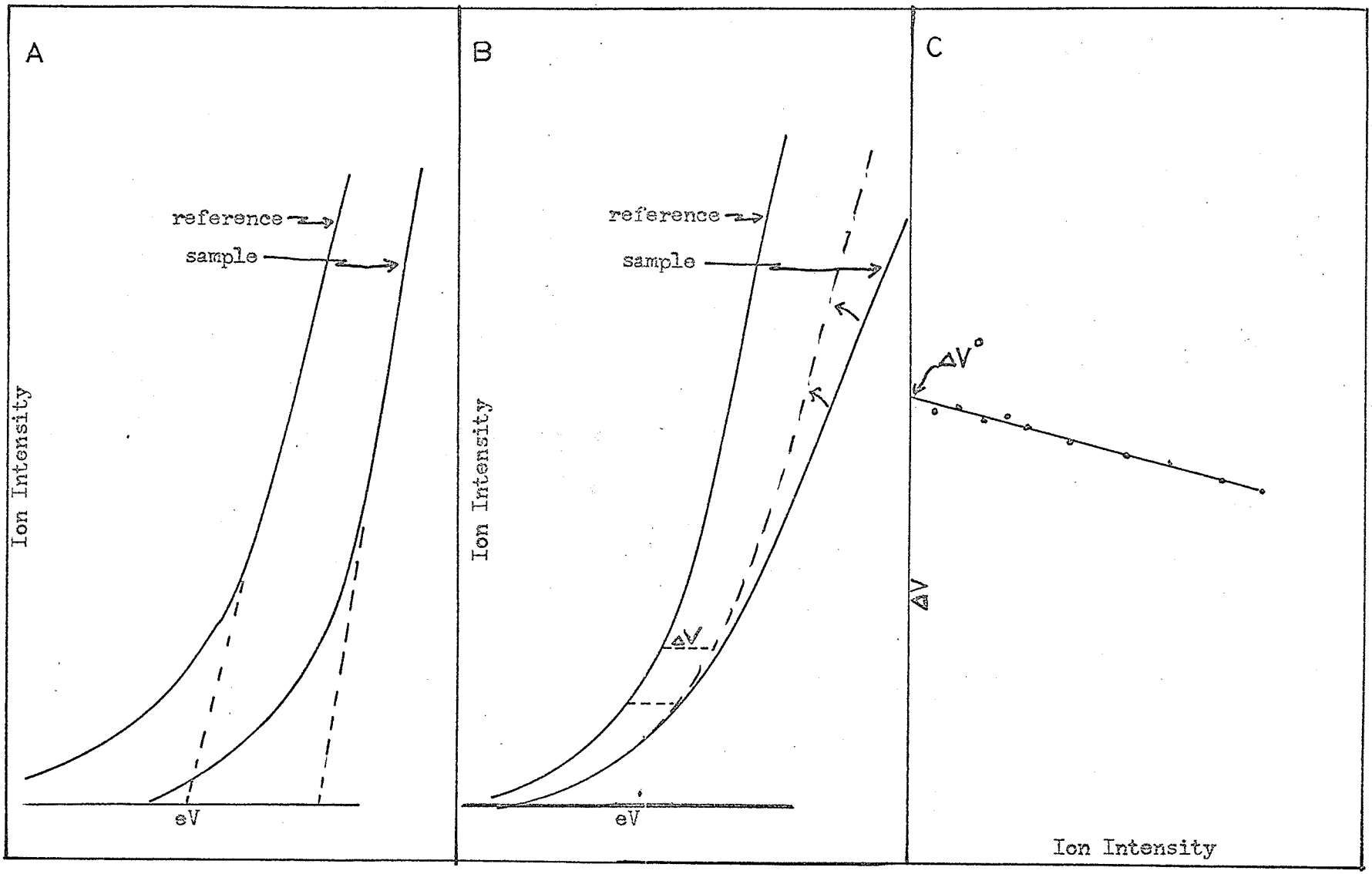
A
reference
sample
Ion Intensity
eV
B
reference
sample
Ion Intensity
ΔV
eV
C
ΔV°
ΔV
Ion Intensity

polated to zero ion current to give ΔV the difference between the appearance potentials of sample and reference gas.

This method is simply a variation of the vanishing current method, and as such appears to have essentially the advantages and disadvantages of the latter.

3. The Critical Slope Method

Honig (14) assumed that the "tail" of the graph is manifestly a property of the distribution of electron energies about the mean. If the electrons have a Maxwellian energy distribution of the type

$$dN_e(U) = \frac{4\pi mA}{h^3} U \exp\left(-\frac{\phi + U}{kT}\right) dU \qquad (12)$$

where $dN_e(U)$ is the number of electrons of energies between U and U + dU per sec., U is the thermal energy of electrons, m is the mass of an electron, h,k, are the Planck and Boltzmann constants and ϕ is the work function for the filament. The energy of the electrons, after acceleration by a potential V, is

$$E = U + V \qquad (13)$$

The number of ions $N_i(V)$ produced per sec., for an electron accelerating voltage V, is then

$$N_i(V) = \int_{U=0}^{U=\infty} N_e(U)\, p(E)\, dU \qquad (14)$$

where p(E) measures the probability (probability density) that an electron of energy E produces an ion which will reach the collector.

Honig then assumes that p(E) is proportional to the square of the "excess energy" of the electrons above the appearance potential V_c:

$$p(E) = 0 \text{ for } E \leq V_c$$
$$p(E) = C_1(E - V_c)^2 \text{ for } E \geq V_c \qquad (15)$$

On substitution of equations (12) and (15) into (14), the following expression for the ion current, $N_i(V)$ is obtained.

$$N_i(V) = 2 C_2 k T^3 \left[(N_c + V) + 3k T \right] \exp \left(- \frac{\phi + V_c - V}{k T} \right) \text{ for } V < V_c \qquad (16)$$

and

$$N_i(V) = C_2 T^2 \left[6 k^2 T^2 + 4k T (V - V_c) + (V + V_c)^2 \right] \exp \left(- \frac{\phi}{kT} \right) \text{ for } V \geq V_c \qquad (17)$$

If $\ln N_i$ is now plotted as a function of V, the curve will approximate to a straight line, below V_c, with a slope of

$$\frac{d}{d V} (\ln N_i) = \frac{1}{kT} + \frac{-1}{V_c - V + 3kT} \qquad (18)$$

If the temperature of the filament is known, then at the critical voltage $V = V_c$

$$\frac{d}{d V} (\ln N_i)_{V_c} = \frac{2}{3kT}, \qquad (19)$$

and thus the value of V_c may be determined by finding the point of critical slope (Fig. 4a).

Even though this method has yielded some excellent results (14) it is delicate in application since the exact temperature of the filament is not generally known. The assumption of a square law for the p(E) function is disputed (15, 16) for most cases except, perhaps, very close to the critical potential.

Figure 4

Determination of Appearance Potentials

A. Honig Critical Slope Method

B. Lossing, Tickner, Bryce Method

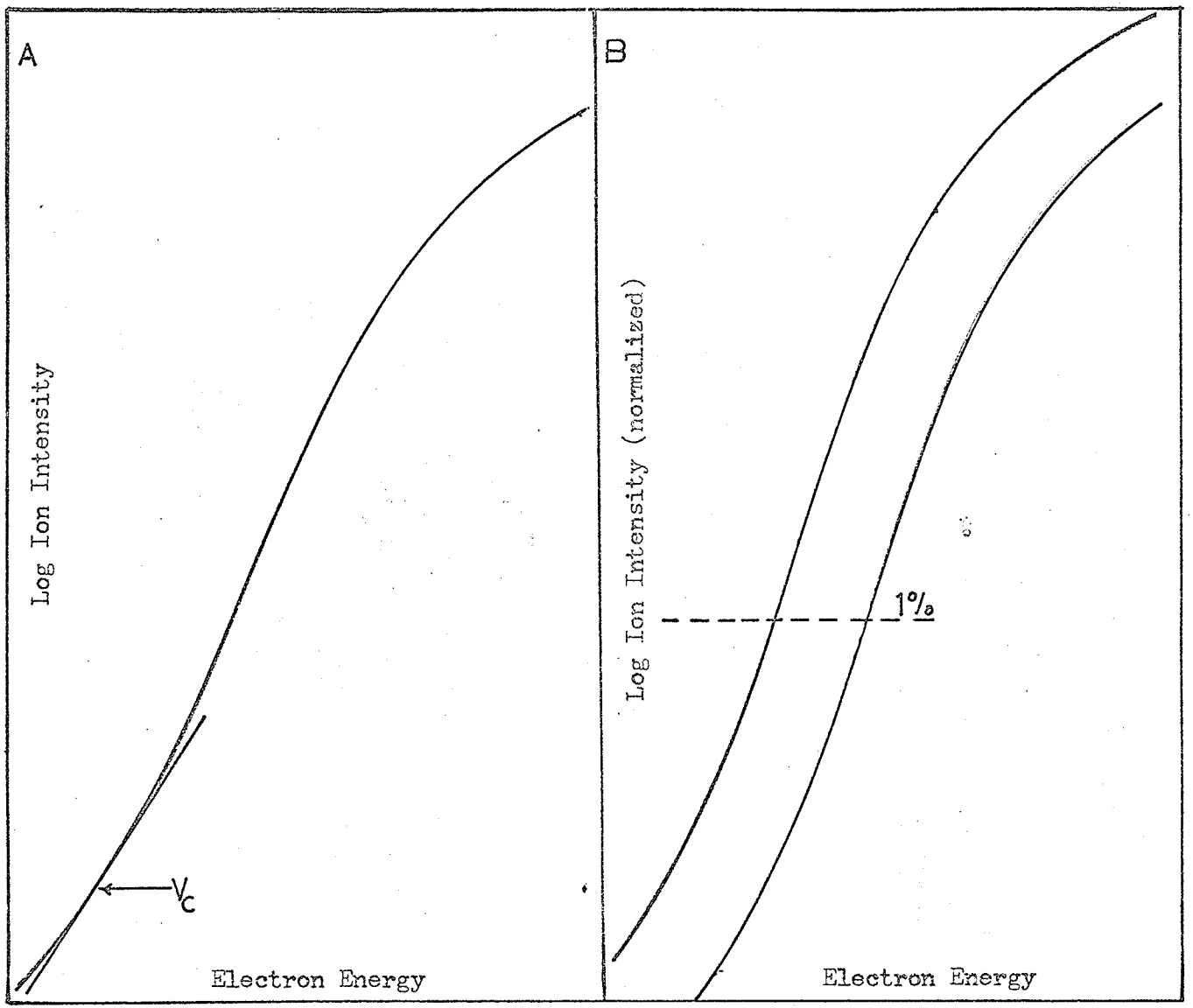
A
Log Ion Intensity
V_c
Electron Energy
B
Log Ion Intensity (normalized)
1%
Electron Energy

4. Semi-Logarithmic Plot Method

A modification of Honig's method proposed by Lossing, Tickner and Bryce (17) gives excellent and reproducible results. Lossing et al. found that plots of the logarithm of the ion current versus electron energy were parallel in the region of about 1% of the 50 eV ion current for very many substances (see Figure 4B).

For curves that are parallel to that of the calibrating gas in the 1% region the appearance potentials obtained by this method, when Δ V is measured at 1% for the two curves, compare very favorably with those given by the Warren method and with adiabatic values.

5. Monoenergetic Electron Impact Methods

As seen from the methods discussed the main difficulties encountered in the interpretation of ionization efficiency curves come from the important energy spread of the bombarding electrons.

Nottingham (7) as early as 1939 succeeded in getting fine structure in the ionization efficiency curve for Hg^+ by using a magnetic selection of electrons of a particular energy. Improvements in electron energy selectors (20-22) have narrowed the electron energy spread to 0.04 - 0.02 eV.

Another technique for obtaining monoenergetic electrons proposed by Fox (6) called the "Retarding Potential Difference" is becoming widely used for studying fine structure in ionization efficiency curves.

Reported comparisons of methods (23) of studying first, second and higher ionization potentials point to the reliability of these methods though many problems have not yet been solved.

Several methods have been developed more recently in an attempt

to improve interpretation of ionization efficiency curves, obtained by using inhomogeneous electron beams, by removing theoretically the blurring effect of the energy spread (18, 19). Some of these methods require considerable computer calculations and even then do not improve the appearance potentials to a great extent even though they may be useful for studying fine structure due to vibrational energy levels.

D. Thermochemical Considerations

The appearance potential of an ion is simply the heat of reaction by which the ion is formed, if no excess energy is involved in the ionization. It is therefore possible to treat the process by the usual methods of thermochemistry

For a reaction such as

$$AB + e \longrightarrow A^+ + B + 2e \qquad (20)$$

the appearance potential of A^+ is related to the heats of formation of the different species by the relation:

$$A.P.\ (A^+) = \Delta H_f\ (A^+) + \Delta H_f\ (B) - \Delta H_f\ (AB) \qquad (21)$$

If, however, excess energy is involved in the reaction, appropriate terms must be added, or the equation as is can be used as an approximation.

The above equation can also be written as

$$A.P.\ (A^+) = \Delta H \text{ reaction} = D\ (A - B) + I\ (A) \qquad (22)$$

so that if the ionization potential of A is known and the appearance potential of A^+ determined experimentally, the bond dissociation energy, can be calculated.

Even though these equations have been widely used for calculating dissociation energies, an unambiguous quantity is obtained only if a certain number of questions are answered:

a) the ionization potential of A must be accurately known;

b) the configuration of the products has to be ascertained;

c) the kinetic energy of fragments has to be measured;

d) the excited states of fragments have to be known.

Thus one can readily see that application and interpretation of appearance potential measurements can be very difficult and require considerable care and caution.

IV METAL COMPLEXES

The first chelate to be recognized as such was described by Werner (24), who stated that a cyclic structure was necessary to satisfy the coordination requirements of potassium dichloro-acetyl acetonato platinite. Further studies by Werner and his contemporaries led to the idea that ligands are groups which can in some way donate electron pairs to metal ions forming the so-called coordinate link.

Different theoretical approaches to the bonding in complexes has led to four major bonding theories:

1) The valence bond theory as developed by Pauling (25).

2) The crystal field theory (26), which gives quite good values for the energies of electronic transitions which are more or less localized on the central metal, the ligands being merely the source of an electrostatic perturbing potential.

3) The ligand field theory (27, 28) as developed by Van Vleck is best used for complexes where there is strong interaction between the metal ion and the ligand orbitals.

4) Molecular orbital theory (29) which is the most cumbersome to utilize.

A large number of publications have appeared in the literature concerning the interpretation of the absorption spectra of transition metal complexes (30) using the different theories.

A brief description of ligand field theory and molecular orbital

theory will be given to help in the understanding of the discussion of the data to follow.

A. Ligand Field Theory (31, 32, 33)

In a gaseous transition metal ion the five d-orbitals are degenerate, oriented as shown in Fig. 5. If we now have six ligands located at the corners of a regular octahedron, i.e. equal distances along the positive and negative extensions of the x, y and z axes, the five d-orbitals are no longer all equivalent due to repulsion between the negative charge on the ligands and the electrons in the orbitals. Some of the orbitals are concentrated in regions closer to the negative ions than others, and the electrons will obviously prefer to occupy the orbital(s) as far from the anions as possible. Looking at Fig. 5 we see that in an octahedral field the $d_{x^2-y^2}$, and d_{z^2} orbitals are pointing directly at the ligands and thus will be of higher energy than the d_{xy}, d_{yz} and d_{xz} which are pointing between the ligands. The d_{xy}, d_{yz}, and d_{xz} orbitals are usually referred to as the t_{2g} or d_ϵ orbitals while the $d_{x^2-y^2}$ and d_{z^2} orbitals are referred to as the e_g or d_γ orbitals. Fig. 6 shows the splitting diagramatically.

The energy difference between the t_{2g} and e_g levels is represented as $10\ D_q$ or Δ which varies for different complexes.

For a tetrahedral complex we see that arrangement of the ligands would be such that the t_{2g} orbitals would be of higher energy than the e_g.

If we take a metal with five d-electrons the electrons will occupy the orbitals in such a way that

Figure 5

Orientation of d Orbitals.

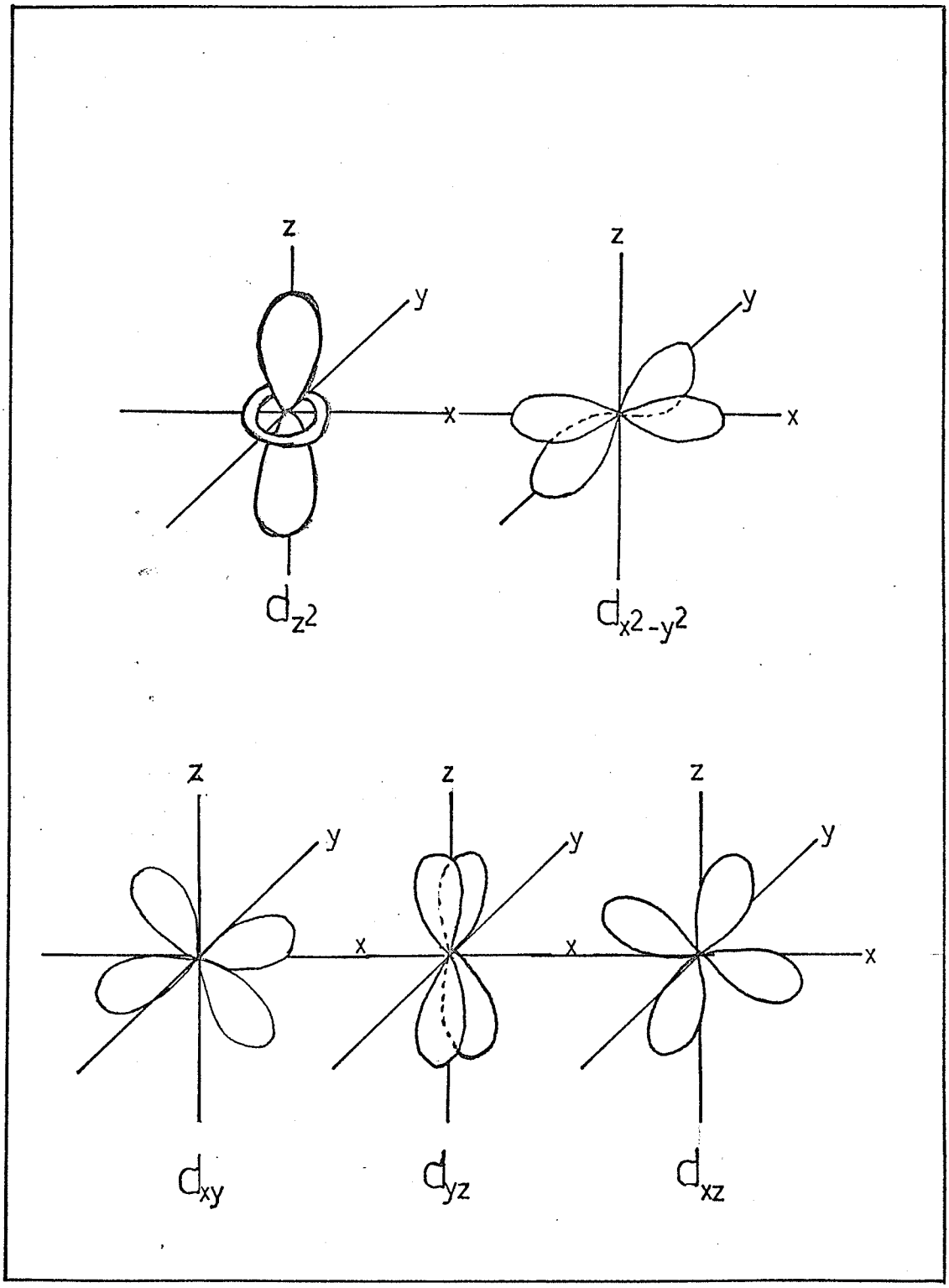
z
y
x
d_{z^2}
z
y
x
$d_{x^2-y^2}$
z
y
x
d_{xy}
z
y
x
d_{yz}
z
y
x
d_{xz}

Figure 6

Splitting of the d Orbitals for

Various Geometries.

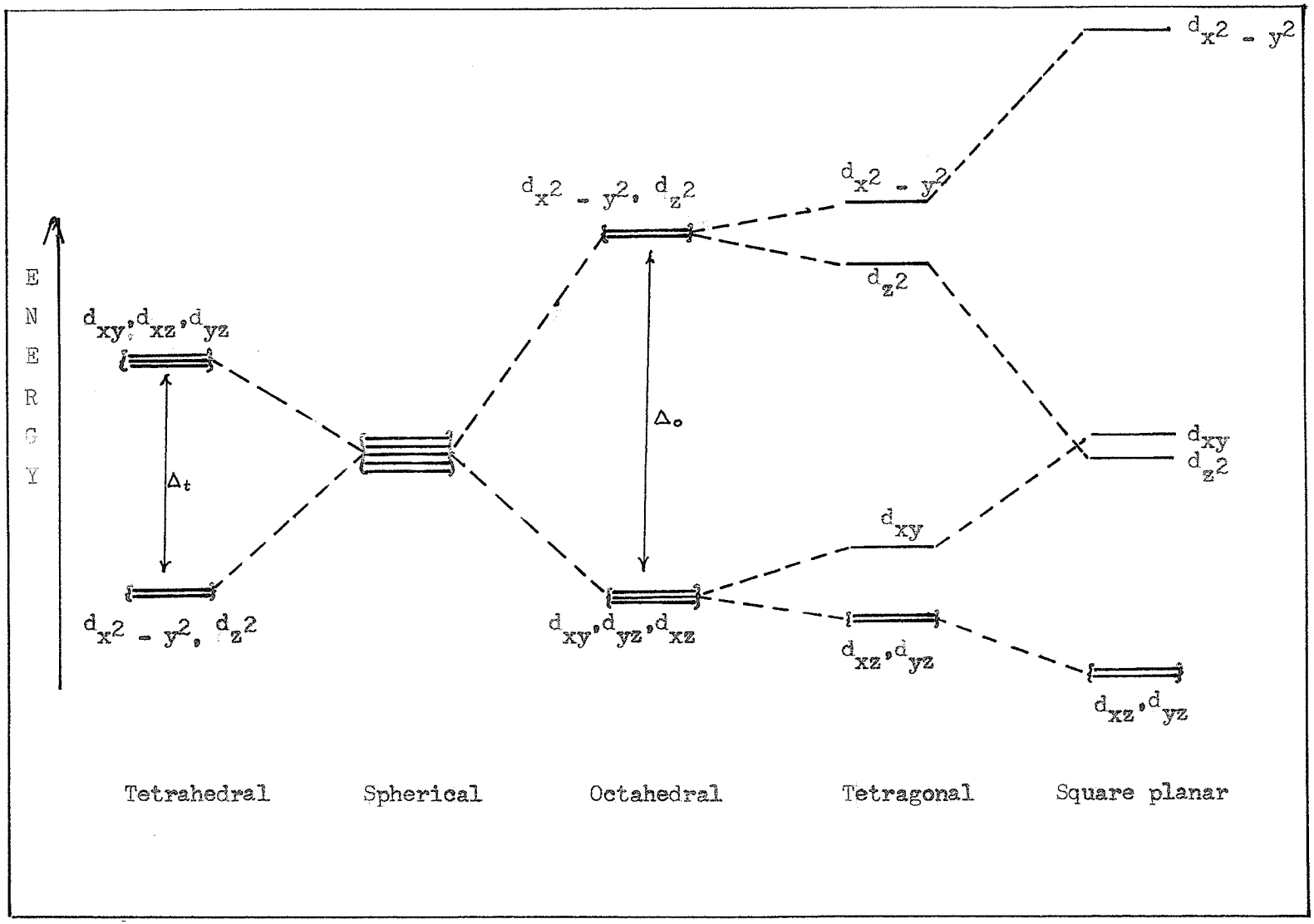
ENERGY
d_{xy}, d_{xz}, d_{yz}
Δ_t
$d_{x^2-y^2}, d_{z^2}$
$d_{x^2-y^2}, d_{z^2}$
Δ_o
d_{xy}, d_{yz}, d_{xz}
$d_{x^2-y^2}$
d_{z^2}
d_{xy}
d_{xz}, d_{yz}
$d_{x^2-y^2}$
d_{xy}
d_{z^2}
d_{xz}, d_{yz}
Tetrahedral
Spherical
Octahedral
Tetragonal
Square planar

1) the lower energy orbitals are filled first,

2) Hund's rule (electrons have a tendency not to pair giving a maximum of unpaired electrons).

Thus for ligands that produce a weak field the splitting Δ will be small enough that the energy required for pairing of electrons will be higher than Δ. We thus see that for a weak field an electron will be located in each of the five orbitals. However, if Δ is large, pairing will by necessity have to take place.

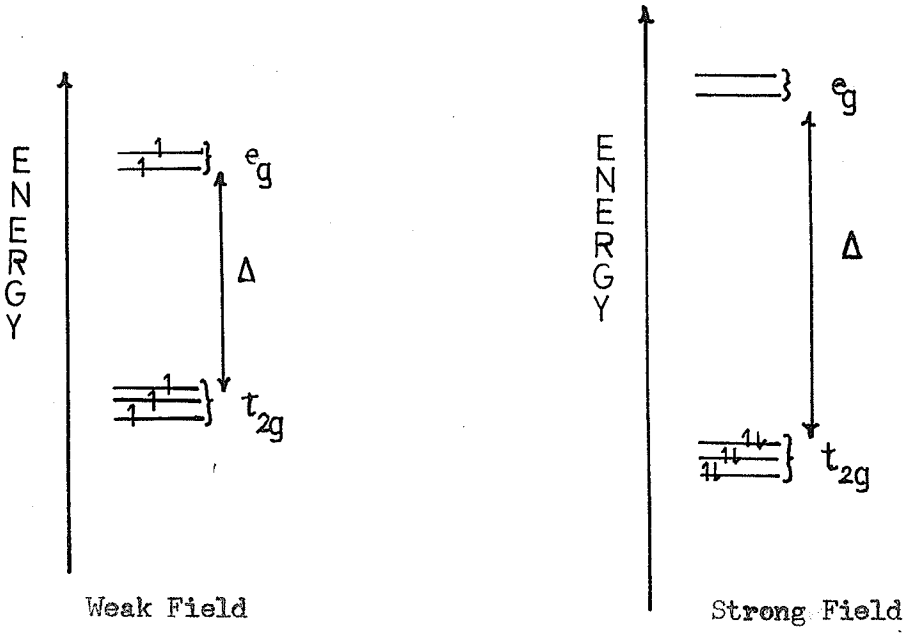

Distortion of octahedral or tetrahedral symmetry is possible as described by Jahn and Teller (34) in their theorem. Their theorem states: "Any nonlinear molecule possessing orbital degeneracy in a given symmetrical arrangement of its nuclei will distort from this arrangement so as to remove the degeneracy". Thus if a subshell (t_{2g} or e_g) is neither filled, half filled, nor empty, a distortion will occur to remove any

possible degeneracy. For example a Cu(II) complex, which is d^9, will in a weak field distort to form a tetragonal complex

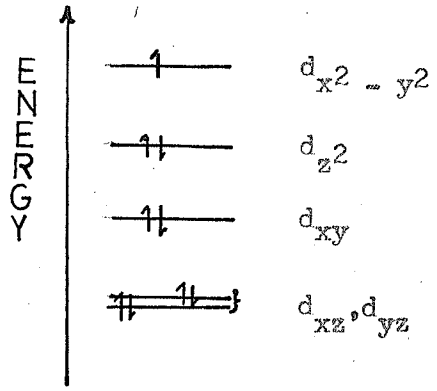

In a strong field a square planar complex will be formed.

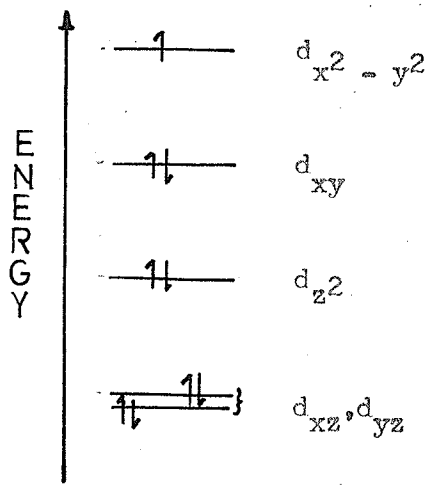

So far all that has been said was developed from the assumption that the interactions between metal ions and the surrounding anions or dipolar molecules are strictly electrostatic in the sense that the metal ion orbitals do not in any way mix with the ligand orbitals. However, overlap of metal and ligand orbitals does occur and as long as the interaction is not excessively large, considerable information can be gained by making only small changes to the strictly electrostatic theory so far discussed.

The simplest modifications to allow for orbital overlap involve using all parameters of interelectronic interaction as variable rather than taking them equal to the values found for the free ions.

B. Molecular Orbital Theory (32, 33, 35)

Molecular orbital theory is based on the overlap of orbitals, to some degree, whenever symmetry permits. It thus allows for no overlap, maximal overlap and all stages intermediate to the extremes.

The molecular orbitals used are obtained by a linear combination of atomic orbitals and can be constructed, for an octahedral complex, by a method using the following steps (see Fig. 7 and 8).

1) There are nine valence shell orbitals of the metal ion to be considered. The s, p_x, p_y, p_z, d_{z^2} and $d_{x^2-y^2}$ have lobes lying along the metal-ligand bond direction and are thus suitable for σ bonding. The d_{xy}, d_{yz}, d_{zx} are so oriented (see Fig. 5 for d orbital orientation) as to be suitable for π bonding only.

2) The assumption is made that each of the six ligands possesses one σ orbital and their individual σ orbitals must then be combined into six "symmetry" orbitals. Each of these is so constructed as to overlap effectively with a particular one of the six metal ion orbitals which are suitable for σ bonding. The ligand "symmetry" orbitals are now combined with the metal orbitals to give bonding and an anti-bonding molecular orbitals.

3) If the ligands posses π orbitals, these must also be combined into "symmetry" orbitals constructed so as to overlap effectively with the

Figure 7

The molecular orbital energy level diagram, (qualitative) for an octahedral complex between a metal ion of the first transition series and six ligands (π bonding effects and electrons are not included).

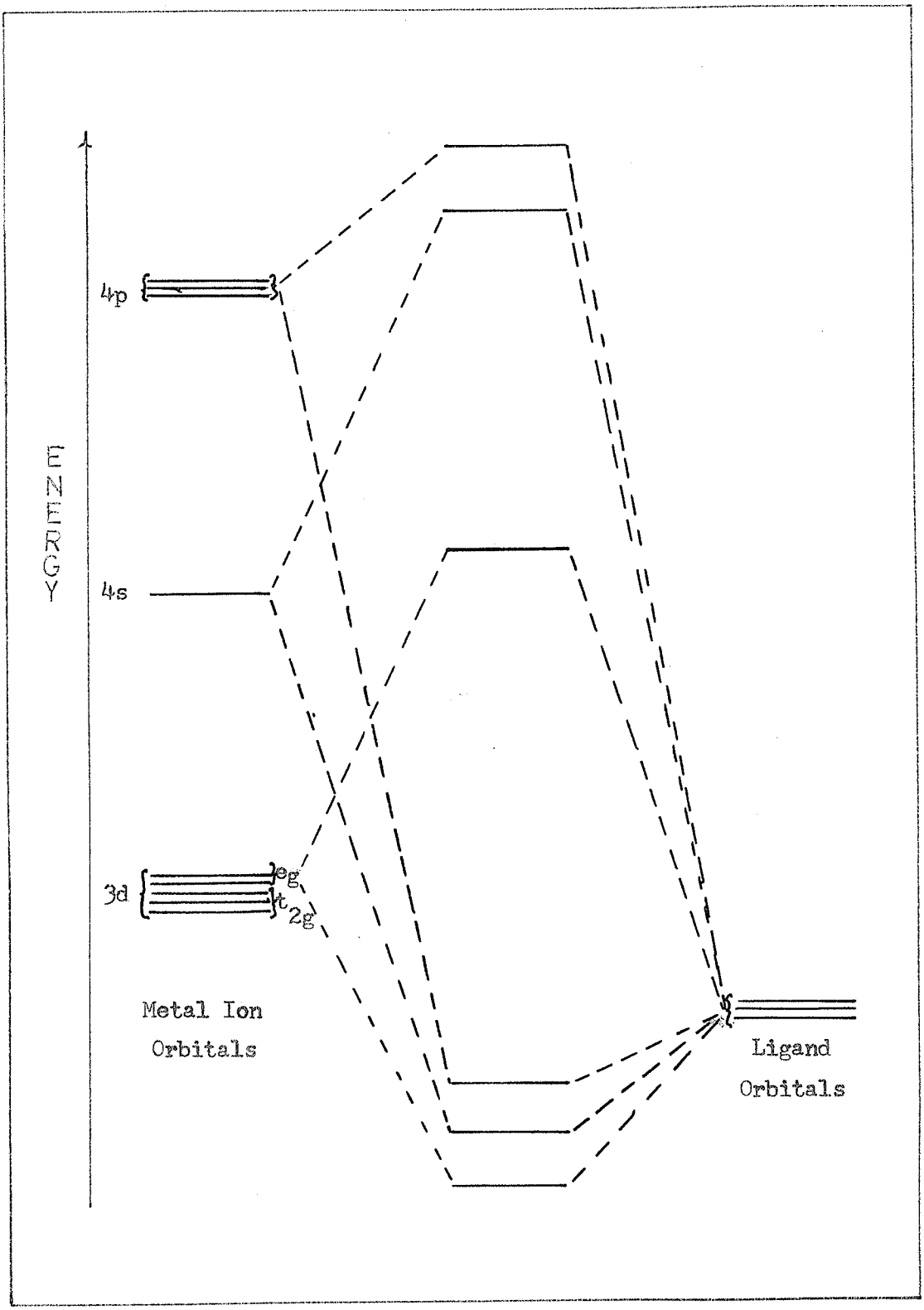
ENERGY
4p
4s
3d
e_g
t_{2g}
Metal Ion
Orbitals
Ligand
Orbitals

Figure 8

Molecular orbital description of

π bonding in a complex.

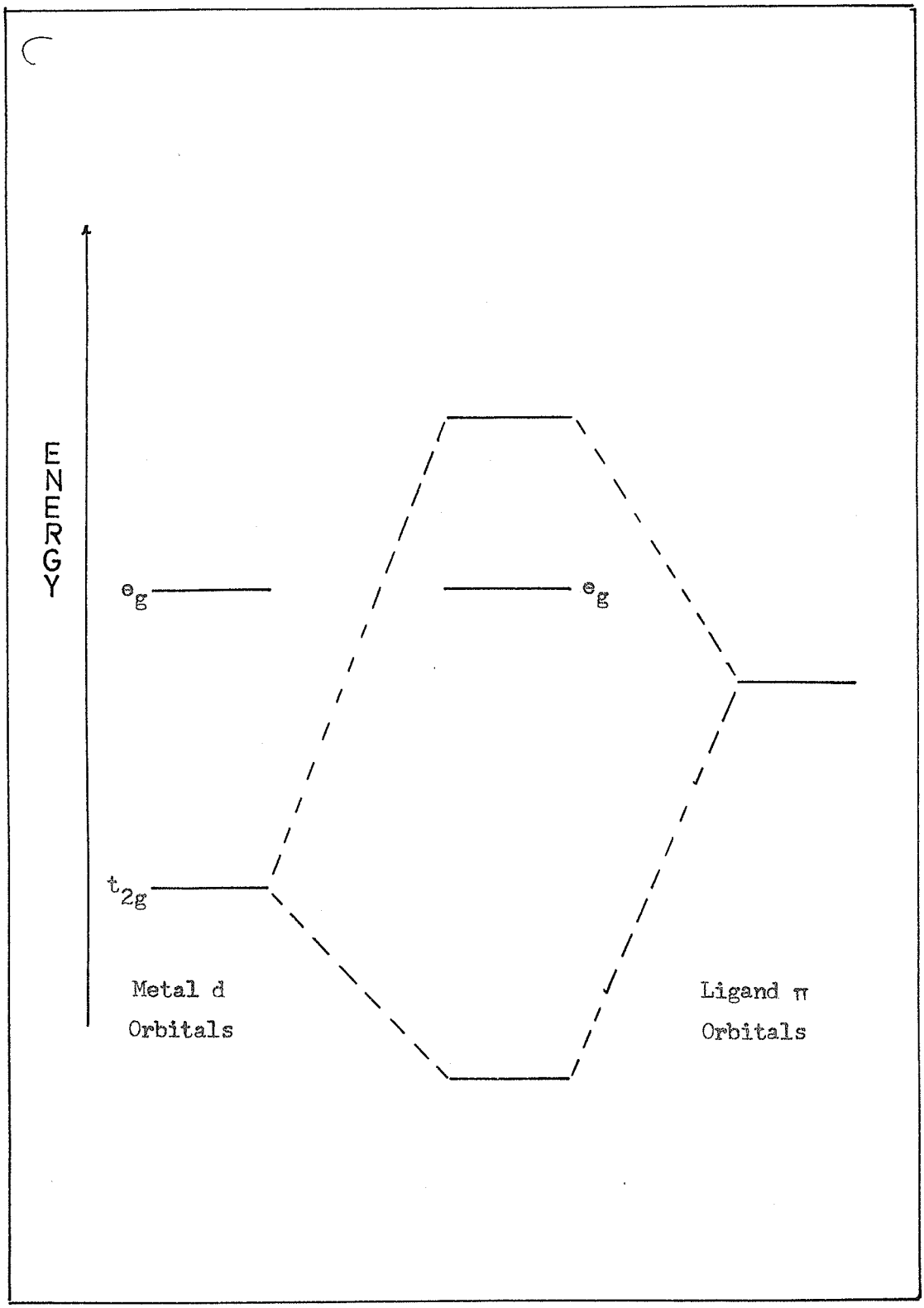
ENERGY
e_g
e_g
t_{2g}
Metal d
Orbitals
Ligand π
Orbitals

metal ion π orbitals. Again we obtain bonding and anti-bonding molecular orbitals as shown in Fig. 8.

V TRANSITION METAL ACETYLACETONATO COMPLEXES

Organic molecules containing one acidic and one co-ordinating group can form stable complexes with metals through chelation. The β-diketones

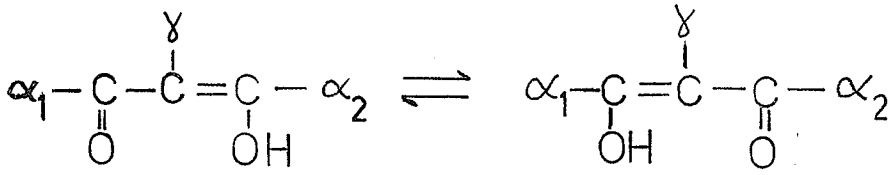

are a group of such compounds that form stable, nonionic and volatile chelate rings with most metals. The chelate ring formed, as shown schematically below, is planar for most β-diketones.

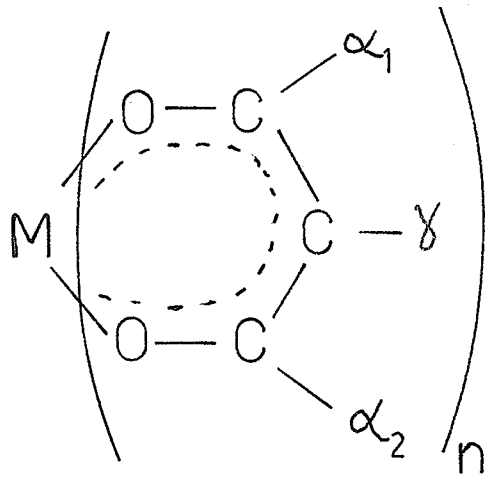

If bulky groups are present in α and γ positions (41, 42) steric hinderance may force the ring to buckle slightly to reduce the strain. X-ray crystalographic studies of copper acetylacetonate (19), where α_1, α_2 are methyl

TABLE 1

Dimensions in β-diketone complexes (42)

Compound	Cu-O	C-O	C-C(ring)	C-C(non ring)	Cu - - - C
$Co(acac)_2H_2O$....		1.275	1.420	1.480	
$VO(acac)_2$.....		1.285	1.398	1.518	
$Zr(acac)_4$		1.270	1.399	1.517	
$Cr_2(acac)_4R$[a]...		1.268	1.395	1.519	
$Mn(acac)_3$.....		1.288	1.378	1.517	
$Cr(acac)_3$.....		1.263	1.388	1.517	
$Cu(acac)_2$.....	1.921	1.260	1.404	1.545	3.075 ± 0.014
$Zn(DPM)_2$[b].....		1.274	1.405	1.517	
$Ni(DPM)_2$[b].....		1.314	1.390	1.514	
		Av. 1.277 ± 0.016	1.397 ± 0.012	1.516 ± 0.016	
$Cu(Et\ acac)_2$[c]..	1.91	1.30	1.35	1.51	3.12 ± 0.02
$Cu(Ph\ acac)_2$[d]..	1.914 ± 0.008	1.282 ± 0.008	1.397 ± 0.010	1.495 (phenyl)	3.02 ± 0.01
	1.931 ± 0.005	1.244 ± 0.008	1.406 ± 0.010	1.519 (methyl)	
$Cu(3\text{-}Ph\ acac)_2$[e]	1.906 ± 0.007	1.256 ± 0.014	1.446 ± 0.013	1.536 ± 0.015	3.5
$Cu(3\text{-}Me\ acac)_2$.	1.908 ± 0.004	1.285 ± 0.007	1.409 ± 0.009	1.496 ± 0.010	3.216 ± 0.007
TAE[f].....		1.302 ± 0.006	1.403 ± 0.006	1.489 ± 0.006	

[a] $R = [OPPh_2O]$. [b] DPM = $Me_3C{\cdot}CO{\cdot}CH{\cdot}CO{\cdot}CMe_3^-$. [c] Et acac = $EtO{\cdot}CO{\cdot}CH{\cdot}COMe^-$. [d] Ph acac = $PhCO{\cdot}CH{\cdot}COMe^-$.
[e] 3-Ph acac = $MeCO{\cdot}CPh{\cdot}COMe^-$. [f] TAE = $[MeCO{\cdot}CH{\cdot}COMe]_2$.

groups and γ is a hydrogen, show that C-O and C-C(ring) bond distances are 1.3Å and 1.4Å respectively which is intermediate between double and single bond character. The C-C(non ring) is 1.5Å. From Table 1 (42) which shows the bond distances for a number of these complexes, we see that the M-O bond distances are slightly larger than C-O distances as expected. However we see that all M-O bond distances are the same for a particular compound.

A number of papers (30, 36-43) have appeared in the literature in the past decade concerning the interpretation of absorption spectra of acetylacetonates as well as other complexes. Crystal field theory and ligand field theory produced a standard qualitative picture of bonding in these chelates; however for quantitative results molecular orbital theory must be used.

Piper and Belford (44) by re-analysing crystal spectra of $Cu(acac)_2$ by Ferguson (45) attempted to assign the observed absorptions to particular electronic transitions. They used the simple crystal field model along with esr data (46-47) available to attack the problem. They found that not enough information was available to them to make unambiguous assignments.

Molecular orbital calculations by Barnum (36) on the acetylacetonates of the trivalent metals of the first transition series appear to be more encouraging. From his calculations it appears that he obtained good agreement with absorption spectra as shown in Table 2.

TABLE 2

Comparison of Calculated and Observed Transition Energies

in some tris(Acetylacetonato) Complexes (36)

Calculated transition energies are in parenthesis

Transition \ Complex, βMO, cm^{-1}	$Ti(acac)_3$ βMO = -2000	$V(acac)_3$ βMO = -6000	$Cr(acac)_3$ βMO = -11000	$Mn(acac)_3$ βMO = -12000	$Fe(acac)_3$ βMO = -12500	$Co(acac)_3$ βMO = -14000
$\pi_3(e) \longrightarrow \pi_4(a_1)$	32400 (32400)	~35900 (35600)	39300 (40600)	39500 (42400)	42500 (41800)	43900 (44000)
$\pi_3(e) \longrightarrow \pi_4(e)$ $\pi_3(a_2) \longrightarrow \pi_4(a_1)$		~ 34500 (34500) (33500)	37100 (37100) (37000)	~ 36800 (38300) (36400)	36800 (37200) (37400)	39000 (38800) (37500)
$\pi_3(a_3) \longrightarrow \pi_4(e)$		--- (32500)	33900 (32600)	--- (32300)	--- (32500)	~ 33900 (32300)
$d\ (a_1) \longrightarrow \pi_4(e)$ $d\ (e) \longrightarrow \pi_4(a_1)$	27500 (30000)	29200 (30400) (29500)	30200 (30800) (29800)	31400 (32000) (30700)	28500 (30000) (29500)	31000 (31700) (31000)
$d\ (e) \longrightarrow \pi_4(e)$		--- (28400)	26300 (26800)	~ 25000? (26700)	32300? (25000)	~ 25000? (25600)

In Fig. 9, taken from Barnum's publication (36), the calculated energy level diagram of the free acetylacetonato ion is shown with its six electrons in the π_1, π_2, and π_3 orbitals. According to his calculations when this ion complexes with a metal the π orbitals are all raised slightly in energy and the d_ϵ and d_γ orbitals fall in between the π_3 and π_4 orbitals. Also the calculations show that the effect of metal-ligand π interaction is to shift the $\pi_3 \longrightarrow \pi_4$ transition to higher energy. From this he concluded that metal-ligand π bonding increases throughout the series $Ti(acac)_3$, $V(acac)_3$, $Cr(acac)_3$, $Mn(acac)_3$, $Fe(acac)_3$ and $Co(acac)_3$.

The literature contains contradictory remarks about the extent of π bonding in acetylacetonato complexes. As mentioned above Barnum's calculations for $\pi_3 \longrightarrow \pi_4$ transition energies indicate strong π interaction in some complexes. Nakamoto (48) from infrared absorption spectra and a normal coordinate treatment of $Cu(acac)_2$ concludes that the metal ligand π bonding is intermediate in strength between that found in $Ni(CO)_4$ and in $Fe(CN)_6^{4-}$ in which π bonding is believed to be quite strong.

Nuclear magnetic resonance studies (49, 50) indicate that electron spin is delocalized from the metal atom to the ligand. The work of Eaton (49) indicates that the extent of the metal-to-ligand charge transfer decreases smoothly in the series from Ti(III) to Fe(III). He found ligand-to-metal charge transfer as well which was very dependent upon the number of metal d orbitals present. Maki and McGarvey (45) from their paramagnetic resonance data conclude that for the copper acetylacetonate, "...the out of plane π bonding is ionic".

Figure 9

Molecular orbitals of the acetylacetonate anion and of a trivalent transition metal complex.

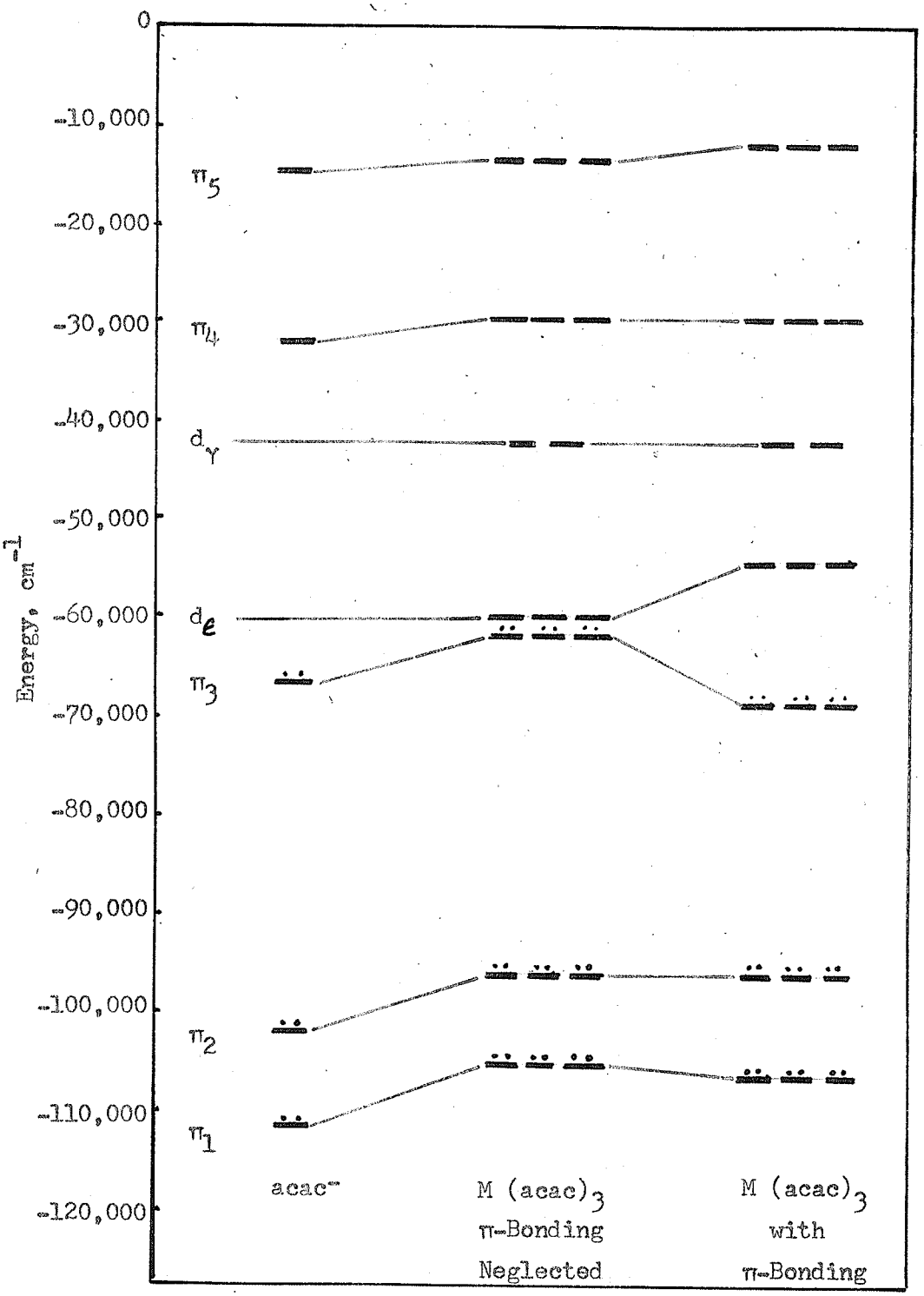
0
-10,000
-20,000
-30,000
-40,000
-50,000
-60,000
-70,000
-80,000
-90,000
-100,000
-110,000
-120,000
Energy, cm-1
π5
π4
dγ
dε
π3
π2
π1
acac⁻
M (acac)3
π-Bonding
Neglected
M (acac)3
with
π-Bonding

Fackler and Cotton (37, 38) studying α and γ substituted copper acetylacetonates in an attempt to show that the ring is quasi-aromatic tried to correlate the $\pi - \pi^*$ shifts in the absorption spectrum of the complexes to the shifts seen in benzene for the same substituents. They found however that a simple comparison could not be made and they concluded that "due to the presence of the copper atom in the chelate ring, benzenoid aromaticity cannot be assumed without making some unreasonable assumptions concerning the bonding".

All the theoretical methods of calculating energy levels used to date have not resolved all the controversial interpretations of the spectra. Price (51) has stated that "the simpler changes which occur in ionization potentials are easier to assess and can be regarded as being a first step in elucidating those which occur in absorption bands". Consequently it appears that considerable work must still be done to clarify the bonding and energy levels.

Assignment of vibrational frequencies to particular vibrations has been as controversial as interpretation of the electronic absorptions but because of the greater number of workers in the field appears to be slowly sorting itself out.

In studying the bonding in acetylacetonates possibly the most important bands observed in the IR region are the metal-oxygen stretching frequencies observed below 500 cm^{-1}. The M-O stretching band appearing at approximately 450 cm^{-1} is metal sensitive and gives information on the nature of the coordinate bond. Comparison of the M-O stretching frequencies,

for different metals or different ligands, should give directly the relative strengths of the M-O bonds. Table 3 gives a list of M-O frequencies for a number of metals and ligands. Unfortunately enough infrared studies in this region have not been carried out as yet to make adequate correlations between M-O frequencies and stability constants of acetylacetonate complexes.

TABLE 3

Metal-Oxygen Vibrational Frequencies in the Infrared for a number of Acetylacetonates of Divalent and Trivalent Metals (Cm^{-1}).

Metal	Vibrational Frequencies						
Al^{III}			496[f]		657[f]		
Cr^{III}		416[d]	456[d]	592[d]		678[d]	
Mn^{III}		434[d]		566[d]		592[d]	670[d]
Fe^{III}	298[b]	415[e]	433[e]	548[e]		559[e]	
Co^{III}	386[b]	432[b]	466[b]	635[e]			
Fe^{II}			414[c]				
Co^{II}			422[c]		659[a]		672[a]
Ni^{II}			452[a]				666[a]
Cu^{II}			455[a]		654[a]		684[a]
Zn^{II}			422[a]		651[a]		666[a]

(a) see reference 48
(b) see reference 52
(c) see reference 53
(d) see reference 54
(e) see reference 55
(f) see reference 56

VI APPARATUS AND EXPERIMENTAL PROCEDURE

A. Preparation of Complexes

The acetylacetonates of all the metals except those discussed individually were prepared using the method discussed by Fernelius and Bryant (57). In this method an alcoholic solution of redistilled acetylacetone is mixed with an aqueous solution of the metal acetate. The complex usually precipitates from the solution. In certain cases such as the chromium complexes evaporation of the water and alcohol was required to recover the complex. In each case the precipitate was filtered off and recrystallized from aqueous ethanol solution and then fractionally sublimed in a vacuum of approximately 0.01 mm. of mercury.

In the preparation of copper acetylacetonates, with methyl or phenyl substituents in the γ-position of the ketone, it was necessary to add a few drops of ammonium hydroxide before the ketone would react.

The titanium (III) acetylacetonate was prepared using the method of Barnum (36). In a nitrogen atmosphere, 0.10 moles of distilled acetylacetone was dissolved in 40 ml. of oxygen-free water by dropwise addition of 6N ammonium hydroxide and vigorous stirring. This solution was then added dropwise and with stirring to a solution of 50 ml. of water and 25 gms. of a 20% solution titanium trichloride. The blue precipitate of $Ti(acac)_3$ was filtered off, washed with oxygen free water and dried in vacuum. The $Ti(acac)_3$ was purified by sublimation in vacuum of 0.001 mm. of mercury.

The vanadium (III) acetylacetonate was made using the method described by McKaveney and Freiser (58). A 0.8 gram sample of vanadyl sulfate, 45 ml. of water, 5.0 ml. of concentrated sulfuric acid, and 1.0 grams of zinc powder were placed in a 200 ml. round bottomed flask. The mixture was refluxed for 1 hour under a steady stream of nitrogen gas. After the mixture cooled it was transferred to a 400 ml. beaker and concentrated ammonium hydroxide added to bring the pH to a value of 2.0. The mixture was extracted with 100 ml. portion of 1:1 chloroform-acetylacetone. The organic extract was evaporated leaving the vanadium (III) acetylacetonate and zinc acetylacetonate as residue. The vanadium complex was separated from the zinc complex by vacuum sublimation.

The iron (II) trifluoro acetylacetonate and acetylacetonate were prepared using a modification of the method used by Buckingham et al. (59). The ligand was added to a solution of $FeSO_4$ in deoxygenated water containing a couple of drops of H_2SO_4 and a few drops of hydrazine to reduce the iron (III) impurities. The precipitate was filtered and washed with a large volume of deoxygenated water. It was then dried in vacuum before sublimation.

The mixed acetylacetonato complexes of copper were prepared as described by Farona et al. (60) adding an equimolar mixture of the two ligands to a small excess of $CuCO_3 \cdot Cu(OH)_2$ suspended in chloroform. After filtering off unreacted material the solvent was evaporated away. The complex was then purified by vacuum sublimation.

The halogen- and nitro-substituted chromium acetylacetonates were obtained from Dr. W.K. Ong (Chemistry Department, University of Singapore). Before using they were purified by sublimation at reduced pressure. The $Cr(Iacac)_3$ contained small amounts of impurities of chelates in which Cl was substituted for I, presumably because ICl had been used in the preparation (61,62). However, these impurities did not give rise to difficulties in interpreting the mass spectrum.

The pure ligands were obtained from the companies listed below.

	Company
acetylacetone (Hacac)	Fisher Scientific Company
trifluoroacetylacetone (Htfacac)	Peninsular Chem. Research Inc.
hexafluoroacetylacetone (H hfacac)	Peninsular Chem. Research Inc.
1-benzoylacetone (H bzacac)	Aldrich Chemical Co. Inc.
dibenzoylmethane (H dbzm)	Aldrich Chemical Co. Inc.
Thenoyltrifluoroacetone	Fisher Scientific Company
4,4,4-Trifluoro-1-phenyl-1,3 butanedione	Eastman Organic Chemicals
4,4,4-Trifluoro-1-(2-naphthyl)-1,3-butanedione	Eastman Organic Chemicals
4,4,4-Trifluoro-1-(2-furyl)-1,3-butanedione	Eastman Organic Chemicals
3-methylacetylacetone	made in laboratory
3-phenylacetylacetone	made in laboratory

Only the 3-methyl and 3-phenyl substituted acetylacetones were made in the laboratory. The 3-methyl acetylacetone was prepared by the

method described by Morgan and Rawson (63). Sodium ethoxide was prepared by gradual addition of small pieces of sodium to absolute ethyl alcohol under a reflux condenser. After the metal had dissolved, pure acetylacetone was added slowly. The white needles of sodium acetylacetonate were filtered off and washed with alcohol and ether.

10 grams of the sodium acetylacetonate were then heated with 60 grams of methyl iodide in a sealed tube for several hours at approximately 100°C. The methylated β diketone was distilled off under reduced pressure yielding 4 grams of the desired product.

3 phenyl acetylacetone was made using Hauser's method (64). A mixture of 0.4 moles of phenyl acetone, 0.8 mole of acetic anhydride, and 0.12 mole of p-toluenesulfonic acid was stirred for five minutes and then saturated at 0 - 10°C with boron trifluoride for three to four hours. The mixture was then allowed to warm to room temperature over a three-hour period. The reaction mixture was poured into a solution of sodium acetate and refluxed until all the boron fluoride complexes were hydrolyzed. The mixture was cooled and extracted with ligroin. The product of 3-phenyl acetylacetone was purified by recrystallization from ligroin.

B. Measurement of Mass Spectra

All the spectra were obtained using a Hitachi-Perkin-Elmer RMU-6D single focusing mass spectrometer and recorded on a Honeywell model 1508 visicorder. The samples were introduced into the ion source by means of (a) the heated gas inlet system or (b) via a direct probe depending upon the volatility of the particular compound. In the first method the compound

was vaporized into a reservoir of approximately 1 liter capacity from which it effused into the ionization chamber through a pinhole leak. The whole system can be heated at temperatures up to 250°C. In the second method the sample was introduced into the ion source on a probe which could be inserted through a vacuum lock.

The sample temperatures were different for each compound depending on its particular volatility. The ionization chamber temperature was either 150°C or 250°C as indicated in the tables of the spectra. All the spectra were recorded at an ionizing voltage of 50 V.

C. Measurement of Appearance Potentials

The appearance potential measurements were performed on the same instrument using a Hewlett-Packard Model 3459A digital voltmeter to monitor both the amplified ion current and the chamber voltage (electron accelerating voltage). Fig. 10 shows a schematic diagram of the ion source. The grid voltage in the ion source was maintained at -0.5 V relative to the filament. The grid thus pushes the electrons toward the ion source, rather than operating in the usual way a grid operates in a vacuum tube. The target (trap) voltage was set at +10 volts relative to the chamber. Repeller voltages were set for maximum sensitivity at all times.

For the measurement of the ion current versus ionizing voltage the calibrating gas xenon was introduced into the ion source simultaneously with the compound under study. The xenon pressure was adjusted so that its ion current was very nearly the same as the intensity of the ion being studied.

Figure 10

Schematic Diagram of the T-2M Source Used.

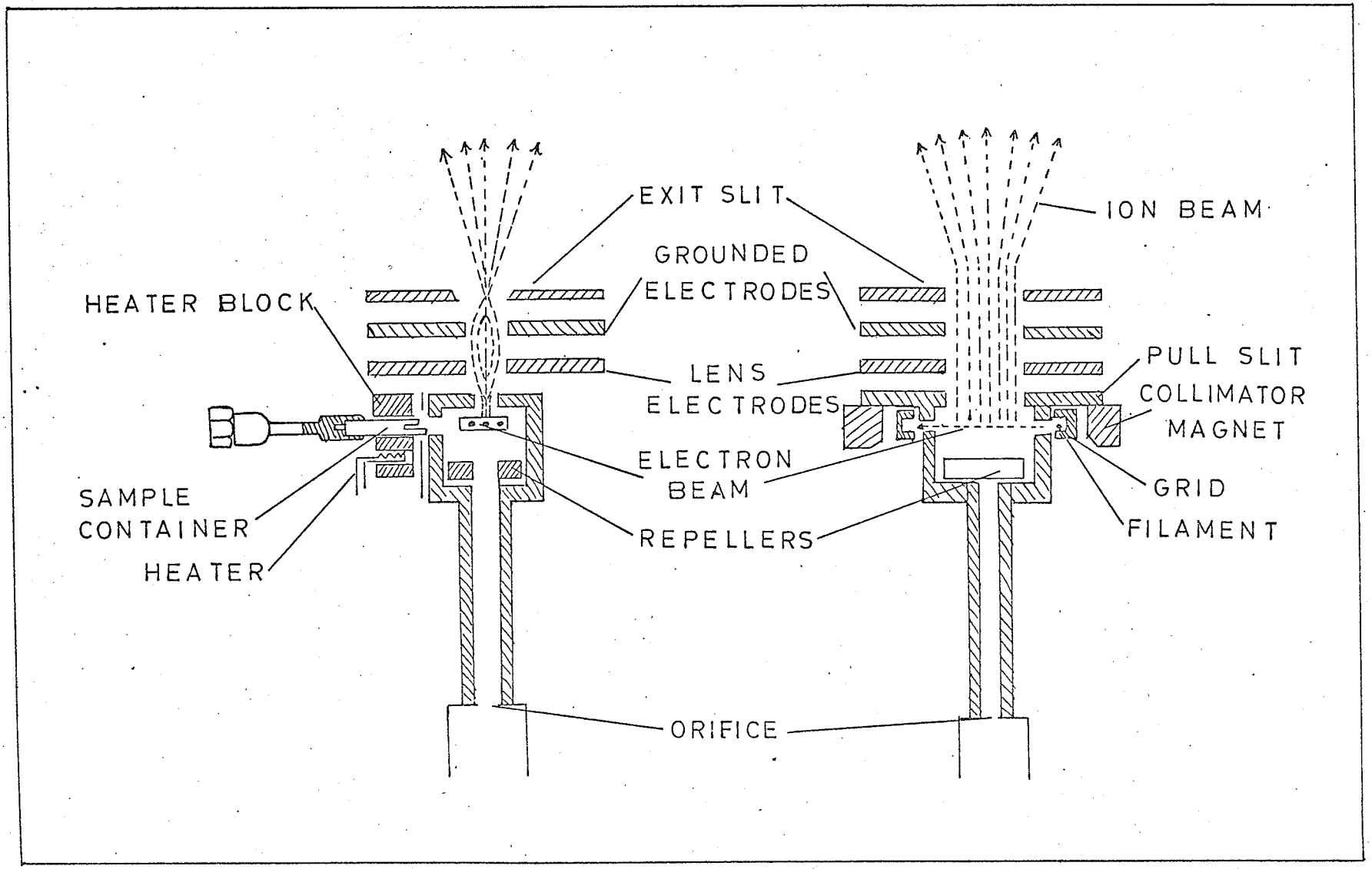
EXIT SLIT
ION BEAM
GROUNDED
ELECTRODES
HEATER BLOCK
PULL SLIT
COLLIMATOR
MAGNET
LENS
ELECTRODES
ELECTRON
BEAM
GRID
SAMPLE
CONTAINER
REPELLERS
FILAMENT
HEATER
ORIFICE

The appearance potential data were treated mathematically to account for pressure drop off durring the time of measurement and normalized to make the 50 eV reading equal to 100%. Where the curves were parallel to the xenon curve the data was plotted on semi logarithmic graph paper to obtain the appearance potentials by the method of Lossing et al. (17). The voltage difference between the xenon and sample ion at 1% of the normalized values was obtained from the graph. If the curves were not parallel then the Warren method was also used and compared to the semi-logarithmic plot at 0.1%.

VII NATURE OF THE PROBLEM

The object of this research is to gain information about transition metal acetylacetonates, by studying their "break up" under electron impact in a mass spectrometer as well as by studying the appearance potentials of the parent ions and the more prominent fragment ions.

Considerable work has been done on metal acetylacetonates in the fields of visible and ultraviolet spectroscopy (30,36-45), infrared spectroscopy (48,52-56), and theoretical calculations of molecular orbitals (36). From a study of the mass spectra and appearance potentials an attempt is made to correlate some of the results obtained by the other methods and thus shed some light on structure and bonding of transition metal complexes.

VIII RESULTS AND DISCUSSION

A. Acetylacetonates of the Trivalent Metals of the First Transition Series

1. The Mass Spectra

The mass spectra obtained for the chelates, by the direct insertion method, for 50V electrons and an ionizing chamber temperature of 150°C are summarized in Table 4. The mass spectra for $Fe(acac)_3$, $Co(acac)_3$ and $Cr(acac)_3$ are in good agreement with those reported by MacDonald and Shannon (65), except that no evidence was found of any polymeric species.

The effect of the method of sample introduction and temperature was investigated in this series because of the difference in spectra obtained for $Fe(acac)_3$, $Co(acac)_3$, and $Cr(acac)_3$ by Sasaki et al. (66) and the inability of MacDonald and Shannon (65) to obtain a spectrum of $Mn(acac)_3$. For $Cr(acac)_3$, as shown in Table 5, the method of introduction and the temperature had very little effect on the mass spectrum and the reproducibility is considered acceptable. For $Mn(acac)_3$, $Fe(acac)_3$ and $Co(acac)_3$ vaporization via the heated inlet system led to a much less abundant molecular ion peak and a lower appearance potential for $M(acac)_2^+$ than those obtained when the compound was vaporized directly into the ionization chamber. The relative ion intensities and the appearance potentials of the $M(acac)_2^+$ ion were also not reproducible under these conditions. However, if the compound was vaporized directly into the ion source, variation of the ionization chamber temperature from 150°C to 250°C had very little effect on the form of the spectrum or the value of the measured appearance potential.

TABLE 4

Relative intensities of metal-containing ions in the mass spectra of acetylacetonates of trivalent metals of the first transition series at an electron energy of 50 volts. (P = Parent Ion)

Ion	$Ti(acac)_3$	$V(acac)_3$	$Cr(acac)_3$	$Mn(acac)_3$	$Fe(acac)_3$	$Co(acac)_3$	Assignment
P	100	32	23	16	16	29	$(ML_3)^+$
P-15	-	-	-	-	-	4	$(ML_3-CH_3)^+$
P-42	-	-	-	-	-	2	$(ML_3-CH_2CO)^+$
P-57	-	-	-	-	-	6	$(ML_2COCH_2)^+$
P-82	37	3	-	-	-	-	$(L_2MOH)^+$
P-83	-	4	-	-	-	-	$(L_2MO)^+$
P-99	55	100	100	100	100	100	$(ML_2)^+$
P-100	80	-	-	-	-	-	$(ML_2-H)^+$
P-114	-	-	5	32	47	47	$(ML_2-CH_3)^+$
P-118	12	-	-	-	-	-	$(ML_2-H_2O)^+$
P-124	7	-	-	-	-	-	
P-141	-	-	-	6	-	-	$(ML_2-CH_2CO)^+$
P-164	7	-	-	-	-	-	$(LM(OH)_2)^+$
P-165	-	7	-	-	-	-	$(LMO(OH))^+$
P-180	16	-	-	-	-	-	$(LMOH_2)^+$
P-181	36	10	12	-	8	-	$(LMOH)^+$
P-182	64	26	-	-	-	-	$(LMO)^+$
P-197	-	3	-	-	-	-	
P-198	-	5	45	70	74	66	$(ML)^+$
P-200	18	3	-	-	-	-	$(ML-2H)^+$
P-213	-	-	4	3	-	7	
P-216	-	-	3	3	-	-	$(ML-H_2O)^+$
P-218	17	-	-	-	-	-	
P-281	-	34	-	-	-	-	$(MO)^+$
P-282	-	-	-	14	12	-	$(MCH_3)^+$
P-297	-	-	2	7	5	2	$(M)^+$

TABLE 5

Relative intensities of major ions from $Cr(acac)_3$ with different conditions of sample introduction. Electron energy = 50 volts.

	Via heated inlet		Direct insertion	
Chamber temp.	150°	250°	150°	250°
P^+	22	22	25	23
$(P-.acac)^+$	100	100	100	100
$(P-.acac-.CH_3)^+$	5	5	6	4.5
$(P-2.acac)^+$	50	50	59	46

The first step in the electron impact of these compounds is the loss of an electron to give the parent ion P^+ (molecular ion). Subsequent fragmentation as briefly discussed and generalized by MacDonald and Shannon (65) depends upon:

1) odd- or even- electron character of an ion (McLafferty(67))

2) the ability of the metal to change its valency state, and

3) the substituent groups on the ligand.

It may be advantageous at this point to discuss "even-electron" and "odd-electron" species (67). The valence electrons of most molecules are paired (exceptions are odd electron molecules such as NO, ClO_2, and paramagnetic molecules like O_2) that is, the molecule is an "even-electron" species. Removal of one of these electrons in ionization destroys the stabilizing effect of one of the pairings to give an "odd-electron ion". Homolytic cleavage of a bond in an "odd-electron ion" will usually produce a neutral radical (odd-electron species) and an even-electron ion. Since the even-electron fragment usually has the much greater stability and therefore the greater influence on the course of the degradation reaction an over-all increase in stability in comparison to the parent ion is observed. To produce an even electron neutral fragment it would be necessary for the molecular ion to undergo multiple bond cleavages or rearrangement which requires more energy than simple one bond cleavage. The loss of even electron fragments from odd-electron ions thus will not occur unless a driving force is present (e.g. loss of extremely stable even electron fragments such as H_2O, CO, etc.).

Even-electron ions can conceivably fragment by either loss of an odd-electron neutral fragment (radical) or an even-electron neutral fragment. Since loss of an odd-electron neutral fragment is accompanied by the formation of the usually less stable odd-electron ion this process is not very favorable. The loss of an even-electron neutral fragment entails multiple bond cleavage or rearrangement requiring considerable energy. From this we can conclude that even-electron ions along with their higher stability due to electron pairing should be the predominant peaks with only minor fragmentation of even-electron ions if sufficient excitation energy is present. Studies on organic compounds (67) shows that the loss of even-electron fragments from even-electron ions is usually energetically more favorable than the loss of odd-electron neutral fragments and corresponding formation of an odd-electron ion.

Based mainly on the proposals of MacDonald and Shannon (65) a general outline of possible fragmentation processes for the $M(acac)_3$ species is shown schematically in Figure 11. Table 6 gives a summary of the metastable peaks observed in the mass spectra related to the fragmentation processes shown in Figure 11.

The predominant step as seen from Table 4 is the loss of an odd electron neutral species, acac$\cdot$(L$\cdot$) in this case, for all but $Ti(acac)_3$. The peaks due to loss of even-electron neutral fragments from the parent ion are generally very small except for $Ti(acac)_3$ if at all present. With the loss of the odd-electron neutral fragment the resulting ion $M(acac)_2^+$ is an even-electron species and not likely to lose an odd-

Figure 11

Some suggested decomposition pathways for the formation of ions in the mass spectra of acetylacetonates of trivalent metals of the first transition series. Other pathways are possible, and only one canonical form of each ion is shown. In many cases, confirmation of the suggested pathway was given by the presence of a metastable peak (see Table 6).

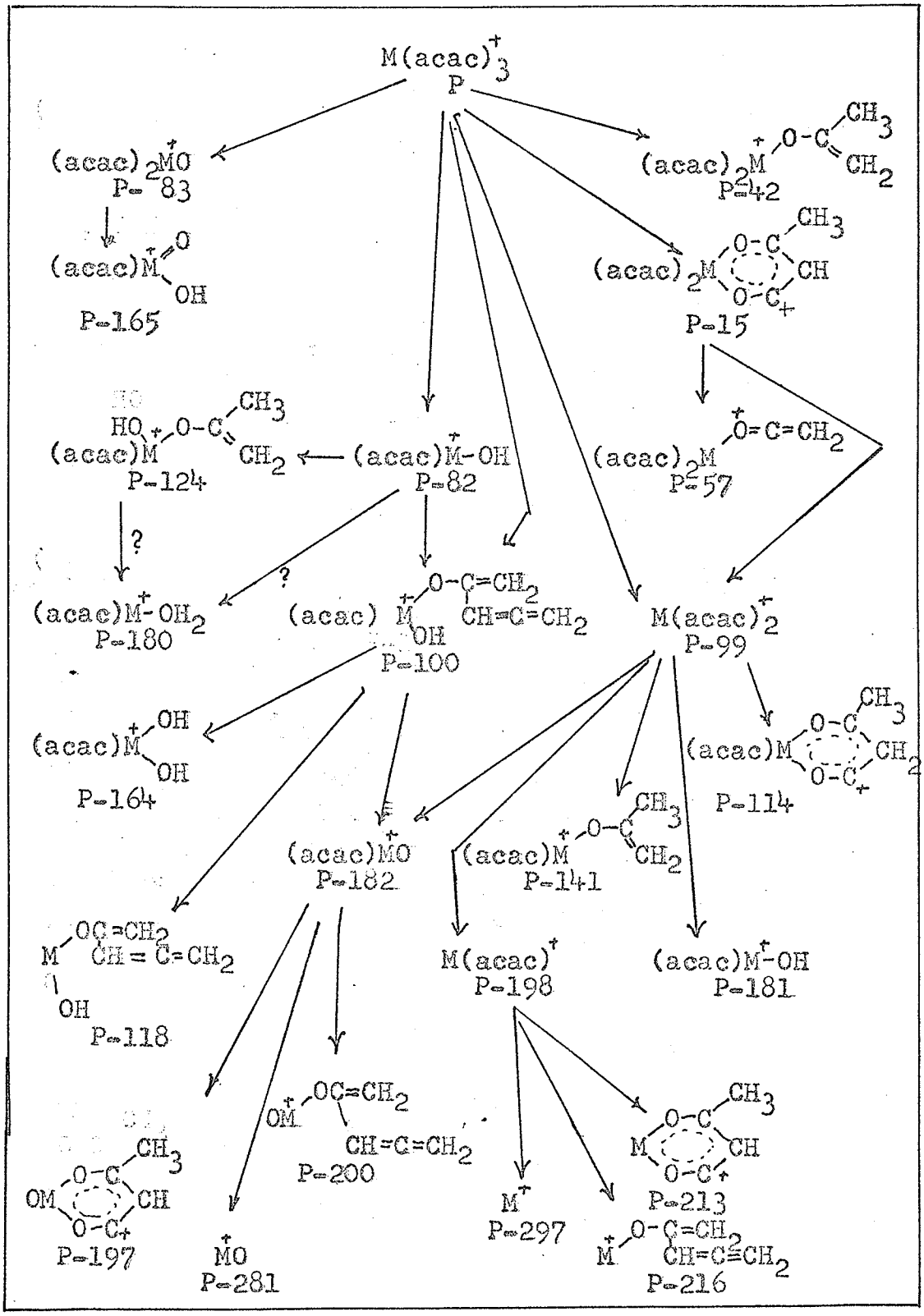
M(acac)3+
P
(acac)2MO+
P-83
(acac)M+(=O)OH
P-165
(acac)2M+-O-C(CH3)=CH2
P-42
(acac)2M+ (O-C(CH3)-CH=C-O+)
P-15
HO(acac)M+-O-C(CH3)=CH2
P-124
(acac)M+-OH
P-82
(acac)2M+-O+=C=CH2
P-57
(acac)M+-OH2
P-180
(acac)M+(OH)-O-C=CH2 CH=C=CH2
P-100
M(acac)2+
P-99
(acac)M+(OH)2
P-164
(acac)M+ (O-C(CH3)-CH2-C-O+)
P-114
(acac)MO+
P-182
(acac)M+-O-C(CH3)=CH2
P-141
M(OC=CH2)(CH=C=CH2)(OH)
P-118
M(acac)+
P-198
(acac)M+-OH
P-181
OM+-OC=CH2 CH=C=CH2
P-200
(OM)(acac) (O-C(CH3)-CH-C-O+)
P-197
MO+
P-281
M+
P-297
M (O-C(CH3)-CH-C-O+)
P-213
M+(O-C=CH2)(CH=C=CH2)
P-216

TABLE 6

Calculated Positions of Metastable Peaks and Related Transitions Observed in the Mass Spectra of Acetylacetonates of the Trivalent Metals of the First Transition Series.

$(ML_3)^+ \longrightarrow (ML_2)^+$	174.0	178.2	179.1	181.8	182.8	
$(ML_3)^+ \longrightarrow (L_2MOH)^+$	200.5					
$(ML_3)^+ \longrightarrow (ML_3 - 42)^+$						277.0
$(ML_3)^+ \longrightarrow (C_4H_5O_2)^+$				20.5		
$(ML_2OH)^+ \longrightarrow (ML_2)^+$	228.2?					
$(ML_2OH)^+ \longrightarrow (L\,MOH(L - 42))^+$	185.7					
$(ML_2OH)^+ \longrightarrow (LM(L - 83)OH)^+$		125.9				
$(ML_20)^+ \longrightarrow (LM(L - 82)O)^+$		126.4				
$(ML_20)^+ \longrightarrow (LMOH)^+$		105.2				
$(ML_20)^+ \longrightarrow (ML)^+$		84.9				
$(ML_2)^+ \longrightarrow (ML_2 - H_20)^+$	210.3					
$(ML_2)^+ \longrightarrow (ML_2 - CH_3)^+$			220.9	223.9	224.9	227.9
$(ML_2)^+ \longrightarrow (LM(L - 42))^+$				176.0		
$(ML_2)^+ \longrightarrow (LM(L - 82))^+$	108.4					
$(ML_2)^+ \longrightarrow (LM(L - 83))^+$		110.7				
$(ML_2 - CH_3)^+ \longrightarrow (ML)^+$				99.7	100.5	103.2
$(ML_2 - CH_3)^+ \longrightarrow (MCH_3)^+$?				20.6		
$(ML_2 - 82)^+ \longrightarrow (ML - H)^+$	129.0					
$(ML)^+ \longrightarrow (MCH_3)^+$				31.8	32.5	
$(ML)^+ \longrightarrow (ML - 16)^+$					124.7	

electron neutral fragment. Further fragmentation can occur by two methods. For the resulting ion to be an even-electron species rearrangement or multiple bond cleavage must take place with loss of an even electron species such as 42($CH_2{=}C{=}O$) as seen for Mn or 82($CH_3{-}C{\equiv}CH = C = CH_2$) as seen for Ti, V, Cr, and Fe.

If the metal is also stable in another valency state it is possible for an electron to be transferred from the ligand to the metal or vice versa thereby changing the valency of the metal (65) by one unit. A change in valency will also result in changing the odd electron ion to an even electron ion or vice-versa. Thus for metals such as Co^{III}, Fe^{III}, Mn^{III}, Cr^{III} after the loss of one acac• radical the valency of the metal can change from +III to +II by an electron transfer from a ligand orbital to a metal orbital as another odd electron neutral species such as acac• or CH_3• is lost. We see from Table 4 that the intensities of these peaks (i.e. the $(P-114)^+$ and $(P-198)^+$ peaks formed by loss of an odd electron fragment from $M(acac)_2^+$) closely parallel the ease with which the +II state is formed from the +III state in the established chemistry of these metals. That is the +II state increases in stability in the sequence Ti ⟹ Co. This follows closely the trend observed in general chemistry for these metals.

Loss of additional odd electron neutral species does not occur, as would be expected, since these metals are not known to be stable in the +I oxidation state. Further fragmentation must occur by multiple bond cleavage or rearrangement if even-electron ions are to be formed. However, since

these processes are energetically expensive, the resulting peaks are generally quite small (usually less than 5 or 10% of the base peak).

Interesting peaks at masses 71 and 70 for iron and manganese respectively, as well as metastables calculated to be for processes leading to these peaks, are seen in the spectra (see Table 6). The metastables indicate a process involving the loss of the ligand moiety less a methyl group, i.e. $CH_3COCHCO$, indicating a methyl migration to the metal. A more detailed discussion of migrations of a similar nature will be carried out in a later section (see section VIII (C) and (E)). The metastable peak seen for manganese in the vicinity of 20.5 can be explained by two possible processes. One of these could be the elimination of a neutral fragment CH_3ML_2 from ML_3; the other could be the formation of MCH_3^+ from $(ML_2\text{-}CH_3)^+$. Unfortunately with the instrument used the process occurring could not be verified.

The fragmentation of $Ti(acac)_3$ and $V(acac)_3$ proceeds somewhat differently than the rest of the series as would be expected from the normal chemistry of these metals. These metals form their most stable compounds in the +IV oxidation state and thus a valency change from +III to +II would not be expected to occur readily; instead a change from +III to +IV with the formation of oxy and hydroxy species is preferred.

On the loss of an electron from the $Ti(acac)_3$ and $V(acac)_3$ molecules, fragmentation by the loss of an odd-electron neutral fragment can occur to a certain extent as for the rest of this series. There is, however, in competition with the loss of the odd-electron fragment another process,

that of valency change of the metal to the +IV state. The transfer of the electron from the orbital localized mainly on the metal to the orbital localized mainly on the ligand produces a pairing of electrons to produce an even-electron ion. The stability gained from this may account for the slight increase in the molecular-ion intensity for $V(acac)_3$ and the large increase for $Ti(acac)_3$.

Fragmentation of the even-electron ion may now occur by the loss of even-electron neutral species. The largest fragment ion for $Ti(acac)_3$ is the ion after loss of mass 100. Mass 100 can be accounted for by either a one step process i.e. loss of the even-electron species Hacac or a two step process i.e. first loss of 82 presumably $CH_3\overset{O}{\overset{\|}{C}}CH = C = CH_2$ and then loss of 18 (H_2O). Unfortunately no metastable peaks are present to verify either process.

Important fragmentations observed for $Ti(acac)_3$ and $V(acac)_3$ are the loss of the even-electron fragment of mass 82 presumably $CH_3\overset{O}{\overset{\|}{C}}CH = C = CH_2$ and the odd-electron fragment of mass 83 presumably $CH_3\overset{O}{\overset{\|}{C}}CH = \dot{C}CH_3$. From general chemistry it is well known that Ti and V form very strong bonds with oxygen. The stability gained from the formation of Ti = O or V = O bonds could possibly be the driving force for the reaction. MacDonald and Shannon suggest a mechanism for the loss of the species of mass 82 from $VO(acac)_2$.

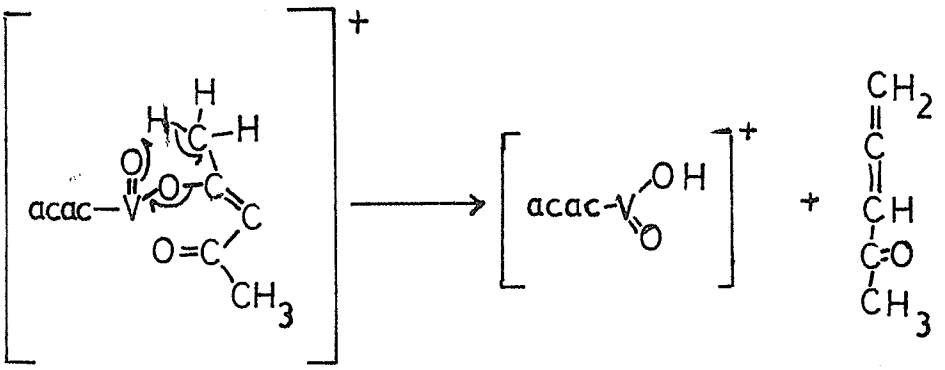

(The "halved" arrowheads ⟶ indicate one electron shifts.) However this mechanism is not possible in the case of $Ti(acac)_3^+$ or $V(acac)_3^+$. Loss of mass 82 from these molecular ions may proceed through the formation of a four membered intermediate such as below.

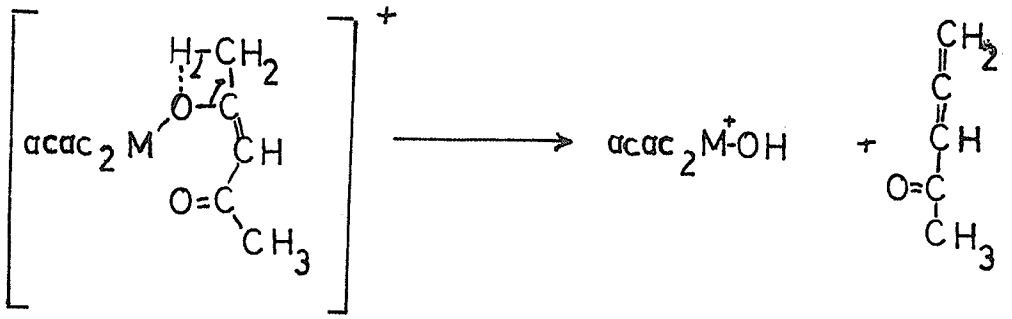

The loss of mass 83 an odd-electron fragment appears to be lost from odd-electron ions by the breaking of two bonds, an O - C bond

and an M - O bond. As mentioned above the driving force for this process may be the subsequent formation of M = O which is known to be relatively strong for these metals.

2. Appearance Potentials

The two processes considered to be of most importance in this series of compounds are

$$M(acac)_3 + e \longrightarrow M(acac)_3^+ + 2e \qquad (23)$$

$$M(acac)_3 + e \longrightarrow M(acac)_2^+ + acac\cdot + 2e \qquad (24)$$

For the first process the assumption made is that, at the ionization threshold, the excess energy (in the form of kinetic or excitation energy) associated with the process is small, or at least constant, for the series of compounds. Since the ionization efficiency curves, shown in Figure 12, had a similar form the assumption appears to be justified. Thus the measured appearance potentials, given in Table 7, should give at least accurate relative ionization potentials and probably absolute appearance potentials.

The errors quoted here and in succeeding series indicate the reproducibility of the results rather than an assessment of their absolute accuracy. The absolute accuracy is probably within $\pm$ 0.2V. The appearance potentials varied by no more than 0.2V on varying the chamber temperature from 150°C to 250°C.

Recent ionization potentials measured by Schildcrout, Pearson and Stafford (68) show a very good agreement (Table 7) even though they used a different method (the vanishing current method) of obtaining the

Figure 12

Ionization efficiency curves for $M(acac)_3^+$ and $M(acac)_2^+$. The curves for $Mn(acac)_2^+$, $Fe(acac)_2^+$, and $Co(acac)_2^+$ probably reflect the thermal instability of the corresponding tris chelate. The effect is most marked in the curve for $Co(acac)_2^+$, where it has been assumed that the experimental curve is the sum of the contributions indicated by the broken lines. The lower curve is taken as $Co(acac)_2^+$ arising from thermal decomposition; the appearance potential was estimated from the upper broken curve and contains considerable uncertainty. For $Mn(acac)_2^+$ the quoted value of the appearance potential is probably a lower limit.

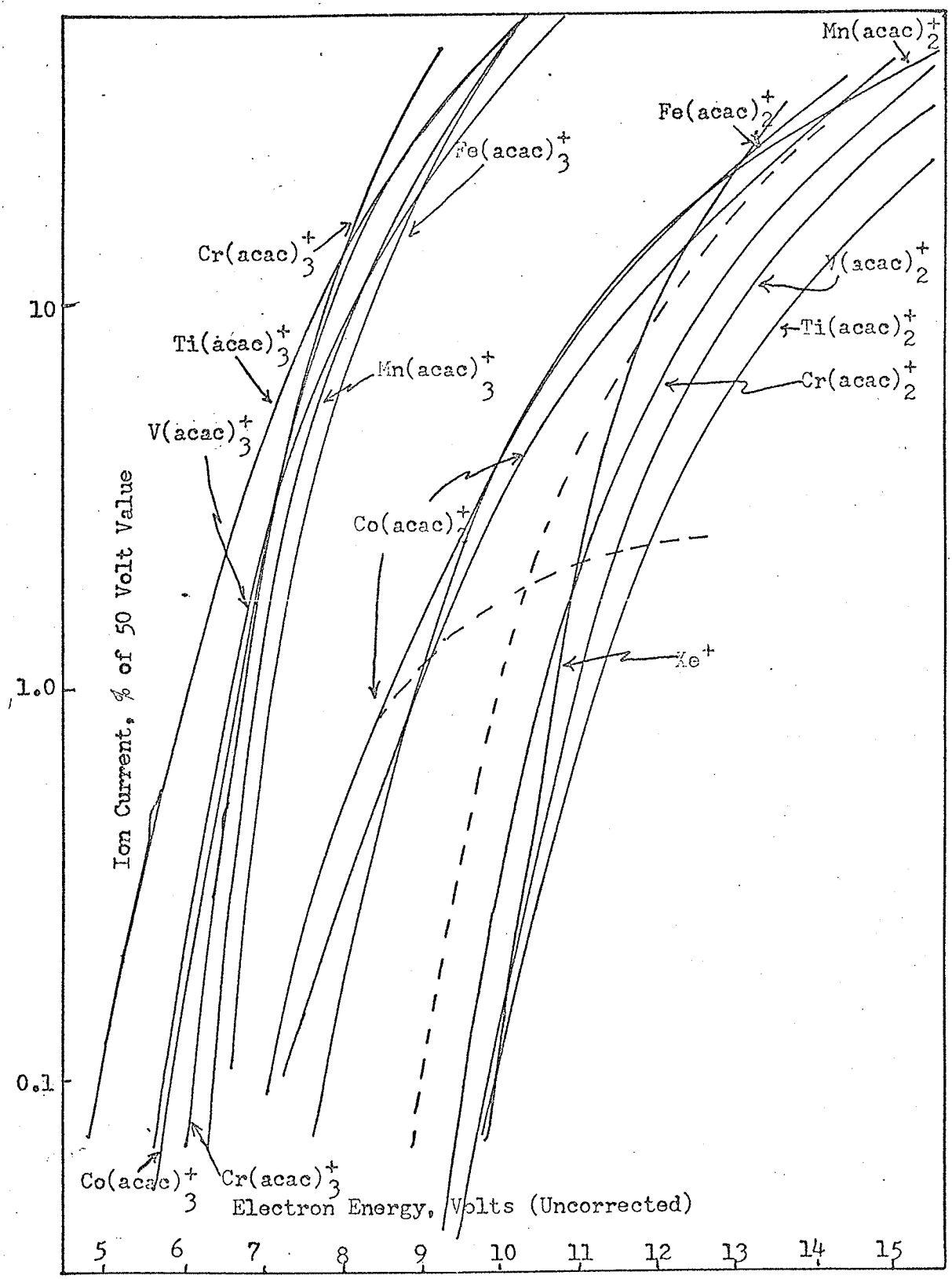
Mn(acac)$_2^+$
Fe(acac)$_2^+$
Fe(acac)$_3^+$
Cr(acac)$_3^+$
V(acac)$_2^+$
Ti(acac)$_2^+$
Ti(acac)$_3^+$
Mn(acac)$_3^+$
Cr(acac)$_2^+$
V(acac)$_3^+$
Co(acac)$_2^+$
Xe$^+$
Co(acac)$_3^+$
Cr(acac)$_3^+$
10
1.0
0.1
Ion Current, % of 50 Volt Value
Electron Energy, Volts (Uncorrected)
5
6
7
8
9
10
11
12
13
14
15

ionization potentials from the ionization efficiency curves.

For the second process, the assumption is that the excess energy is small, so that

$$\text{A.P.}\left[M(acac)_2^+\right] = \text{I.P.}\left[M(acac)_2^+\right] + 2E(M-O) \qquad (25)$$

where E(M - O) is the energy of the metal-oxygen bond. Unfortunately, however, it is not possible to determine the ionization potentials of the bis-chelates of all the metals, so that a correlation of bond energies with electronic structure is not possible. Though not necessarily related to the above reaction, the energy of the process

$$M(acac)_3^+ \longrightarrow M(acac)_2^+ + \cdot acac + 2e \qquad (24)$$

was assumed to be given by

$$\text{A.P.}\left[M(acac)_2^+\right] - \text{A.P.}\left[M(acac)_3^+\right] \qquad (26)$$

and the variation in energy of this process with the transition metal is believed to be of significance.

Studies of proton resonance and ultraviolet spectra of metal acetylacetonates led Holm and Cotton (69) to state that the experimental data could not be correlated with any simple parameter of the complexed metal ion, although they believed that the ability of the metal ion to participate in π-interaction with the chelate ring was important. Similarly, in this study, we were unable to find any simple correlation between the measured appearance potentials and a parameter relating to the complexed ions.

Barnum (36) has calculated energy levels, using molecular orbital

theory and taking account of π-interaction for these compounds. His calculations show that for metals of the first transition series the d-orbitals of the metal are split by the nearly octahedral ligand field and that these orbitals lie higher in energy than the highest filled π orbitals of the acac ligand. This would indicate that the ionization potential would depend to a large degree on the number of d electrons. Figure 13 shows a superposition of the appearance potentials on the calculations of Barnum. If we define the ionization potential as being the minimum energy required to remove the electron from the highest occupied molecular orbital, the results do not correlate with Barnum's simplified calculations. For example, $Mn(acac)_3^+$ should have a much lower ionization potential than $Cr(acac)_3^+$ (at least 1.5V lower). Similarly, low spin $Co(acac)_3^+$ should have a much higher ionization potential than $Fe(acac)_3^+$. It can be seen that these conclusions are not in agreement with the measured appearance potentials.

Since the assumptions about the energetics of processes given by equations 24 and 25 should be essentially correct we are forced to conclude that Barnum's calculations are not even qualitatively correct or that the electron is not removed from the highest occupied molecular orbital in all cases. Even if Barnum's calculations were seriously in error, there is still the trend in the appearance potentials of $M(acac)_2^+$ to be explained. The d_γ orbitals are antibonding. It would be expected, therefore, that for the manganese chelate if the d_γ electron is removed, the difference between the appearance potentials of $Mn(acac)_2^+$ and

Figure 13

Appearance potentials of $M(acac)_3^+$ and $M(acac)_2^+$ from $M(acac)_3$. The energy levels have been estimated from data given by Barnum (36).

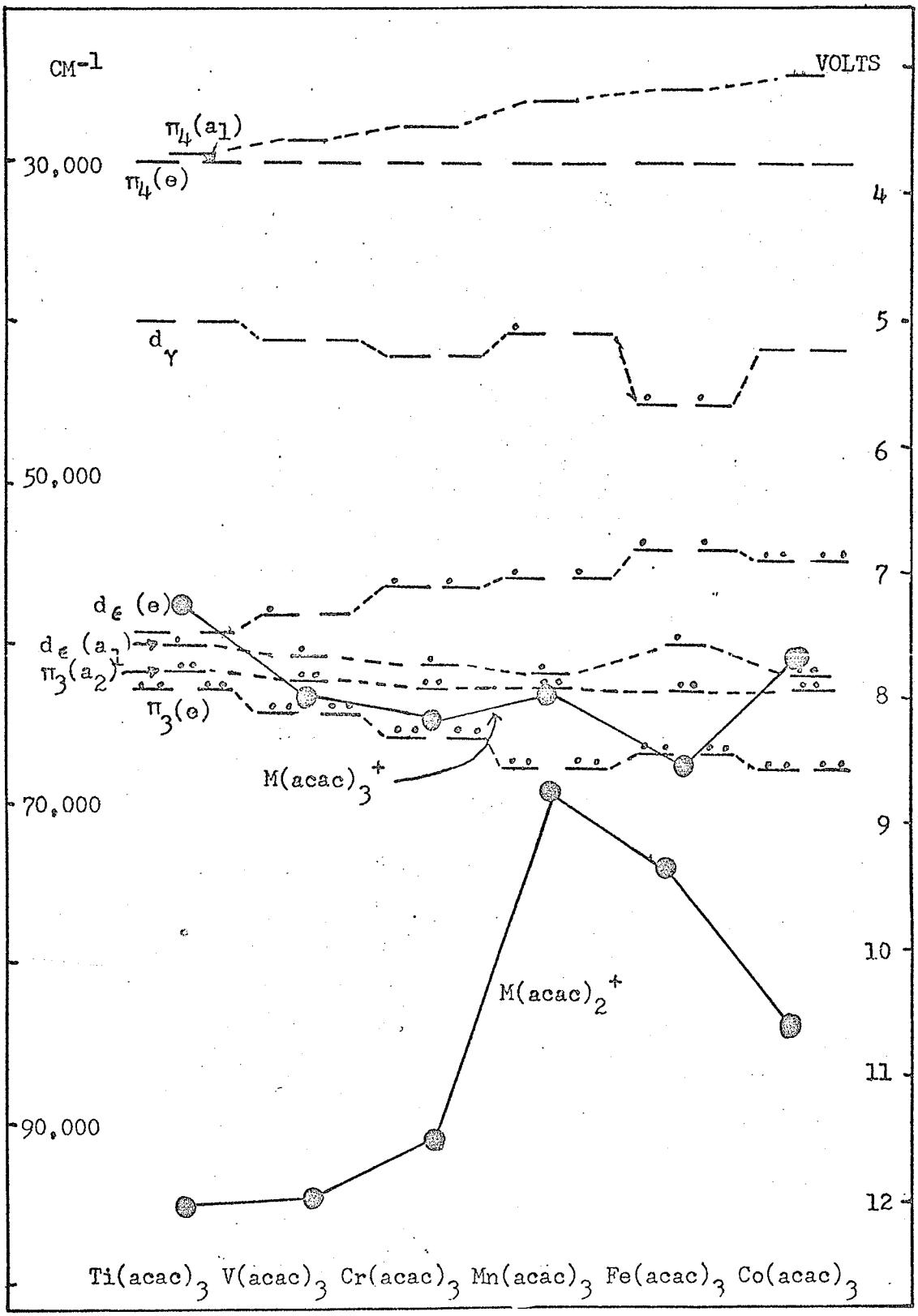
CM-1
VOLTS
30,000
50,000
70,000
90,000
4
5
6
7
8
9
10
11
12
$\pi_4(a_1)$
$\pi_4(e)$
d_γ
d_ϵ (e)
d_ϵ (a_1)
$\pi_3(a_2)$
π_3(e)
$M(acac)_3^+$
$M(acac)_2^+$
$Ti(acac)_3$ $V(acac)_3$ $Cr(acac)_3$ $Mn(acac)_3$ $Fe(acac)_3$ $Co(acac)_3$

$Mn(acac)_3^+$ would be of similar magnitude to that for the chelates of Ti, V, and Cr, instead of the large decrease which is actually observed. If the electron is assumed to be removed from either the d_ϵ or π_3 orbitals, then better correlation with Barnum's calculation is obtained, and furthermore, the variation in appearance potentials of $M(acac)_2^+$ formed from $M(acac)_3$ can be rationalized, although the results could be complicated by structural rearrangement (e.g. to square-planar or tetrahedral ions). It is perhaps worth noting that for $Al(acac)_3$ in which little or no π interaction between metal and ligand is expected that the appearance potential of $Al(acac)_2^+$ is only 1.1V higher than that of $Al(acac)_3^+$.

B. Acetylacetonates of the Divalent Metals of the First Transition Series

1. Mass Spectra

The mass spectra, obtained for the chelates for 50 volt electrons and an ionizing chamber temperature of 150° as tabulated in Table 8, compare favorably to the spectra reported by MacDonald and Shannon (60). Variations which do occur can be attributed in most cases to differences in experimental conditions.

Fragmentation as discussed in some detail by MacDonald and Shannon proceeds in much the same way as for the trivalent acetylacetonates (see Figure 14 and Table 8) with the loss of an acac• odd-electron species accounting for the most abundant peak in the spectra for all but the copper complex. Table 9 lists the metastable peaks found in the spectra.

TABLE 8

Relative intensities of the ions in the mass spectra of acetylacetonates of divalent metals, at an electron energy of 50 volts and ionization chamber temperature of ~150°. The intensities of doubly charged ions are shown in parenthesis. (L = •acac)

Ion	Mn	Fe	Co	Ni	Cu	Zn	Assignment
P	84(0.6)	60	96	98	48	52	ML_2^+
P-15	58(1.6)	42 (0.8)	91	90	35	69	$(ML_2-CH_3)^+$
P-18	1	-	-	-	1	-	$(ML_2-H_2O)^+$
P-30	-(3.3)	-	2	-	35	-	$(ML_2- ML_2-2CH_3)^+$
P-42	9	1	2	-	10	9	$(L_2M-CH_2CO)^+$
P-57	-	-	2	3	-	33	$(LMCOCH_2)^+$
P-82	-	9	-	-	-	-	$LMOH^+$
P-98	-	-	-	41	6	-	LMH^+
P-99	100	100	100	100	50	100	LM^+
P-100	-	-	3	-	5	-	$(LM-H)^+$
P-101	-	-	2	-	-	-	$(LM-2H)^+$
P-114	5	-	12	33	100	-	$(LM-CH_3)^+$
P-115	-	-	3	24	-	-	$(L_2M- CH_3-HL)^+$
P-117	4	-	2	-	-	9	$(LM-H_2O)^+$
P-128	-	-	-	-	12	-	$(L_2M-2CH_3-(L-H))^+$
P-141	-	-	-	-	-	4	$(LM-CH_2CO)^+$
P-142			10				$(LM-CH_3CO)^+$
P-156	-	-	-	30	50	-	$(MCOCH_2)^+$
P-157	-	-	-	-	8	-	$(MCOCH)^+$
P-181	3	-	-	-	-	-	MOH^+
P-182	-	10	-	-	-	-	MO^+
P-183	14	25	-	-	-	-	MCH_3^+
P-198	8	15	6	17	10	5	M^+

Figure 14

Some suggested decomposition pathways for the formation of ions in the mass spectra of acetylacetonates of the divalent metals of the first transition series.

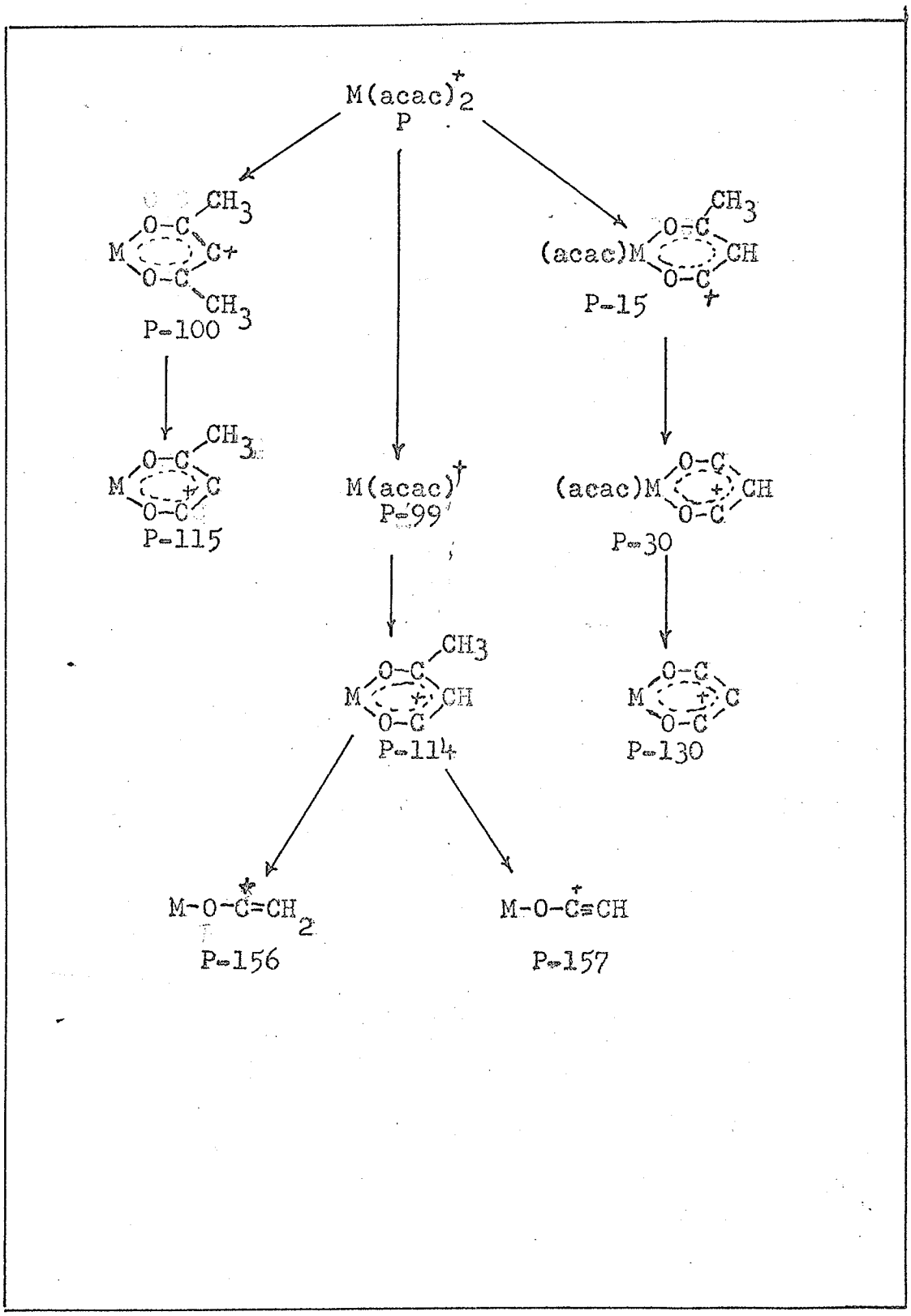
M(acac)2+
P
P-100
P-15
P-115
M(acac)+
P-99
P-30
P-114
P-130
M-O-C=CH2
P-156
M-O-C≡CH
P-157

TABLE 9

Calculated Positions of Metastable Peaks and Related Transitions Observed in the Mass Spectra of Acetylacetonates of the Divalent Metals of the First Transition Series.

	Mn	Fe	Co	Ni	Cu	Zn
$(ML_2)^+ \longrightarrow (ML_2 - CH_3)^+$	223.9	224.9	227.9			232.9
$(ML_2)^+ \longrightarrow (ML_2 - 2CH_3)^+$			200.5			
$(ML_2)^+ \longrightarrow (ML_2 - 42)^+$	176.0		179.9		183.8	
$(ML_2)^+ \longrightarrow (ML - H)^+$			95.9			
$(ML_2)^+ \longrightarrow (ML - CH_3)^+$			79.6			
$(ML_2)^+ \longrightarrow (M(L - H) - CH_3)^+$			78.5			
$(ML_2 - CH_3)^+ \longrightarrow (ML_2 - 2CH_3)^+$					216.9	
$(ML_2 - CH_3)^+ \longrightarrow (ML)^+$	99.7		103.2	102.3	106.7	
$(ML_2 - CH_3)^+ \longrightarrow (MLCOCH_2)^+$			165.3			170.1
$(ML_2 - 2CH_3)^+ \longrightarrow (ML)^+$					133.4	
$(ML_2 - 2CH_3)^+ \longrightarrow (ML - CH_3)^+$					93.6	
$(ML_2 - 2CH_3)^+ \longrightarrow (ML_2 - 2CH_3 - (L-H))^+$					76.6	
$(MC(=O)C = C = O)^+$						
$(MLCOCH_2)^+ \longrightarrow (ML)^+$						129.6
$(ML)^+ \longrightarrow (ML - CH_3)^+$				126.6	113.6	
$(ML - H)^+ \longrightarrow (M(L - H) - CH_3)^+$			128.4			
$(ML - CH_3)^+ \longrightarrow (MCOCH_2)^+$					75	
$(ML - CH_3)^+ \longrightarrow (MCOCH)^+$					73.6	

The effect of valency change on peak intensities is evident in this series. Copper is seen to be the most stable one in the +I state as evidenced by the base peak being a species produced by the successive loss of two odd electron neutral fragments. The Co and Ni compounds are the only others showing evidence for successive loss of two odd electron fragments but have only small peaks due to these processes.

2. Appearance Potentials

The results for the acetylacetonates of the trivalent metals as discussed suggested that on ionization the electron was removed from a π-orbital localized mainly on the ligand since the nature of the ligand had a far greater effect than the metal on the appearance potentials of the metal chelates. In this series variation of the appearance potentials from metal to metal appears to be even less. In Table 10 are tabulated the appearance potentials of the molecular ions, and the ions formed by loss of $CH_3^{\bullet}$ or a ligand radical.

Most of these complexes have different structures in the gaseous and condensed phases. The available evidence (70) suggests that in the gaseous state the acetylacetonates of Mn(II), Fe(II), Co(II) and Zn(II) are tetrahedral (high spin) while those of Ni(II) and Cu(II) are square planar, and in the solid state they are all polymeric with the exception of $Cu(acac)_2$. Electronic absorption spectra can, in principle, be used to evaluate ligand field effects, but solution spectra are not likely to be helpful here. Thus, the usual experimental data are not available

with which to compare the measured appearance potentials and, we are not aware of any theoretical treatment of the gaseous chelate molecules.

In the previous series values were quoted for the appearance potentials of the $M(acac)_2^+$ ions from the tris-chelates of Mn(III), Fe(III) and Co(III). For these chelates it is thus possible to calculate the energy, ΔH_{diss}, of the dissociation

$$M(acac)_3 \longrightarrow M(acac)_2 + acac \qquad (27)$$

Making the usual assumptions that the products of the ionization reaction are formed in their ground states and that their total kinetic energy is small, a lower limit for the energy of the homolytic dissociation is given by:

$$\Delta H_{diss} = \text{A.P.} \left[M(acac)_2^+ \text{ from } M(acac)_3\right] - \text{I.P.} \left[M(acac)_2\right] \qquad (28)$$

The metal-oxygen coordinate bond energies in the $M(acac)_2$ complexes are then given by:

$$E_{M-O}^{bis} = \frac{1}{4} \left(6E_{M-O}^{tris} - \Delta H_{diss} \right) \qquad (29)$$

Values calculated using these equations are given in Table 11.

TABLE 10

Appearance Potentials of ions from $M(acac)_2$ at an ionization chamber temperature of approximately 150°.

Metal	Sample temp. (approx.)	P^+ eV	$(P-CH_3)^+$ eV	$(P-L)^+$ eV
Mn	120°	8.34 ± 0.05	11.7 ± 0.1	13.7 ± 0.1
Fe	100°	8.10 ± 0.05	11.7 ± 0.1	13.9 ± 0.1
Co	25°	8.54 ± 0.05	11.5 ± 0.1	13.9 ± 0.2
Ni	100°	8.23 ± 0.05	11.6 ± 0.1	13.5 ± 0.2
Cu	30°	8.31 ± 0.05	10.9 ± 0.1	13.1 ± 0.2
Zn	100°	8.62 ± 0.05	10.9 ± 0.1	14.1 ± 0.2
H	-	9.2 ± 0.1	10.7 ± 0.1	-----

TABLE 11

Coordinate Bond Energies

Metal	A.P. $\left[M(acac)_2^+\right]$ From $M(acac)_3$	H_{diss} kcal/mole	$E_{M-O,tris}$[a]	$E^{bis}_{M-O,}$ kcal/mole
Mn	$\geqslant$ 8.7 ± 0.1	$\geqslant$ 9 ± 4	44.8 ± 0.5	$\leqslant$ 65 ± 2
Fe	$\geqslant$ 9.4 ± 0.1	$\geqslant$ 30 ± 4	55.9 ± 0.6	$\leqslant$ 76 ± 2
Co	10.7 ± 0.1	$\geqslant$ 51 ± 4	50.9 ± 0.7	$\leqslant$ 63 ± 2

(a) see reference (71).

C. Metal Fluorinated Acetylacetonates

1. The Mass Spectra

The relative intensities of all metal containing ions in the mass spectra of the tri and hexafluoroacetylacetonates of Al(III), Cr(III), Fe(III), Fe(II), Cu(II) and Zn(II) are given in Tables 12 and 13. In assigning the base peak, mass 69(CF_3^+), which was often the most abundant peak, was ignored. Tables 14 and 15 give the metastable peaks found in the spectra as well as the process related to each peak.

The results are consistent with the facile loss of one odd-electron neutral fragment, as discussed for the acetylacetonates, after which further odd-electron neutral fragments are not readily lost unless the metal can undergo a valency change. Figures 15 and 16 give a schematic diagram of these processes. When no further odd-electron neutral fragments can be easily lost, then loss of even-electron fragments can occur, as shown in the scheme.

Compared with the spectra of the acetylacetonates, it is apparent that substitution of CF_3 for CH_3 leads to a more extensive fragmentation of the molecule under electron impact. The greater fragmentation of the fluorinated chelates can be attributed to:

1) the relative instability of the molecular ion due to, for example, weak C-CF_3 bonds;
2) the relative stability of some of the products due to the high M-F bond energies; and
3) the stabilization of the positive charge on the carbon via the electron withdrawing power of CF_3.

TABLE 12

Relative intensities of metal containing ions in the mass spectra of the bis-complexes of fluorinated acetylacetonates, at an electron energy of 50 volts and an ionization chamber temperature of 150°C.

Ion	$Fe(hfacac)_2$	$Cu(hfacac)_2$	$Zn(hfacac)_2$	$Fe(tfacac)_2$	$Cu(tfacac)_2$	$Zn(tfacac)_2$
$(L_2M)^+$	83	9	9	100	5	44
$(L_2M-F)^+$	4					
$(L_2M-CH_3)^+$	-			6	1	21
$(L_2M-CF_2)^+$	30			28		
$(L_2M-CH_2CO)^+$					8	
$(L_2M-CFO)^+$					8	
$(L_2M-CF_3)^+$	44	24	27	31	11	100
$(L_2M-(CF_3+CH_2CO))^+$				4		40
$(L_2M-138)^+$		23	2.5		27	
$(LMF)^+$	8			6		
$(LM)^+$	13	1.5	19	23	8	54
$(LM-CH_3)^+$					10	
$(L_2M-(2CF_3+CH_3CO))^+$?						9
$(LM-CF_2)^+$	100		100	71		67
$(LM-CF_3)^+$		100	12		100	

Table 12 Continued

Ion	$Fe(hfacac)_2$	$Cu(hfacac)_2$	$Zn(hfacac)_2$	$Fe(tfacac)_2$	$Cu(tfacac)_2$	$Zn(tfacac)_2$
$(MCOCH_2)^+$					59	
$(MCOCH)^+$		11	6		18	12
$(LMF-CF_2)^+$	9					
M^+		82	46		44	28

TABLE 13

Relative intensities of metal containing ions in the mass spectra of the tris-complexes of fluorinated acetylacetonates, at an electron energy of 50 volts and an ionization chamber temperature of 150°C. (Only peaks greater than 1% of base peak)

Ion	$Al(hfacac)_3$	$Cr(hfacac)_3$	$Fe(hfacac)_3$[a]	$Al(tfacac)_3$	$Cr(tfacac)_3$	$Fe(tfacac)_3$
L_3M^+	5	20	18	3	24	10
$(L_3M-F)^+$	1	4	2	-	2	-
$(L_3M-CF_3)^+$	6	6	7	-	-	0.5
L_2M^+	100	100	100	100	100	100
$(L_2M-CH_3)^+$	-	-	-	-	-	3
$(L_2M-CF_2)^+$	17	21	37	9	8	27
$(L_2M-CF_3)^+$	3	3	21	1.5	21	20
$(L_2M-2CF_2)^+$	1	-	-	7	-	0.5
$(LMOC\ CH)^+$	-	-	-	-	-	3
$(L_2M-CF_3-CF_2)^+$	1	-	-	-	-	4
LMF^+	-	70	8	12	40	5
LM^+	-	64	7	3	30	20
$(LMF-CF_2)^+$	10	23	6	39	25	-
$(LM-CF_2)^+$	11	35	57	-	40	80
$(LM-CF_3)^+$	-	38	-	-	3	-

(a) 75°C.

TABLE 14

Calculated Positions of Metastable Peaks and the Related Transitions observed in the Mass Spectra of Fluorinated Acetylacetonates of some Divalent Metals of the First Transition Series.

$(L_2M)^+ \longrightarrow (L_2M\text{-}CF_3)^+$		349.0	350.0			244.9
$(L_2M)^+ \longrightarrow (L_2M\text{-}CF_2)^+$	375.3			268.9		
$(L_2M)^+ \longrightarrow (L_2M\text{-}COF)^+$					289.8	
$(L_2M\text{-}F)^+ \longrightarrow (L_2M\text{-}CF_3)^+$	356.5	363.5				
$(L_2M\text{-}CF_3)^+ \longrightarrow (LM)^+$	172.5		179.6			
$(L_2M\text{-}CF_3)^+ \longrightarrow (L_2M\text{-}2CF_3)^+$		281.7				
$(L_2M\text{-}CF_3)^+ \longrightarrow (LMCH_3)^+$					177.9	
$(L_2M\text{-}CF_3)^+ \longrightarrow (LMCOCH_2)^+$						222.9
$(L_2M\text{-}CH_3)^+ \longrightarrow (LM)^+$						132.6
$(L_2M\text{-}CF_2)^+ \longrightarrow (L_2M\text{-}CF_3)^+$				275.2		
$(L_2M\text{-}2CF_3)^+ \longrightarrow (LM\text{-}CF_3)^+$		119.2			93.6	
$(LMCH_3)^+ \longrightarrow L^+$					101.3	
$(LMCOCH_2)^+ \longrightarrow (LM)^+$						181.8
$(LM)^+ \longrightarrow (LM\text{-}CF_2)^+$	172.5		180.2			128.5
$(LM\text{-}CF_3)^+ \longrightarrow (M)^+$		19.8				
$(LM\text{-}CF_3)^+ \longrightarrow (MCOCH_2)^+$					75.0	

TABLE 15

Calculated Positions of Metastable Peaks and the Related Transitions Observed in the Mass Spectra of Fluorinated Acetylacetonates of Some Trivalent Metals.

	$Al(hfacac)_3$	$Cr(hfacac)_3$	$Fe(hfacac)_3$	$Al(tfacac)_3$	$Cr(tfacac)_3$	$Fe(tfacac)_3$
$(ML_3)^+ \longrightarrow (ML_2)^+$	300.13	322.7		228.2		
$(ML_3)^+ \longrightarrow (ML_3 - CF_3)^+$	517.3	542.1				
$(ML_3)^+ \longrightarrow (ML_3\text{-}F)^+$	612					
$(ML_3\text{-}F)^+ \longrightarrow (L_3M\text{-}CF_3)^+$	532	557.8				
$(ML_3\text{-}F)^+ \longrightarrow (ML_2\text{-}CF_3)^+$		241.0				
$(ML_3\text{-}CF_3)^+ \longrightarrow (ML_2)^+$	335.9	359.5				
$(ML_3\text{-}CH_3)^+ \longrightarrow (ML)^+$					84.7	
$(ML_2)^+ \longrightarrow (ML_2\text{-}CF_2)^+$	346.7	371.4	375.3	240.5		268.9
$(ML_2)^+ \longrightarrow (ML_2\text{-}CH_3)^+$						125.9
$(ML_2)^+ \longrightarrow (MFL)^+$		165.8				
$(MFL)^+ \longrightarrow (FML\text{-}CF_2)^+$		187.0		111.6	135.2	
$(L_2M\text{-}CF_2)^+ \longrightarrow (L_2M\text{-}CF_3)^+$		378.9			271.2	
$(L_2M\text{-}CF_2) \longrightarrow (CF_3)^+$	12.2					
$(L_2M\text{-}2CF_2)^+ \longrightarrow (FML\text{-}CF_2)^+$				95.3		
$(L_2M\text{-}CF_2)^+ \longrightarrow (ML)^+$			172.5	139.9	136.4	
$(FML\text{-}CF_2)^+ \longrightarrow (CF_2 \cdot CO \cdot CHCO)^+$	36.2	62.1				

Table 15 Continued

	$Al(hfacac)_3$	$Cr(hfacac)_3$	$Fe(hfacac)_3$	$Al(tfacac)_3$	$Cr(tfacac)_3$	$Fe(tfacac)_3$
$(L_2M\text{-}CF_3)^+ \longrightarrow (ML)^+$		169.0	172.5			
$(ML)^+ \longrightarrow (ML\text{-}CF_2)^+$		168.7	164.7			121.0
$(ML\text{-}CF_2)^+ \longrightarrow (C_4HF_2O_2)^+$			66.5			

Figure 15

Some suggested decomposition pathways for the formation of ions in the mass spectra of the fluorinated acetylacetonates of the divalent metals.

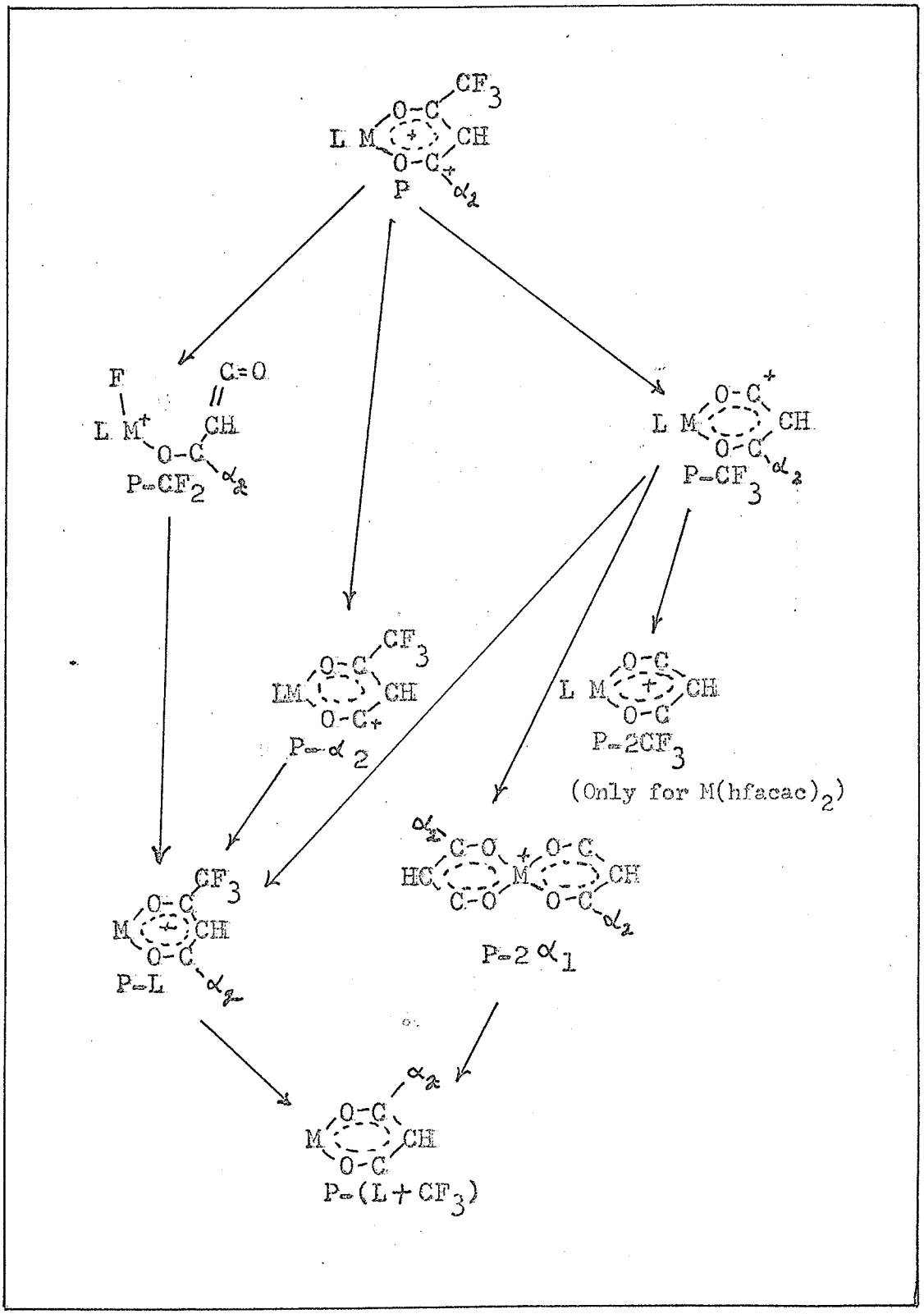
P
P-CF2
P-CF3
P-α2
P-2CF3
(Only for M(hfacac)2)
P-L
P-2α1
P-(L+CF3)

Figure 16

Some suggested decomposition pathways for the formation of ions in the mass spectra of the fluorinated acetylacetonates of the trivalent metals.

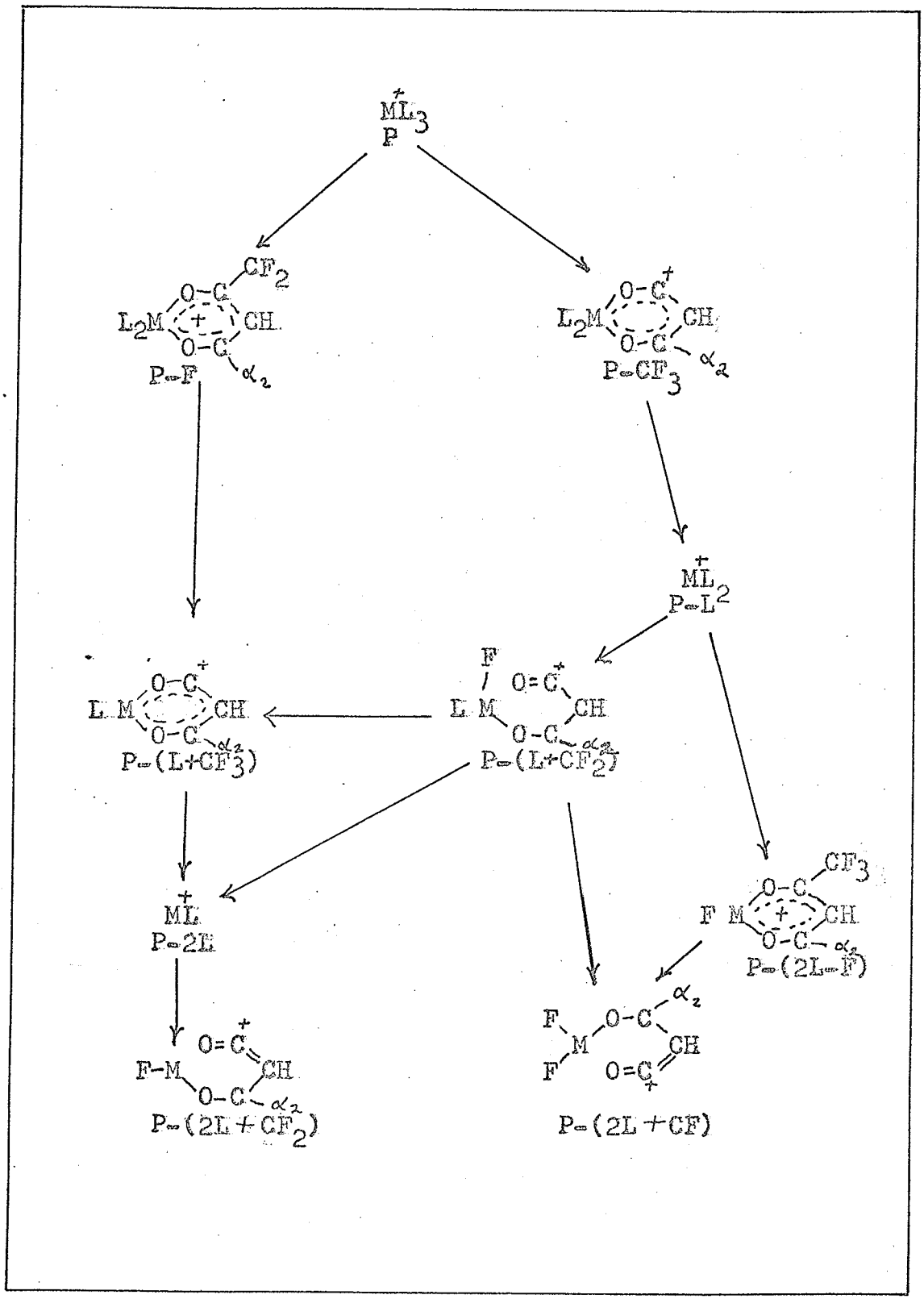
ML3
P
L2M
CH
O-C
CF2
P-F
α2
P-CF3
ML2
P-L2
F
O=C
L M
P-(L+CF3)
P-(L+CF2)
ML
P-2L
F-M
P-(2L+CF2)
CF3
F M
P-(2L-F)
F
P-(2L+CF)

For example, when it is present in the spectrum, the peak corresponding to the loss of a CF_3 radical is always considerably more intense than the corresponding peak due to the loss of a CH_3 radical. In fact, the latter peak is insignificant or undetectable in most of the spectra of the trifluoro compounds presented here. Only in the case of $Zn(tfacac)_2$, in which the appearance potentials of both $(P-CF_3)^+$ and $(P-CH_3)^+$ could be measured, can a direct comparison of the bond dissociation energies in the same molecule be made. The values as seen in the next section are in agreement with the suggestion (see Table 16) that $C-CF_3$ bonds are somewhat weaker than the $C-CH_3$ bonds in these chelates.

A number of rearrangement peaks involving the loss of a CF_2 group with the assumed formation of a metal-fluorine bond are present in the spectra for some of the metals studied. The migration of the fluorine presumably proceeds by a concerted process involving the fission of one of the metal-oxygen bonds followed by a suitable rotation of part of the ligand about the 2,3 C-C bond, bringing one of the fluorines of the CF_3 group close to the metal.

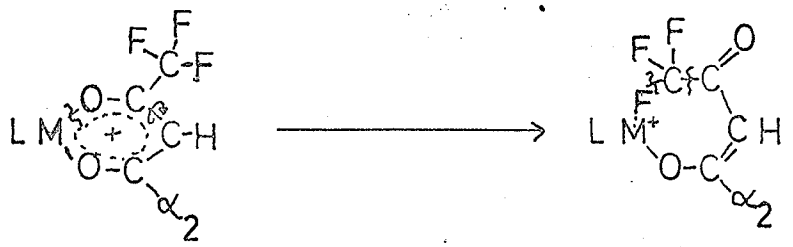

This concerted process would probably be sterically hindered in the tris chelates and thus no $(L_3M\text{-}CF_2)^+$ peaks are recorded. The elimination of the CF_2 species has been well documented recently in the mass spectra of certain organometallic compounds (72,73) and is favored both by the formation of strong M-F bonds, and elimination of the comparatively stable CF_2 species. These peaks are more intense for the hexafluoro compounds than in the trifluoro compounds, because of the greater statistical probability of the processes and also because the other CF_3 group remaining will by its electron withdrawing power stabilize the positive charge on the ring.

Proof of migration of the fluorine to the metal is given by the presence of metastable peaks for the elimination of MF_2 and MF_3 neutral species for $Cr(hfacac)_3$, $Al(hfacac)_3$ and $Fe(tfacac)_3$ as pointed out by Clobes et al. (74).

$Al(hfacac)_3$ also loses another metal containing neutral fragment. The even electron ion $(LAlF{\cdot}OC(CF_3)CHCO)^+$ fragments to lose (LAlFOC·CHCO) as the neutral fragment leaving the CF_3 group with the positive charge.

$Cu(hfacac)_2$ and $Cu(tfacac)_2$ show major peaks for the loss of mass 138. $Zn(hfacac)_2$ the only other compound to lose mass 138 from the molecular ion has only a minor peak at this mass. For $Cu(hfacac)_2$ mass 339 can conceivably be formed by the loss of two CF_3 groups or $CF_3\overset{O}{\overset{\|}{C}}\,CH\overset{O}{\overset{\|}{C}}$, both of mass 138. Using ligand deuterated in the γ position would make the latter fragment mass 139. However in the mass spectrum no loss of mass 139 occurred. Similarly mass 207 could conceivably be accounted for by loss of three CF_3

groups, however using deuterated ligand the fragment lost was of mass 208 rather than 207 as would be found for three CF_3 groups. This suggests that one ring will be removed before the fragmentation of the other ring begins.

Fragmentation of $Cu(tfacac)_2$ is unique. Using $Cu(tfacac)_2$ deuterated in the γ position it was proved that loss of two CF_3 groups or loss of CF_3 CCHC can occur each by means of a two step process. When two CF_3 groups are lost successively this is followed by loss of CCHC to give the ion of mass 147 (non deuterated chelate). In the second process, after the loss of the CF_3 group, a methyl migration occurs, presumably to the metal, with the elimination of CCHC. This ion of mass 231 then loses a $CuCH_3$ neutral radical leaving the positive charge on the ligand.

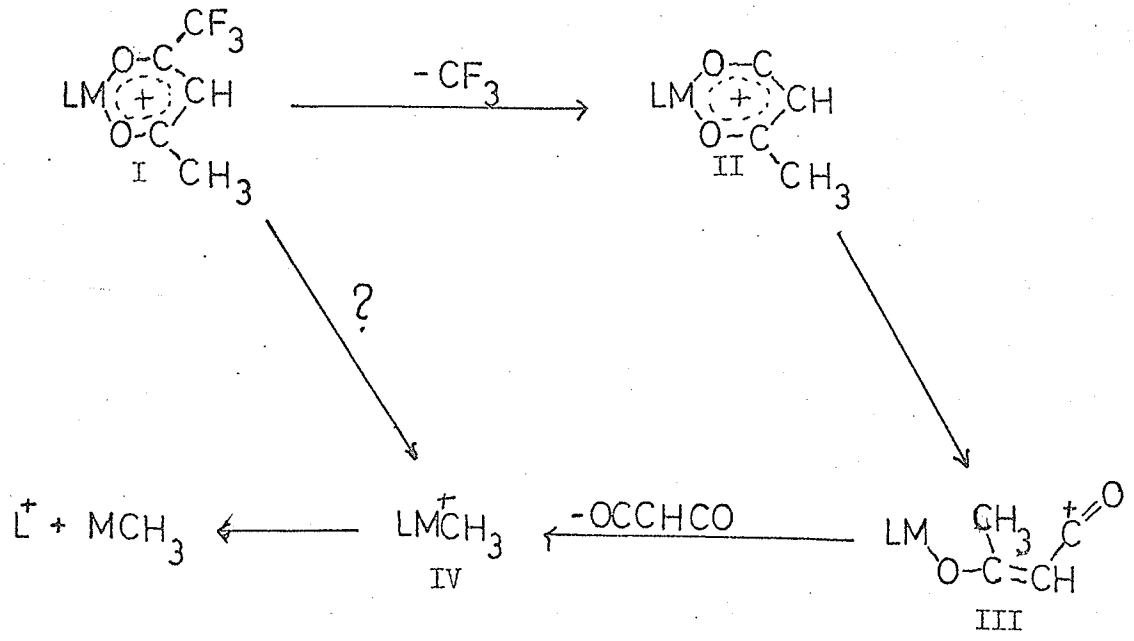

The one step process going from I to IV may be occurring as well, however there is no metastable peak present to verify this process.

2. The Appearance Potentials

As has been seen from the previous series the appearance potentials of the molecular ion depend much more upon the nature of the ligand than upon the nature of the metal. Thus, for all the bis and tris hexafluoroacetylacetonates listed here, Table 16, the appearance potentials lie within the range 9.95 $\pm$ 0.25 volts; while the bis and tris trifluoroacetylacetonates are within the range 9.05 $\pm$ 0.35 volts (Table 16). Replacement of a CH_3 substituent by a CF_3 substituent increases the appearance potential by 0.6 to 1.1 volts. These generalizations are thus consistent with the suggestion that the electron removed on ionization of the molecule comes from an orbital which has mainly ligand character, i.e. a π orbital localized mainly on the ligand. This is in contrast to the ionization of metal carbonyls and cyclopentadienyls in which it was concluded that the electron was removed from an orbital locallized mainly on the metal (75).

In some of the chelates in this series it is possible to measure the energy required to dissociate a $\cdot CF_3$ or $\cdot CH_3$ radical from the molecular ion. The energies required vary widely from compound to compound. In a neutral molecule AB the bond dissociation energy, D(A-B), is the enthalpy change for the process

$$A\text{-}B \rightleftharpoons A^{\cdot} + B^{\cdot} \qquad \Delta H = D(A\text{-}B) \qquad (30)$$

TABLE 16

Appearance potentials of selected ions in the mass spectra of fluorinated acetylacetonates. Ionization chamber temperature 150°. All values are in volts with experimental error of ±0.1 volts unless otherwise stated. Error in values is ± 0.2 volts in most cases.

	P^+	$(P-CF_3)^+$	$(P-CH_3)^+$	$(P-L)^+$	(CF_3)	(CH_3)	(L)	P^+(Lit.)
$Al(hfacac)_3$	9.80	10.7	-	11.2	0.9	-	1.4	10.30[a]
$Cr(hfacac)_3$	10.13±0.05	-	-	14.3±0.1	-	-	4.2	9.97[a]
$Fe(hfacac)_3$	10.21	11.1	-	10.2[c]	0.9	-	0[c]	10.34[a]
$Fe(hfacac)_2$	9.7	13.2±0.2	-	-	3.5	-	-	-
$Cu(hfacac)_2$	9.86±0.05	11.6	-	-	1.7	-	-	-
$Zn(hfacac)_2$	10.07±0.05	11.35	-	15.3±0.2	1.3	-	5.2	-
$Al(tfacac)_3$	9.05	-	-	10.2	-	-	1.15	-
$Cr(tfacac)_3$	9.09±0.05	-	-	11.9±0.1	-	-	2.8	-
$Fe(tfacac)_3$	9.10±0.05	-	-	9.2±0.1[c?]	-	-	0.1[c]	9.38[a]
$Fe(tfacac)_2$	8.75	12.6	-	14.5	-	-	5.75	-
$Cu(tfacac)_2$	9.05	11.5	-	13.1	2.45	-	4.05	-
$Zn(tfacac)_2$	9.40	11.28	11.7	14.6	1.9	2.3	5.2	-
$Al(acac)_3$	7.95±0.05	-	-	9.1±0.2	-	-	1.15	8.27[a]
$Cr(acac)_3$	8.10±0.05	-	-	11.3±0.1	-	-	3.2	7.87[a]
$Fe(acac)_3$	8.45±0.05	-	-	9.4±0.1	-	-	0.95	8.64[a]
$Fe(acac)_2$	8.1±0.05	-	11.7±0.1	13.9±0.1	-	3.6	5.8	-
$Cu(acac)_2$	8.31±0.05	-	10.9±0.1	13.1±0.2	-	2.6	4.8	-

Table 16 Continued

	P^+	$(P-CF_3)^+$	$(P-CH_3)^+$	$(P-L)^+$	$\Delta(CF_3)$	$\Delta(CH_3)$	$\Delta(L)$	P^+ (Lit.)
$Zn(acac)_2$	8.62±0.05	-	10.9±0.1	14.1±0.2	-	2.3	5.5	-
H(hfac)	10.55±0.05	11.2±0.1	-	-	0.6	-	-	10.68[a]
H(tfac)	9.82	10.6±0.2	11.7±0.1	-	0.8	1.9	-	9.96[a]
H(acac)	9.2±0.1	-	10.7±0.1	-	-	1.5	-	8.87[b]

(a) see reference (68)

(b) see reference (3)

(c) May be low because of the possibility of thermal decomposition to the bis chelate in the ion source.

and is given by

$$D(A\text{-}B) = \Delta H_f(A\cdot) + \Delta H_f(B\cdot) - H_f(AB) \qquad (31)$$

The appearance potential of A^+ in the reaction

$$AB + e \longrightarrow A^+ + B + 2e \qquad (32)$$

is related to the heats of formation of the different species by the relation:

$$A.P.(A^+) = \Delta H(A^+) + \Delta H(B) - \Delta H(AB) \qquad (33)$$

If excess energy is small it is possible to write

$$A.P.(A^+) = \Delta H_{reaction} = D(A\text{-}B) + I(A) \qquad (34)$$

In principle, contributions to D(A-B) can be divided into σ- and π-bond energy terms (76), but the situation is actually more complicated than this. For example, when the A-B bond is breaking, adjustments of the other bonds in the product radicals may occur. This contribution has been called the "reorganizational energy". To avoid this difficulty, the assumption is made that the σ-bond term in D(A-B) is identical to that in an analogous system which involves no π-conjugation, and the difference between the D values for the two systems, is associated mainly with the π-energies as the bond is broken. The term "stabilization" energy is used instead of "resonance" or "delocalization" energy.

The stabilization energy of the $\cdot CF_3$ radical is of importance. The bond dissociation energies are : $D(CF_3\text{-}CF_3)$ = 86 Kcal/mole, $D(CH_3\text{-}CH_3)$

= 88 kcal/mole, $D(CF_3\text{-}H)$ = 106 kcal/mole, $D(CH_3\text{-}H)$ = 104 kcal/mole. These values suggest that the energy required to dissociate a $\cdot CH_3$ or $\cdot CF_3$ radical from the chelate ring in the neutral metal chelates studied should be about 85-90 kcal/mole, i.e. slightly less than 4eV/molecule. The energies required to dissociate these radicals from the parent molecular ions are, however, always lower than this, usually much lower, indicating considerably higher stabilization energies for the fragment ions than for the parent ion. These dissociation energies are expressed as $\Delta(CF_3)$ and $\Delta(CH_3)$ in Table 16. The smaller the value of $\Delta(CF_3)$ and $\Delta(CH_3)$ the greater is the relative stabilization energy of the fragment ion. An explanation for the variations in $\Delta(CF_3)$ and $\Delta(CH_3)$ must be sought in the structures of the molecular and fragment ions. Upon ionization of the molecule an electron is removed presumably from the π-system of one of the chelate rings to give I below. Homolytic dissociation of α_1 from the ring will leave an unpaired electron on the ring carbon atom.

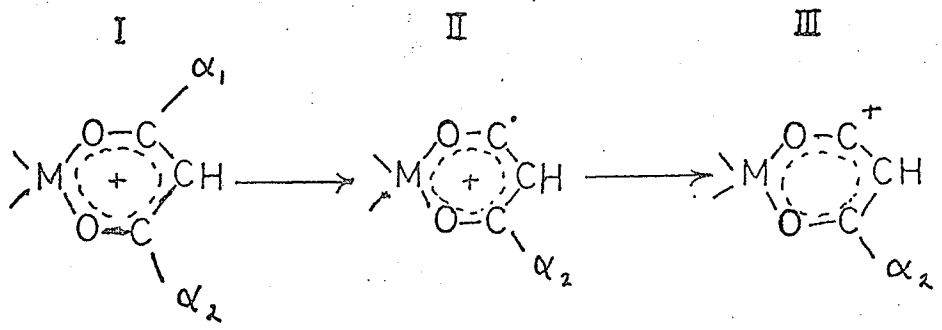

which may then transfer to a partially empty delocalized bonding π molecular orbital on the chelate ring to give III. This should give considerable π stabilization to the fragment ion with respect to the molecular ion. Furthermore, little structural or geometrical rearrangement should accompany this process. The metal ion should have little effect on the stabilization of III, and thus we assume that the large variations in $\Delta(CF_3)$ which are observed are due to the different stabilizations of the molecular ion. The smallest $\Delta(CF_3)$ are observed with Al(III), Fe(III) and Zn(II) and the largest $\Delta(CF_3)$ with Fe(II). For the Cr(III) chelates no values could be obtained due to the low relative intensities of the $(L_3M\text{-}CF_3)^+$ and $(L_3M\text{-}CH_3)^+$ peaks. This probably means that the energy required to dissociate a CF_3 or CH_3 group from the molecular ion is high ($\Delta(CF_3)$, $\Delta(CH_3)$ are high) indicating a large π-stabilization of the molecular ion.

It is proposed that the stabilization of the molecular ion by the metals is accomplished via π donation from the metal d_ϵ orbitals to the partially empty ligand π orbital. For the Al(III) chelates, the molecular ion cannot be stabilized in this way and the process I $\longrightarrow$ III goes more readily. For Cr(III), stabilization of the molecular ion can occur, which should make the process I $\longrightarrow$ III more difficult. In the trivalent metals of the first transition series the amount of metal-to-ligand charge transfer decreases in the sequence $Ti^{III} \longrightarrow Fe^{III}$ according to the work reported by Eaton (49). Considering that Cr(III) is d_ϵ^3 and Fe(III) is $d_\epsilon^3 d_\gamma^2$ if the ligand field splitting lowers d_ϵ in Fe(III) relative to Cr(III)

than transfer of charge to the ligand would be more difficult for Fe(III) than for Cr(III), via the d_ϵ orbital. The d_ϵ orbitals have suitable symmetry for the charge transfer while the d_γ orbitals do not. Since no peaks were observed for loss of CF_3 for the Cr(III) complexes presumably ΔCF_3 would be large possibly in the order of ΔL which is 4.2v for $Cr(hfacac)_3$. Thus the data appears to support the greater stabilization of Cr(III) than Fe(III).

For the Fe(II) chelates the high value of $\Delta (CF_3)$ suggests stabilization of the molecular ion, I, presumably by the electron transfer to the ligand. This would be in agreement with the well-known ready conversion of Fe(II) to Fe(III). Oxidation of Zn(II) and Cu(II) occurs much less readily and in agreement with this, much lower values of $\Delta(CF_3)$ and $\Delta(CH_3)$ are observed. As might be expected it seems electron transfer from metal to ligand is slightly easier for Cu(II) than for Zn(II).

Although the data is rather limited it appears that, when the electronegative CF_3 group remains attached to the chelate ring in the fragment ion, greater stabilization of the fragment ion results than when the CH_3 group remains. For example, $\Delta(CF_3)$ is 1.7 volts for $Cu(hfacac)_2$ and 2.45 volts for $Cu(tfacac)_2$; it is 1.3 volts for $Zn(hfacac)_2$ and 1.9 volts for $Zn(tfacac)_2$; $\Delta (CH_3)$ is 2.3 volts for both $Zn(tfacac)_2$ and $Zn(acac)_2$. It seems that electronegative groups on the ring enhance transfer of the unpaired electron from the ring carbon of II to the π system. This observation is consistent with the arguments presented in the inter-

pretation of the mass spectra of the substituted chromium acetylacetonates discussed in section VIII (D).

It is difficult to assess the energies involved in the dissociation of a ligand radical from the molecular ion. Apart from electronic reorganization, there may be, and probably are in many cases, structural rearrangements, and, for small metal atoms, steric relaxations to consider. However for the compounds studied here we see that it is more difficult to remove a ligand from the molecular ion of a bis chelate than from a tris chelate. An interesting feature of the Δ L values are the extremely small values for the Fe^{III} acetylacetonates. They may however be larger than the values obtained in this study since some decomposition was evident in the spectra, with the value of the appearance potential of the $Fe^{III}L_2^+$ species probably being affected somewhat by $Fe^{II}L_2^+$.

D. Substituted Acetylacetonates of Trivalent Chromium

In the series of acetylacetonates of the trivalent metals of the first transition series it was concluded that valency changes of the metal account for the trends in the mass spectra. In the mass spectra of Ti $(acac)_3$ and $V(acac)_3$ there were found species evidently characteristic of the +IV valency state. On the other hand, in the mass spectra of $Cr(acac)_3$, $Mn(acac)_3$, $Fe(acac)_3$ and $Co(acac)_3$ a general increase was seen in intensity of peaks believed to be characteristic of the +II valency state. $Cr(acac)_3$ did not appear to exhibit any peaks characteristic of the +IV state and only very small peaks in evidence of the +II state.

A number of substituted chromium acetylacetonates (see Table 17) were studied to see the effects of electron withdrawing groups and electron donating groups on the fragmentation patterns and appearance potentials of the complex.

1. The Mass Spectra

As for the other series previously discussed the mass spectra can be rationalized in terms of preferred formation of even-electron ions and elimination of odd-electron neutral species.

Mechanisms to account for the important peaks in most of these spectra are summarized in Figure 17. The first step in the electron impact process, as discussed earlier, is the removal of an electron from the π system to give I, the odd electron ion. Homolytic fission of the C-α or C-γ bonds (with transfer of one electron of the bond to the π-system to give species such as II or III) yields an even-electron ion and a neutral radical. Only in $Cr(Iacac)_3$, as seen in Table 18, does this process give rise to a large peak, although small peaks are present in the $Cr(Bracac)_3$ and $Cr(hfacac)_3$ spectra. Such a process would be expected to be significant when the C-α or C-γ bonds are weak, or when there are no other electronegative groups on the ring to increase the positive charge on the ring. The former appears to be important for the present series of γ-substituted acetylacetonates where the intensity of the peak due to III is consistent with the relative bond strengths $C\text{-}I < C\text{-}Br < C\text{-}Cl \leq C\text{-}NO_2$ in aromatic compounds, but not consistent with the order $C\text{-}NO_2 < C\text{-}I < C\text{-}Br < C\text{-}Cl$ in aliphatic compounds. The second factor is probably of im-

TABLE 17

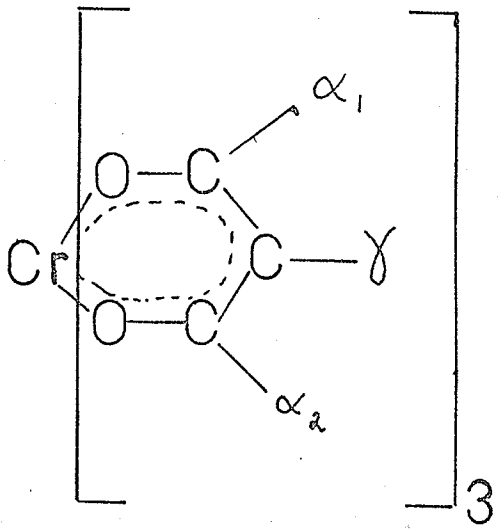

Designation	α_1	α_2	Y
$Cr(acac)_3$	CH_3	CH_3	H
$Cr(CH_3acac)_3$	CH_3	CH_3	CH_3
$Cr(Clacac)_3$	CH_3	CH_3	Cl
$Cr(Bracac)_3$	CH_3	CH_3	Br
$Cr(Iacac)_3$	CH_3	CH_3	I
$Cr(NO_2acac)_3$	CH_3	CH_3	NO_2
$Cr(tfacac)_3$	CF_3	CH_3	H
$Cr(hfacac)_3$	CF_3	CF_3	H

Figure 17

Schematic diagram showing some of the fragmentation processes possible for the substituted chromium acetylacetonates.

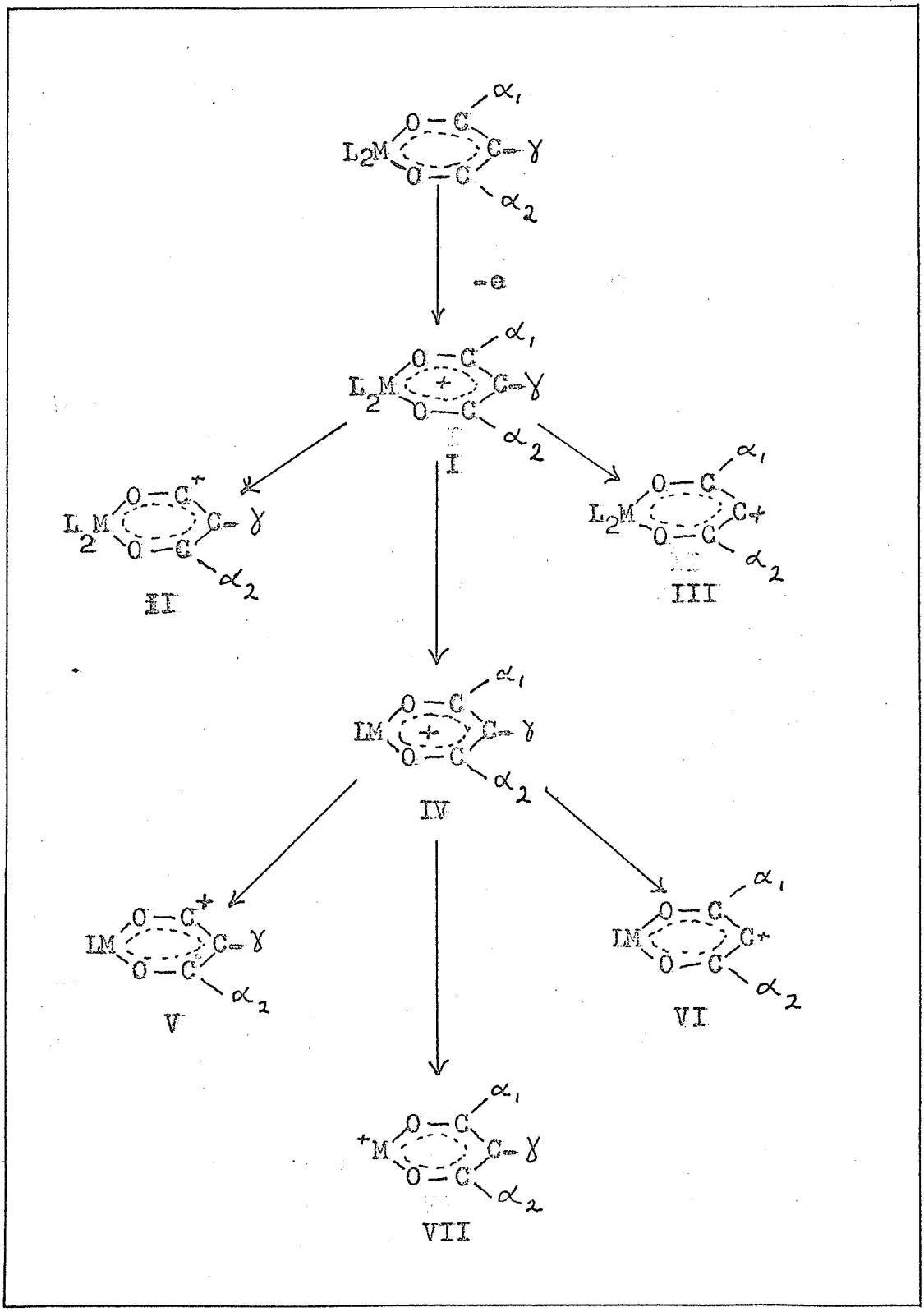
-e
I
II
III
IV
V
VI
VII

TABLE 18

Relative intensities in the mass spectra of substituted acetylacetonates of chromium (only peaks greater than 1% of base peak). (L = ligand; α and γ as in Table 17. Other symbols are chemical symbols.)

Ion	$Cr(acac)_3$	$Cr(CH_3acac)_3$	$Cr(Clacac)_3$	$Cr(Bracac)_3$	$Cr(Iacac)_3$	$Cr(tfacac)_3$	$Cr(hfacac)_3$	$Cr(NO_2acac)_3$
L_3Cr	23	24	18	32	16	24	20	23
L_3Cr-O								1
L_3Cr-F				1		2	4	
$L_3Cr-\gamma$					22			
$L_3Cr-\alpha_1$							6	
L_2CrO								100
L_2Cr	100	100	100	100	54	100	100	8
$L_2Cr-\gamma$				5	100			
$L_2Cr-\alpha_1$	5	1				21	3	
L_2Cr-CF_2						8	21	
$LCr\gamma$			23	17				
LCrF						40	70	
$LCrF-CF_2$						25	23	
LCrO.OH								24
LCrOH	12	9	3	4				
LCrO			1	2				27

Table 18 Continued

Ion	$Cr(acac)_3$	$Cr(CH_3acac)_3$	$Cr(Clacac)_3$	$Cr(Bracac)_3$	$Cr(Iacac)_3$	$Cr(tfacac)_3$	$Cr(hfacac)_3$	$Cr(NO_2acac)_3$
LCr	45	22	11	22	17	30	64	2
$LCr-\alpha_1$	4					23	38	
$LCr-CF_2$						40	35	
$LCr-H_2O$	3							
$Cr\gamma$			1					
Cr	2							

In addition there are several small peaks at masses less than LCr^+ to which no structural significance can be assigned. These peaks may arise from fragmentation of the ligand or from background. Mass 43 is often very abundant and is assigned to CH_3CO^+.

portance in explaining the non-existence of II in the spectrum of Cr $(tfacac)_3$, whereas there is a small peak in the spectrum of $Cr(hfacac)_3$. The CF_3 group will increase the positive charge on the ring more than will a CH_3 group.

An alternative process to the above is the loss of a ligand to give ions such as IV. This process is preferred in nearly all these compounds. An exception is the nitro-substituted chelate which exhibits different behavior from the others, and will be discussed separately later. The precursor of IV could be II or III but metastable peaks (Table 19) indicate that IV will usually be formed on decomposition of I. There appears to be no significant trend in the intensities of these peaks.

The even-electron ion IV can decompose to either V or VI. We postulate that this process includes both (a) the breaking of a C-α or C-γ bond, and (b) transfer of an electron from ligand to metal. The electron transfer seems reasonable in this reaction since in the series of acetylacetonates of the trivalent metals the intensity of the peak due to species V increased in the same order as the normal ease of reduction of the central metal atom. Part (a) of the process would be favored by weak C-α or C-γ bonds, whereas part (b) would be hindered by electron withdrawing substituents on the same ring because the ligand electrons would be more tightly held, even though the chromium atom becomes more electronegative itself due to electron withdrawing substituents on the other ring. The relative intensities of the peaks due to VI in the

TABLE 19

Calculated Positions of Metastable Peaks and the Related Transitions Observed in the Mass Spectra of Some Chromium Acetylacetonates.

	acac	CH_3acac	Clacac	Bracac	NO_2acac	tfacac	hfacac
$(L_3Cr)^+ \longrightarrow (L_2Cr)^+$	179.1	199.	224.2	286.0			322.7
$(L_3Cr)^+ \longrightarrow (LCr)^+$						82.2	
$(L_3Cr)^+ \longrightarrow (L_2CrO)^+$					261.9		
$(L_3Cr)^+ \longrightarrow (L_3Cr\text{-}\alpha)^+$							542.1
$(L_3Cr\text{-}F)^+ \longrightarrow (L_3Cr\text{-}\alpha)^+$							557.8
$(L_3Cr\text{-}F)^+ \longrightarrow (L_2Cr\text{-}\alpha)^+$							241.0
$(L_3Cr\text{-}CH_3)^+ \longrightarrow (LCr)^+$						84.7	
$(L_3Cr\text{-}\alpha)^+ \longrightarrow (L_2Cr)^+$							359.5
$(L_2Cr)^+ \longrightarrow (LCrOH)^+$			128.3				
$(L_2Cr)^+ \longrightarrow (LCr)^+$			107.6				
$(L_2Cr)^+ \longrightarrow (LCr\gamma)^+$			152.2				
$(L_2Cr^+)^+ \longrightarrow (L_2Cr\text{-}\alpha)^+$	220.9						
$(L_2Cr)^+ \longrightarrow (L_2Cr\text{-}CF_2)^+$							371.4
$(L_2Cr)^+ \longrightarrow (CrFL)^+$							165.8
$(L_2Cr\text{-}CF_2)^+ \longrightarrow (L_2Cr\text{-}\alpha)^+$						271.2	378.9
$(L_2Cr\text{-}CF_2)^+ \longrightarrow (LCr)^+$						136.4	
$(L_2CrO)^+ \longrightarrow (L_2Cr)^+$					324.7		
$(L_2CrO)^+ \longrightarrow (LCrO)^+$					126.3		

Table 19 Continued

	acac	CH_3acac	Clacac	Bracac	NO_2acac	tfacac	hfacac
$(LCr)^+ \longrightarrow (LCr)^+$				170.3			
$(LCrF)^+ \longrightarrow (LCrF\text{-}CF_2)^+$						135.2	187.0
$(LCrF\text{-}CF_2)^+ \longrightarrow (C_4HF_2O_2)^+$							62.1
$(L_2Cr\text{-}CF_3)^+ \longrightarrow (LCr)^+$							169.0
$(LCr)^+ \longrightarrow (LCr\text{-}CF_2)^+$							168.7

γ-substituted chromium chelates again reflect the strengths of the C-γ bonds. However, in the γ-substituted compounds, only $Cr(acac)_3$ has a significant peak due to V which indicates that part (b) of the process is difficult when electron withdrawing groups are present on the ring. This view is supported by the relative intensities of this peak in the $Cr(tfacac)_3$ and $Cr(hfacac)_3$ spectra (i.e. the peak is larger for $Cr(tfacac)_3$).

The even-electron ion IV can also fragment to the ion VII. Again, we postulate a valency change for this reaction because the intensity of this peak in the metal acetylacetonates increases with ease of reduction of the metal atom. In this reaction the strength of the metal-oxygen bonds, and the ease of transfer of an electron from ring to metal again appear to be important. There is considerable evidence from stability constant data (77,78), polarographic half-wave potentials (79-82), and infrared spectra (48,54), that electron withdrawing substituents decrease the metal-oxygen bond strength. On this basis, $Cr(acac)_3$ would be expected to have a smaller VII peak than the other chromium chelates (except for $Cr(CH_3acac)_3$) whereas it is one of the largest. Again, we postulate that electron withdrawing substituents on the ring hinder electron transfer to the metal, making the reaction IV $\longrightarrow$ VII more difficult.

There are a number of noteworthy rearrangement peaks, involving migration of halogen atoms, in the spectra. The site to which the halogen migrates is not known but is presumably the metal atom. Probably the driving force for the reaction is the strength of the metal-

halogen bond. A suggested mechanism for the process involves fission of one Cr-O bond, followed by a suitable rotation of part of the ligand about the 2,3 C-C bond, which brings the halogen atom close to the metal as in VIII and IX or X and XI.

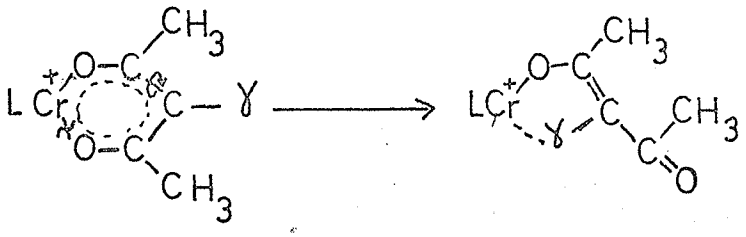

VIII IX

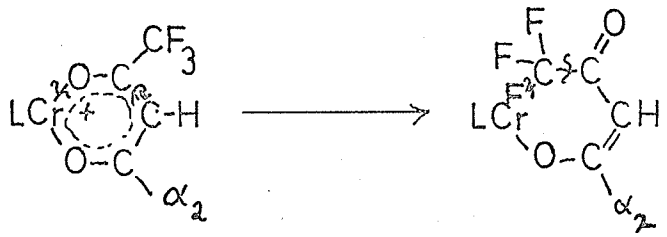

X XI

In a presumed concerted process the metal halogen bond is formed and a neutral species is eliminated. The neutral species is either the rest of the ligand moiety, or in the CF_3 substituted chelates is CF_2. The peaks which may arise in this way are $(L_2Cr\text{-}CF_2)^+$, $LCr\gamma^+$, $LCrF^+$, $(LCr\text{-}CF_2)^+$ and possibly $Cr\gamma^+$. The process

does not seem to occur readily until one ligand has already been lost. This may be due to steric hindrance in the parent molecule ion. The metastable ions seen for most of these processes is considered proof of the presence (see Table 19) of these processes.

Further fragmentation of the chelate to species lighter than VII was not extensive in any of the chelates examined here. A peak at M/e = 43 assigned to CH_3CO^+, was often the only peak which was obviously distinguishable from background peaks.

The NO_2 substituted chelate deserves some separate discussion. A distinctive feature of the spectrum is the relatively great abundance of oxy-ions (the base peak is assigned to $CrO(NO_2acac)^+_2$). The origin of the oxygen atom bonded to the chromium atom has not been confirmed but it seems reasonable to assume that it is not from the NO_2 group. Migration of an oxygen atom from the NO_2 group to the metal would require a rearrangement process similar to the one described above for the halogenated chelates. In the molecular ion this would probably be sterically hindered.

The NO_2 group is a powerful electron withdrawing group; the resonance effect directing the positive charge to the chromium atom. The positive charge on the metal could be reduced by the resonance effect by the formation of chromium-oxygen double bonds, in for example $L_2Cr = O^+$ and $LCr = O^+$. Another prominent oxy species is $LOCrOH^+$. The only other ions worthy of comment in this spectrum are $LO_2CrOCCH_3^+$ and

$LOCrOCCH_3^+$, which are of low abundance and are possibly formed by elimination of $CH_3C \equiv CNO_2$ from L_2CrO^+ and L_2Cr^+, respectively.

Very small $LCrO^+$ peaks are also observed in the $Cr(Bracac)_3$ and $Cr(Clacac)_3$ spectra. For these compounds the resonance effect would be expected to be smaller.

It is perhaps surprising that there are no major peaks due to loss of NO_2 as in aromatic nitro compounds. This is presumably because there are other processes which can occur much more easily here, whereas this is usually not the case in an organic aromatic compound.

2. The Appearance Potentials

All of the chelates gave abundant molecular ions and ions for loss of a ligand (except for $Cr(NO_2acac)_3$ in which the peak was however large enough) for a reasonably accurate measurement of their appearance potentials. The appearance potentials for these two ion types are shown in Table 20.

There has been considerable debate about the supposed aromaticity of the chelate ring in the acetylacetonates. While the theoretical grounds for a truly aromatic ring are not convincing, these chelates do undergo certain reactions characteristic of aromatic compounds, such as direct halogenation and nitration (83,84). It seems worthwhile, therefore, to discuss the variations in appearance potentials of the substituted chromium chelates in terms of ionization by removal of an electron from a quasi-aromatic ring and compare these variations to those in substituted aromatic compounds.

TABLE 20

Appearance potentials and spectral shifts (39) of substituted chromium acetylacetonates.

Compound	$(A.P.)L_3Cr^+$ ±0.05 volts	$(A.P.)L_2Cr^+$ ±0.10 volts	$\Delta\bar{\nu}$, cm^{-1} (relative to $Cr(acac)_3$) Band B	Band C	$\bar{\nu}_{max}$, cm^{-1} $^2E - {}^4A_2$
$Cr(acac)_3$	8.11	11.3	0	0	12,800
$Cr(CH_3acac)_3$	7.81	10.7	-2100	-1300	12,310
$Cr(Clacac)_3$	8.16	11.1	-2300	-1400	12,420
$Cr(Bracac)_3$	8.05	11.0	-2300	-1600	12,390
$Cr(Iacac)_3$	8.03	10.8	-3100	-2200	12,340
$Cr(NO_2acac)_3$	8.63	11.6	+1300	+ 500	12,940
$Cr(tfacac)_3$	9.09	11.9	- 300?	- 700	12,340
$Cr(hfacac)_3$	10.13	14.3	-	- 700	-

Bralsford, Harris and Price (51) have discussed substituent effects on the electronic spectra and ionization potentials of electrons in chromophoric groups, particularly with the regard to the effects of fluorine. The two major contributions are (a) inductive effects, which are important in changing the binding of electrons in the ground state, and (b) resonance effects which stabilize the excited state or molecular ion. Thus we may consider the ionization of a π-electron of the chelate ring in terms of these effects.

The α-substituents in these chromium complexes are either CH_3 or CF_3. For CF_3 only the inductive effect is likely to be of importance. In the γ-substituted complexes both inductive and resonance effects will operate and instead of trying to evaluate the magnitude of these two effects on the π-system it is simpler to compare variations in appearance potentials with those in suitable model aromatic compounds. The γ-substituents are para to the chromium atom but ortho to the methyl groups. In Table 21 the appearance potentials of some substituted benzenes and toluenes are given, so that they can be directly compared with those of the chromium chelates.

The substitution of CF_3 for CH_3 in toluene raises the ionization potential by 0.86 volts from 8.82 to 9.68 volts. Substitution of CF_3 for CH_3 in the α position of the chelate ring causes successive rises of the appearance potential of similar magnitude in the sequence $Cr(acac)_3$, $Cr(tfacac)_3$, $Cr(hfacac)_3$. Although for the γ-substituted chelates the results do not correlate exactly with substituted aromatic

TABLE 21

Ionization potentials of substituted benzene and toluenes.

Substituent X	Ionization potential, volts C_6H_5X	$o\text{-}CH_3C_6H_4X$	$p\text{-}CH_3C_6H_4X$
H	9.245	8.82	8.82
I	8.73	8.62	8.50
Br	8.98	8.78	8.67
Cl	9.07	8.83	8.69
NO_2	9.92	-	9.82
CF_3	9.68	-	-

All values are from photoionization except $p\text{-}CH_3C_6H_4NO_2$ (electron impact). All values from reference 3 except $C_6H_5CF_3$ (reference 51).

compounds the order of magnitude of the variations is certainly similar. For example, the substitution of CH_3 for H reduces the appearance potential from 8.11 volts for $Cr(acac)_3$ to 7.81 volts for $Cr(CH_3acac)_3$ and from 9.245 volts for benzene to 8.82 volts for toluene. Comparison of Tables 20 and 21 shows a similar parallelism for the two groups of compounds.

An exact correlation would not be expected since the presence of the chromium (III) and oxygen atoms in the chelate ring means that benzenoid aromaticity cannot be assumed. The appearance potential of the nitro-substituted chelate is perhaps a little lower than expected. Possibly this is because the nitro-group may be forced out of the plane of the chelate ring by the adjacent methyl groups (85). This probably reduces the effectiveness of this electron withdrawing group via the resonance effect. On the other hand, the electric moment for the $C-NO_2$ group (μ = 3.99D in $Cr(NO_2acac)_3$) is nearly identical to the value $C_{arom}-NO_2$ (μ = 4.0D) (86). It seems, therefore, that the experimental results are not inconsistent with the ionization of a π-electron localized mainly on a ligand.

An alternative to the above suggestion is to consider the ionization by removal of an electron from an orbital locallized mainly on the chromium atom. It is difficult to estimate the magnitude of the inductive and resonance effects of substituents on the chelate ring on the electron density at the chromium atom. It seems reasonable to assume however that it would be a function of the appropriate Hammett σ con-

stants for the various substituents. For the substituents para to the chromium atom representative values (87) taken are CH_3 = -0.170, Cl = 0.227, Br = 0.232, I = 0.276 and NO_2 = 0.778. For the substituent meta to the chromium atom an appropriate value (87) would be CF_3 = 0.43. Consequently, the trend in the appearance potentials should be $Cr(CH_3acac)_3 < Cr(acac)_3 < Cr(Clacac)_3 \approx Cr(Bracac)_3 < Cr(Iacac)_3 < Cr(tfacac)_3 < Cr(NO_2acac)_3 < Cr(hfacac)_3$ which differs from the observed order. It seems that the ionized electron is not removed from an orbital localized mainly on the chromium atom, although in view of the assumptions involved, the evidence must be taken as suggestive rather than conclusive.

On the basis of substituent effects De Armond and Forster (39) have made assignments in the UV and visible spectra of these chelates. The spectral shifts, relative to the acetylacetonate, quoted by them for the B and C bands, and the d-d bands were assigned to π-π^* transitions. There appears to be no simple correlation of the spectral shifts with the measured appearance potentials. This is not surprising since it has been pointed out (51) that it is a much more difficult task to assess the contribution of the inductive and resonance effects to an excited state of a molecule than to the ground state, although inductive effects are relatively smaller in the lower than in the more highly excited states. In addition, there is no general agreement as to the assignment of the observed bands.

In summary we see that in this series there is a general increase in the appearance potentials on addition of electron withdrawing substituents to the ring. The addition of electron withdrawing groups should weaken the Cr-O bond and increase the electronegativity of the chromium atom. Barnum's calculations (36) indicate that as the electronegativity of the central atom increases, the highest energy d_ϵ orbitals increase in energy whereas the π_3 orbitals decrease in energy. This trend then provides further evidence for the postulate that the electron is removed from a π orbital.

E. β-diketonates of Copper II

1. The Mass Spectra

In this series (see Table 22) it is evident that the fragmentation processes depend quite largely on the substituents on the chelate ring (see Table 23). Figure 18 illustrates schematically the fragment ions observed for these β-diketonates with suggested modes of decomposition. Each mode of fragmentation is supported by the presence of a metastable peak in at least one compound. The metastable peaks observed are recorded in Table 24. Steric effects, C-α bond strengths and electron withdrawing power of the substituents can be seen to be the determining factors for peak intensities.

As has been proposed for the other series, the first step in the electron impact is the removal of an electron from the π system to give an odd electron ion, $Cu^{II}L_2^+$.

TABLE 22

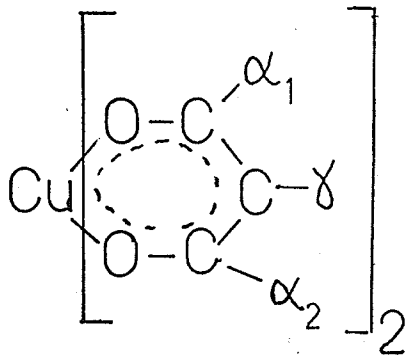

	α_2	γ	α_1
1.	Ph	H	CH_3
2.		H	CF_3
3.	Ph	H	CF_3
4.		H	CF_3
5.	Ph	H	Ph
6.		H	CF_3
7.	CH_3	Ph	CH_3
8.	CH_3	H	CH_3
9.	CH_3	CH_3	CH_3
10.	CF_3	H	CF_3
11.	CH_3	H	CF_3

12. and Cu(acac, hfacac) a mixed ligand complex

Relative intensities in the mass spectra of some Cu β-diketonates at an electron energy of 50 V and an ionization chamber temperature of 150°C.

	$\alpha_2\gamma\alpha_1$ $(PhHCH_3)_2$	$\alpha_2\gamma\alpha_1$	$\alpha_2\gamma\alpha_1$ ϕHCF_3	$\alpha_2\gamma\alpha_1$	$\alpha\gamma\alpha$ $\phi H\phi$	$\alpha_2\gamma\alpha_1$	$\alpha_2\gamma\alpha_1$ $CH_3\phi CH_3$	$\alpha_2\gamma\alpha_1$ CH_3HCH_3	$\alpha_2\gamma\alpha_1$ $CH_3CH_3CH_3$	$\alpha_2\gamma\alpha_1$ CF_3HCF_3	$\alpha_1\gamma\alpha_2$ CF_3HCH_3	acachfacac	
L_2Cu	100	100	100	100	88.5	73.2	62.1	47.7	26.1	9.5	5.1	21.6	
P-1							17.4						
L_2Cu-α_1	11.2	41.9	31.3	35.4		8.9				23.7	10.6	5.1[a]	
P-18	6	4.7			10.3								
L_2Cu-α_2											1.2	13.1[b]	
L_2Cu-$COCH_2$								34.6			8		
L_2Cu-COF		3.9	5.3	4.5		3.9				22.8	8		
L_2Cu-2α	4.8								44.8	1.5	[illegible]	7.5[c]	1.7[d]
L_2Cu-138		26.0	27.8	45.0		11.1					27.0		
P-(L-1)	30.2	8.0	14.4	8.6		61.7	100	70.0					
LCu	25.6	10.6	6.9	6.1		6.1	20	94.4	38.5	1.5	8.2	73[e]	
P-(L+1)	34.5	13.6	13.4	18.5	100	100	15.8		40.1				
P-(L+2)							8.3		100				
LCu-α_1	27.5	75.5	30.4	75.6		56.9	71.4	100	35.2	100	100	100[a]	
LCu-α_2	25.2										10.0		
(CuL-1)-α					20.7			20					
(CuL+1)-2a							13.6	11.8	8.0				
$Cu\alpha_2$	14.4		12.2	11.4		35.8							
Cu(OC-CH)										11.0	18.4		
$CuOC-CH_2$											59.1		
Cu(63)	10		12.9	9		11.1	8.3		20.7	82	44.4	70	

a) loss of CH_3 b) loss of CF_3 c) loss of $2(CF_3)$ d) loss of $2(CH_3)$ e) loss of hfacac

Figure 18

Some suggested decomposition pathways for the formation of ions in the mass spectra of the copper β-diketonates.

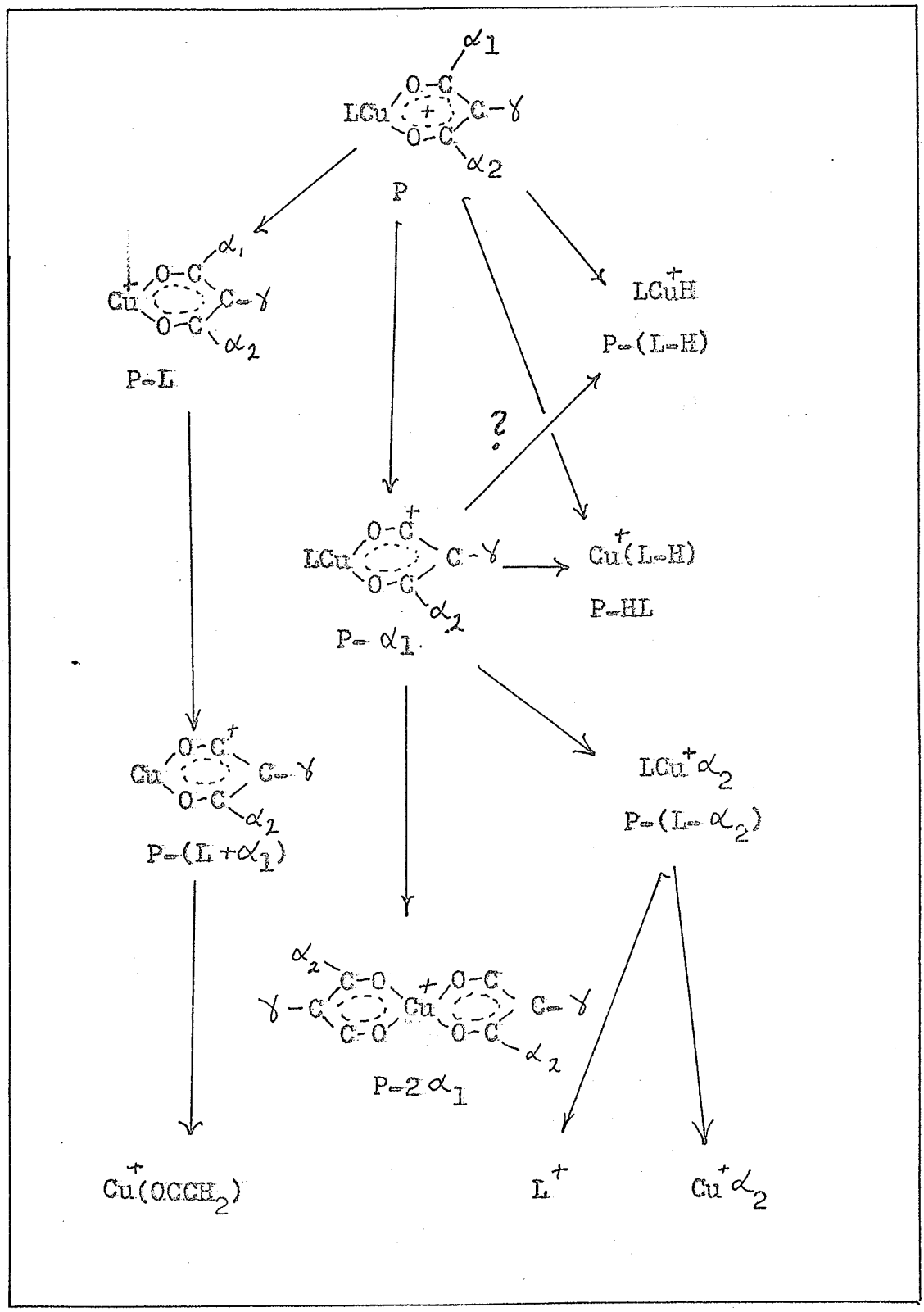
P
P-L
LCuH+
P-(L-H)
?
P-α1
Cu+(L-H)
P-HL
P-(L+α1)
LCu+α2
P-(L-α2)
P-2α1
Cu+(OCCH2)
L+
Cu+α2

TABLE 24

Calculated Positions of Metastable Peaks and Related Transitions seen in the Mass Spectra of the Copper-β-diketonates.

	$\alpha_1\gamma\alpha_1$ $PhHCH_3$	$\square HCH_3$	$PhHCF_3$	$\square HCF_3$	PhHPh	CH_3PhCH_3	$\bigcirc\!\!\!\!\bigcirc HCF_3$	CH_3HCH_3	$CH_3CH_3CH_3$	CF_3HCF_3	$\alpha_1\gamma\alpha_1$ CH_3HCF_3
$(CuL_2)^+ \longrightarrow (CuL)^+$	130.3		156.8	159.7							
$(CuL_2)^+ \longrightarrow (Cu(L+H))^+$						138.3	182.5				
$(CuL_2)^+ \longrightarrow (CuL_2-47)^+$		365.9			159.6						
$(CuL_2)^+ \longrightarrow (CuL_2-42)^+$								183.8			289.8
$(CuL_2)^+ \longrightarrow (CuL_2-\alpha_1)^+$				376.4						349	
$(CuL_2)^+ \longrightarrow (CuL_2-H_2O)^+$	349.8	437.7			473.6						
$(CuL_2-F)^+ \longrightarrow (CuL_2-CF_3)^+$										363.5	
$(CuL_2-\alpha_1)^+ \longrightarrow (CuL_2-2\alpha_1)^+$		277.8	297.2	308.9				216.9		281.7	177.9
$(CuL_2-\alpha_1)^+ \longrightarrow (CuL)^+$								106.7			
$(CuL_2-138)^+ \longrightarrow (CuL-CF_3)^+$											93.6
$(CuL_2-2\alpha_1)^+ \longrightarrow (LCu-\alpha_1)^+$				126.0						119.2	
$(CuL_2-2\alpha_1)^+ \longrightarrow (LCu)^+$								113.6			
$(CuL_2-2\alpha_1)^+ \longrightarrow (LCu-2\alpha_1)^+$								93.6			
$(LCu\alpha_2)^+ \longrightarrow L^+$							154.3				101.3
$(CuL)^+ \longrightarrow (CuL-\alpha_1)^+$			157.1					133.4			
$(CuL-\alpha)^+ \longrightarrow (Cu)^+$									147.3	19.8	
$(CuL-\alpha)^+ \longrightarrow (CuOCCH_2)^+$											75.0
$(CuL-H)^+ \longrightarrow (CuL-\alpha_1)^+$						209.8					

For all but the dibenzoyl methane complex (compound 5 in Table 22) the loss, from the molecular ion, of odd-electron neutral fragments, such as $\alpha_1\cdot$ or L·, is observed to occur. This results in the formation of an even-electron fragment ion. In the copper complexes, as further fragmentation occurs by loss of odd-electron neutral radicals an electron can be readily transferred from a ligand orbital to a metal orbital. This preserves the even-electron character of the resulting fragment ion. Thus most of the copper complexes very readily lose two successive odd-electron fragments as is especially seen for the fluorinated complexes.

As seen from Table 23 the presence of aromatic groups in an α-position on the chelate ring tends to stabilize the molecular ion, i.e. the molecular ion represents a higher percentage of the total ion current. The possible mechanism for the stabilization is the π-donation of electrons from the aromatic group to the π-system (in contrast to σ-donation of CH_3 groups and σ-withdrawl of CF_3 groups). This enhances the transfer of an electron from the ligand to the metal thereby creating an even-electron ion. Even-electron ions are relatively more stable as compared to odd-electron ions since fragmentation to lose an even-electron species will be preferred over loss of an odd-electron fragment, even though this requires multiple bond cleavage and a substantial expenditure of energy. Support for this view is given by the increased importance of fragmentation steps involving the loss of even-electron species (L+H), (L-H), H_2O from the molecular ion.

The presence of a phenyl group in the γ-position on the chelate ring, as in compound 7 in Table 22, would not be expected to stabilize the molecular ion to the same extent as a phenyl group in an α-position since the main effect expected would be that of inductive interaction. For effective π-donation to the chelate ring the phenyl group attempts to become co-planar with the chelate ring. Models of this compound (80) show that there is definitely steric hindrance between a phenyl group in the γ-position and a methyl group in the α-position. Comparing the increase in relative intensity of the molecular ion on replacing a methyl group with a phenyl group we see an increase from 47.7 to 100 on going from $Cu(acac)_2$ to $Cu(\phi\overset{O}{\overset{\|}{C}}CH\overset{O}{\overset{\|}{C}}CH_3)_2$ (α group replacement) while in the γ-position a smaller increase of 26.1 to 62.1, on going from $Cu(CH_3\overset{O}{\overset{\|}{C}}\underset{CH_3}{C}H\overset{O}{\overset{\|}{C}}CH_3)_2$ to $Cu(CH_3\overset{O}{\overset{\|}{C}}\underset{\phi}{C}H\overset{O}{\overset{\|}{C}}CH_3)_2$, is observed.

Replacement of both α-methyls with phenyl groups does not further stabilize the molecular ion but instead destabilizes it enhancing greatly the ability of the chelate to lose the (L + H) species.

In the acetylacetonates of the trivalent metals of the first transition series peaks were observed for migration of a methyl group to the metal for $Fe^{III}(acac)_2$ and $Mn^{III}(acac)_2$ (see sec. VIII (A)). A similar migration of a methyl was discussed for $Cu(tfacac)_2$ in the fluorinated acetylacetonate series (sec. VIII (C)). In this case for the compounds with aromatic groups in the α-position the aromatic group is seen to migrate to the metal.

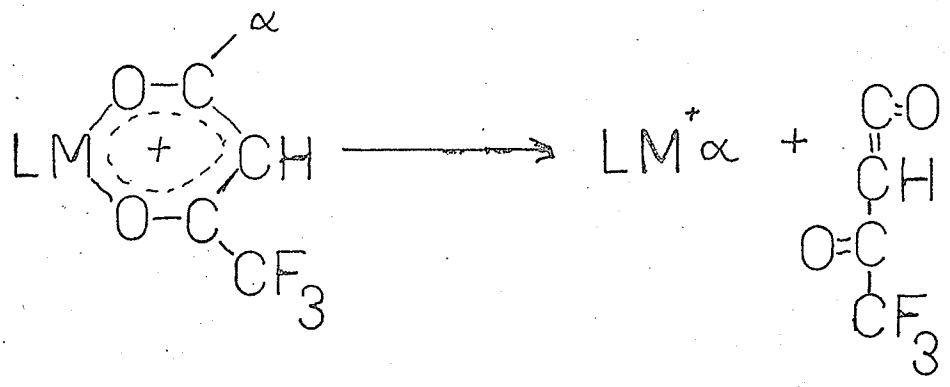

No metastables are present in the spectra to confirm the processes involved or related to the migration. In the $Cu(tfacac)_2$ case metastable peaks showed that the ion (tfacac Cu^+CH_3) fragmented such as to eliminate a neutral metal containing species ($CuCH_3$) with the charge remaining on the ligand moiety. In the case of the compounds with the aromatic group in the α position the $LCu^+\alpha$ ion fragments such as to retain the positive charge on the metal containing species $Cu^+\alpha$ eliminating a neutral ligand moiety.

Ions produced by loss of fragments such as (L + H) and (L - H) arise from hydrogen migration reactions either in one step process or two step processes. Ions of this type were first reported by MacDonald and Shannon (65) for the dibenzoyl methane (dbm) complexes. They discussed a mechanism involving the migration of the γ hydrogen, from one ligand to the other, for the copper complex. (Half headed arrows indicate one electron shifts, full headed arrows indicate two electron shifts.)

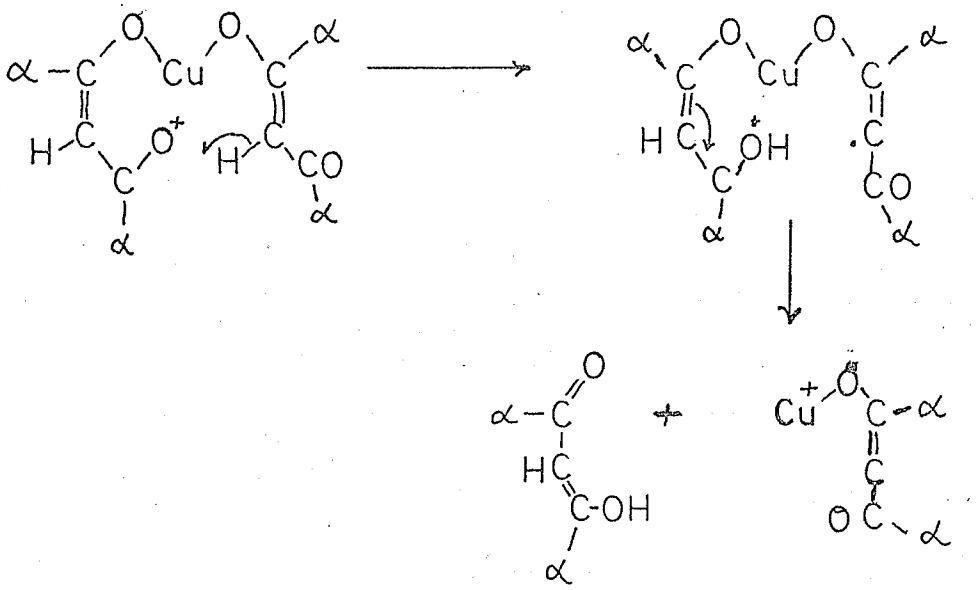

For the Co(II) and Ni(II) complexes they reported that a hydrogen from the ortho position on the phenyl group migrated to the metal.

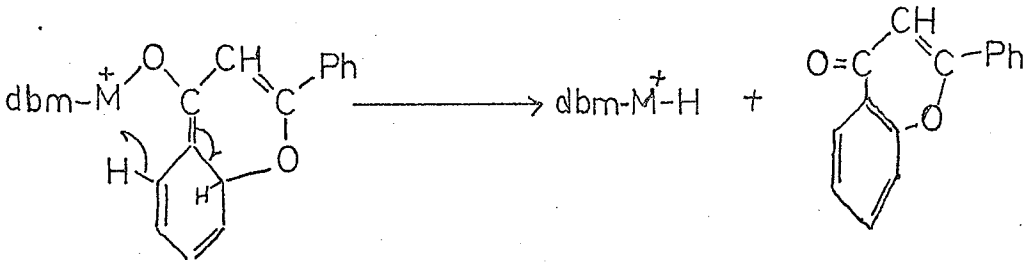

In the copper series peaks are present for both loss of (L + H) and (L - H). For the chelates with no aromatic substituents no analogous mechanism can exist for the latter process.

Table 25 gives the spectra for the Co^{II}, Ni^{II} and Cu^{II} benzoyltrifluoroacetonate complexes. The Cu complex exhibits the three peaks $(P-L)^+$, $(P-HL)^+$ and $(P-(L-H))^+$ while Ni^{II} exhibits $(P-L)^+$ and $(P-(L-H))^+$ and Co^{II} only the $(P-L)^+$ peak. As we see, copper is the only one to give the $(ML-H)^+$ species and we postulate that this species is produced from the parent ion with a valency change in the metal and a hydrogen migration from the γ-position on the ligand (see Table 26). Even though no metastable ion peaks are seen for this process a one step process appears to be indicated by the fact that the more easily an α group is lost (weak C-α bond) from the molecular ion the smaller is the $(CuL-H)^+$ species and no other obvious correlation.

Study of the complexes for which the $(CuLH)^+$ ion is present, using ligands deuterated in the γ position (see Table 26) showed that this peak is due to two competing mechanisms. One mechanism involves a hydrogen from the γ-position while the other process involves a hydrogen from one of the α substituents on the ligand leaving. On reducing the ionizing voltage to a value just above the threshold value no change was observed in the intensity pattern of these three peaks ($(CuL)^+$, $(CuLH)^+$, $(CuL-H)^+$) indicating that they must come from a common parent ion or intermediate. No metastable peaks are present to indicate the nature of the process taking place. The processes possible are:

TABLE 25

Relative intensities of the important ions in the mass spectra of Co(II), Ni(II) and Cu(II) benzoyltrifluoroacetonates ($\alpha_1 = CF_3$)

	Co	Ni	Cu
P	100	100	100
$P - \alpha_1$	80.5	62.1	31.3
$P - 2\alpha_1$			27.8
P - L	17.0	14.5	6.9
P - (L + 1)	-	-	13.4
P - (L - 1)	-	11.0	14.4
$LM - \alpha_1$	-	-	30.4

TABLE 26

Relative intensities for the peaks due to loss of a ligand plus or minus a hydrogen or deuterium for a number of copper complexes.

	P-(L-D)	P-(L-H)	P - L	P-(L+H)	P-(L+D)
$Cu(\phi C(O) CH C(O) CF_3)_2$	-	41	21	39	-
$Cu(\phi C(O) CD C(O) CF_3)_2$	19.0	25.0	22.5	-	33.5
$Cu(\phi C(O) CH C(O) \phi)_2$	-	-	-	100	-
$Cu(\phi C(O) CD C(O) \phi)_2$	-	-	-	-	100
$Cu(\phi C(O) CH C(O) CH_3)_2$	-	33.4	28.4	38.2	-
$Cu(\phi C(O) CD C(O) CH_3)_2$	26.4	18.4	24.5	-	30.7
$Cu(\text{thienyl}\text{-}C(O) CH C(O) CF_3)_2$	-	25.8	18.4	55.8	-
$Cu(\text{thienyl}\text{-}C(O) CD C(O) CF_3)_2$	15.4	11.6	20.2	-	52.8

1) The loss of HL directly from the molecular ion accompanying a valency change in the metal.

2) The loss of the remainder of a ligand moiety plus a hydrogen after an α group has been lost, or

3) Loss of H from $(P - L)^+$.

An interesting species seen is the loss of a hydrogen atom from $Cu(CH_3\overset{O}{\overset{\|}{C}}\overset{\phi}{C}\overset{O}{\overset{\|}{C}}CH_3)_2^+$. The loss of a hydrogen atom usually requires considerable energy and is thus seldom seen. In this case however the peak is relatively abundant.

$Cu(hfacac)_2$ and $Cu(tfacac)_2$ will not be covered here since they were discussed to some extent in section VIII (C).

2. The Appearance Potentials

All of the chelates gave abundant molecular ions and consequently it was possible to measure the appearance potentials of the complete series of compounds. Ions due to the loss of one ligand, however, were sufficiently abundant for only four of the compounds. Table 27 gives the appearance potentials for the molecular ions for the series as well as those for the ion which lost a ligand radical where possible.

From this series it is very evident that the substituent groups electron withdrawing power or electron donating power is the determining factor in the value of the appearance potentials. With the ligands chosen for this series both inductive and resonance effects will influence the ionization potential.

TABLE 27

Appearance potentials of ions from the copper β-diketonates as well as formation constants and polarographic half-wave potentials for these chelates.

	Ion	Volts A.P.	log K_1K_2 (77,78)	$\frac{1}{2}$ wave pot. (80)
1.	$Cu(acacCH_3)_2$ Cu(L)	7.97 10.8		-0.559 v.
2.	$Cu(acac)_2$ Cu(L)	8.31 13.1	22.60	-0.487
3.	$Cu(\phi\overset{O}{\overset{\|}{C}}CH\overset{O}{\overset{\|}{C}}CH_3)_2$ Cu(L)	8.37	23.02	-0.384
4.	$Cu(CH_3\overset{O}{\overset{\|}{C}}\underset{Ph}{C}\overset{O}{\overset{\|}{C}}CH_3)_2$ Cu(L-H)	8.05 10.7		-0.497
5.	Cu(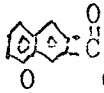 $\overset{O}{\overset{\|}{C}}CH\overset{O}{\overset{\|}{C}}CF_3)_2$	8.39	18.4	
6.	$Cu(Ph\overset{O}{\overset{\|}{C}}CH\overset{O}{\overset{\|}{C}}Ph)_2$ Cu(L-H)	8.28 10.3	25.00	-0.376
7.	Cu( $\overset{O}{\overset{\|}{C}}CH\overset{O}{\overset{\|}{C}}CF_3)_2$ Cu(L)	8.89	17.2	-0.146
8.	Cu( $\overset{O}{\overset{\|}{C}}CH\overset{O}{\overset{\|}{C}}CF_3)_2$ Cu(L)	8.90	19.0	-0.155
9.	$Cu(\phi\overset{O}{\overset{\|}{C}}CH\overset{O}{\overset{\|}{C}}CF_3)$ Cu(L)	9.06	18.8	
10.	$Cu(tfacac)_2$ Cu(L)	9.05 13.1	17.2	-0.173
11.	$Cu(hfacac)_2$	9.86	8	+0.04
12.	Cu(acac hfacac)	9.03		

Considering the acetylacetone ligand as a standard for comparison, from the data in Table 27, the effect upon the appearance potential of the chelate caused by substitution of various groups on the ligand can be evaluated. Substitution of a CF_3 group (strongly electron withdrawing) for a methyl is seen to raise the A.P. by 0.74 volts and another 0.81 volts on the second substitution. A very similar increase (0.70 volts) is seen on going from the benzoylacetonate to the benzoyltrifluoroacetonate.

Substitution of aromatic groups for a methyl group, (e.g. phenyl, naphthyl, furyl, thenyl) in the α position, only the phenyl group raises the appearance potential while the remaining groups lower the appearance potential. However when the phenyl group is substituted for a hydrogen in the γ-position the appearance potential is lowered by 0.26 volts. This is not as much lowering as for a CH_3 group but is still quite substantial. This suggests that, if the inductive effect is the principal determining factor, the phenyl group in the γ-position is donating electrons to a greater extent than hydrogen but less than a methyl group in the same position.

A surprising feature is that on substitution of both α methyls by phenyl groups the appearance potential is neglig bly different from the unsubstituted acetylacetone chelate.

Since it is very difficult to sort out the relative magnitudes of resonance and inductive effects it is very difficult to compare the compounds containing substituents capable of resonance effects to com-

pounds without such groups. However qualitative and even semi quantitative results may be gleaned from their comparison and correlation to studies of these compounds by other methods.

Table 27 gives a list of half-wave reduction potentials obtained polarographically (80) as well as a list of formation constants (77-78) for these chelates. Figures 19 and 20 show plots of the appearance potentials versus the half wave potentials and formation constants respectively to show their relation.

It was shown by Van Uitert et al. (77,78) that pK_d of groups of β-diketonates is directly related to the formation constants ($\log K_f$) of the metal chelates. This means that electron withdrawing and electron donating groups have the same effect on the acidity of the ligand as they have on the stability of the complex. Since the acidity of the ligand depends on the electron density on the oxygen atoms we see that the electron density at the oxygen atoms will effect not only the stability of the complex but the half-wave reduction potentials and the appearance potentials.

Figure 39

Plot of the appearance potentials of the molecular ions for the 4-chlorotropolone of copper versus polarographic half-wave potentials of the chelates. Numbers beside the points refer to the chelates as in Table 27.

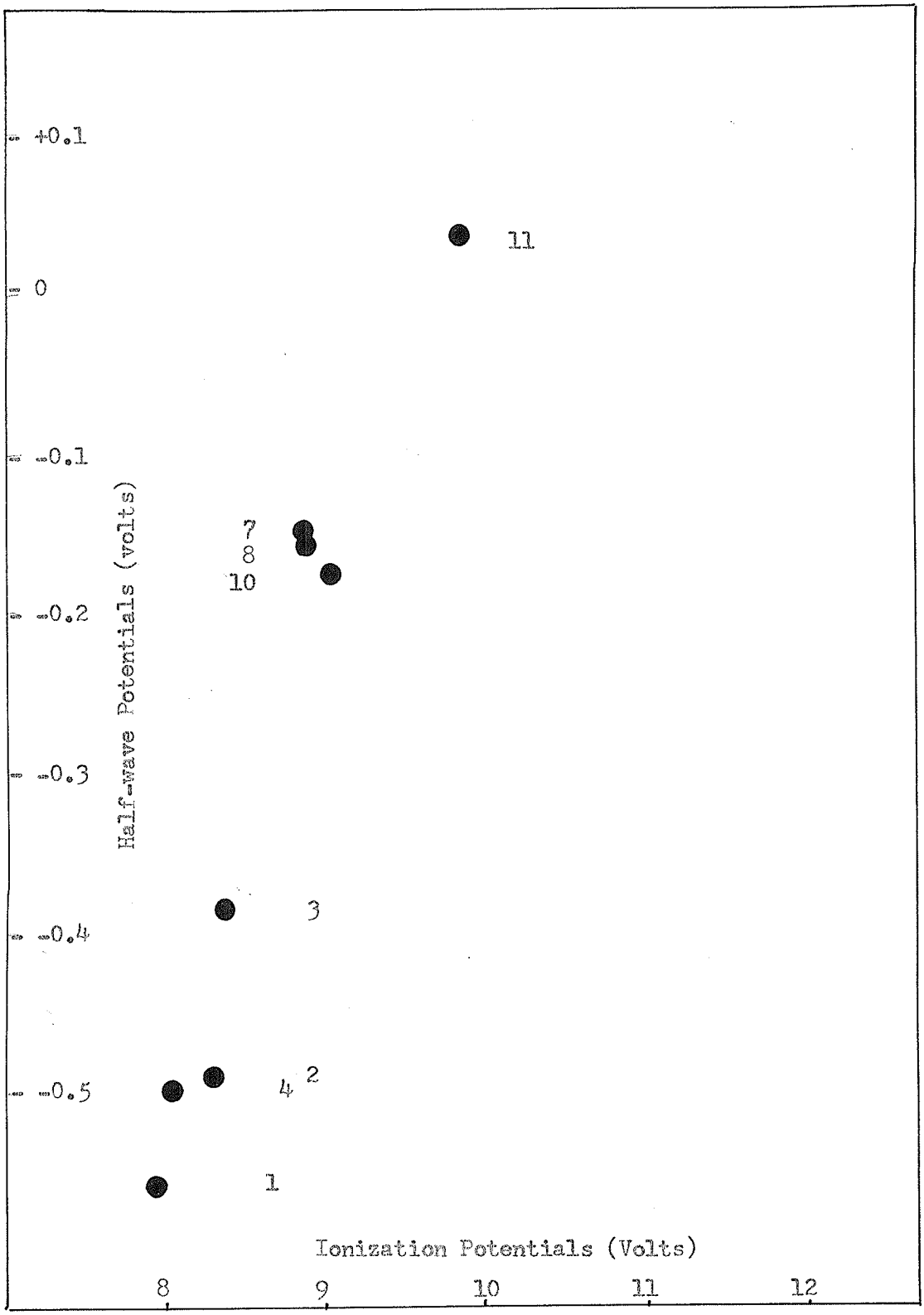
+0.1
0
-0.1
-0.2
-0.3
-0.4
-0.5
Half-wave Potentials (volts)
11
7
8
10
3
2
4
1
Ionization Potentials (Volts)
8
9
10
11
12

Figure 20

Plot of the appearance potentials of the β-dihydroxyethyl
of copper versus the formation constants for the
chelates. Numbers beside the points refer to the
chelates as in Table 27.

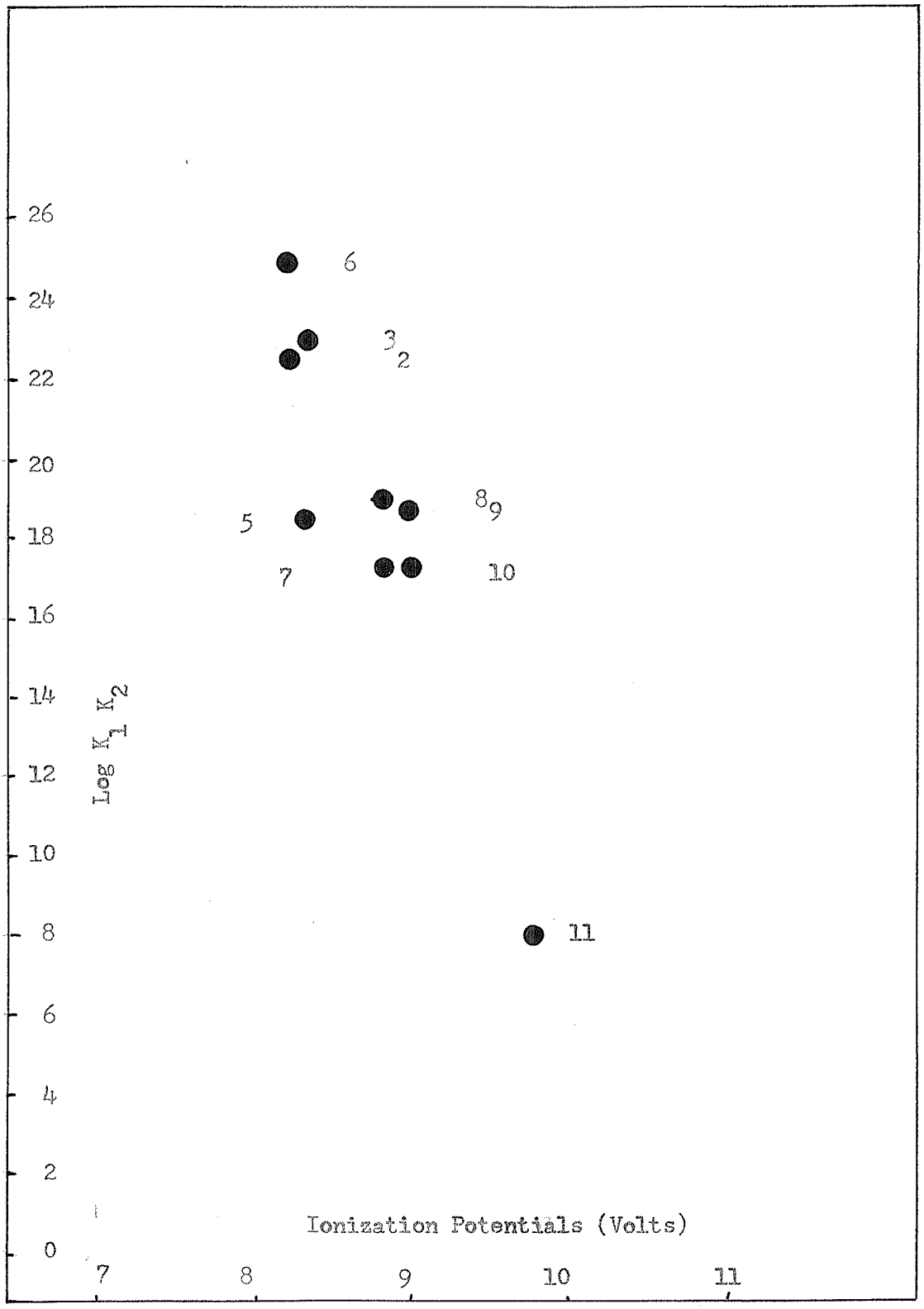
26
24
22
20
18
16
14
12
10
8
6
4
2
0
Log $K_1 K_2$
6
3
2
5
8
9
7
10
11
7
8
9
10
11
Ionization Potentials (Volts)

IX SUMMARY AND CONCLUSIONS

The mass spectra of acetylacetonates and substituted acetylacetonates show that odd electron ions tend to fragment by the elimination of odd-electron neutral radicals with formation of even-electron fragment ions. Even-electron ions tend to fragment less easily but when they do they tend to lose even-electron neutral fragments. Metals that can change valency by one unit and consequently reverse their odd- or even-electron character tend to fragment more than metals that do not change valency. Electron withdrawing and electron donating groups can effect the transfer of electrons between the metal and ligand orbitals and thus can have a large effect on the fragmentation pattern observed.

Appearance potentials of the molecular ion are dependent to the greatest extent on the ligand and substituent groups on the ligand. The effect of the metal is almost negligable indicating that the electron removed on ionization can be regarded as an electron being removed from the π-system related to the ligand.

In general electron withdrawing groups on the chelate ring tend to raise the appearance potential of the molecular ion while for electron donating groups the reverse holds true.

The appearance potentials of the fragment ions are more involved since they are seen to be dependent on factors such as

1) the ligand substituent groups, and
2) the metal and its available electrons.

BIBLIOGRAPHY

1. E. Goldstein. Berl. Ber. 39, 691 (1886).

2. W. Wien. Wied. Ann. 65, 440 (1898).

3. R.W. Kiser. Introduction to Mass Spectrometry and Its Applications, Prentice-Hall (1965).

4. R.I. Reed. Ion Production by Electron Impact, Academic Press (1962).

5. C. Sandorfy. Electronic Spectra and Quantum Chemistry, Prentice-Hall (1964).

6. R.E. Fox, W.M. Hickam , T. Kjeldaas. Rev. Sci. Instr. 26, 1101 (1955); Phys. Rev. 84, 859 (1951).

7. W.B. Nottingham. Phys. Rev. 55, 203 (1939).

8. J.D. Waldron, K. Wood. Mass Spectrometry Conference, Institute of Petroleum, London (1952).

9. H.S.W. Massey, E.H.S. Burhop. Electronic and Ionic Impact Phenomena, Oxford University Press, London (1952).

10. R. Bates. Atomic and Molecular Beams, Academic Press, New York. (1962).

11. H.D. Smyth. Proc. Roy. Soc., A102, 283, (1922).

12. R.H. Vought. Phys. Rev., 71, 93, (1947).

13. J.W. Warren. Nature, 165, 810 (1950).

14. R.E. Honig. J. Chem. Phys. 16, 105 (1948).

15. J.D. Morrison. J. App. Phys. 28, 1409 (1957).

16. W.M. Hickam , R.E. Fox, T. Kjeldaas. Phys. Rev. 96, 63 (1954).

17. F.P. Lossing, A.W. Tickner, W.A. Bryce. J. Chem. Phys. 19, 1254, (1951).

18. J.D. Morrison. J. Chem. Phys. 21, 1767, (1952); 22, 1219, (1954); 39, 200, (1963).

19. R.E. Winters, W.L. Courchene, J.H. Collins. Chem. and Eng. News. 44, June 6, 1966.

20. E.M. Clarke. Can. J. Phys. 32, 764, (1954).

21. P. Marmet, L. Kerwin. Can. J. Phys. 38, 787 (1960).

22. P. Marmet, J.D. Morrison. J. Chem. Phys. 36, 1238 (1962).

23. J.E. Collin. "Physical Meaning of Photon and Electron Impact Ionization Processes", in Mass Spectrometry, Academic Press, London (1964).

24. Werner. Ber. 34, 2584 (1901).

25. L. Pauling, The Nature of the Chemical Bond Cornell University Press (1948).

26. W.G. Penny and R. Schlapp. Phys. Rev. 41, 194 (1932); 42, 666 (1932).

27. C.J. Ballhausen, and A.D. Liehr. J. Molecular Spectr. 2, No4 (1958).

28. J.H. Van Vleck. J. Chem. Phys. 3, 807 (1935).

29. L.E. Orgel, An Introduction to Transition Metal Chemistry, John Wiley and Son Inc. New York.

30. T.M. Dunn, Modern Coordination Chemistry, (Ed. by J. Lewis and R.G. Wilkins) Chap. 4, Interscience, New York (1960).

31. A. Streitweiser. Molecular Orbital Theory for Organic Chemists, John Wiley and Sons, New York (1961).

32. R.S. Drago, Physical Methods in Inorganic Chemistry, Reinhold Publishing Corp. New York.

33. F.A. Cotton and G. Wilkinson. Advanced Inorganic Chemistry, Interscience Publishers. New York. 1962.

34. H.A. Jahn and E. Teller. Proc. Roy Soc., A, 1937, 161, 220.

35. J.N. Murrell, S.F.A. Kettle, J.M. Tedder. Valence Theory, John Wiley and Sons Inc., London.

36. D.W. Barnum. J. Inorg. Nucl. Chem. 21, 221, (1961); 22, 183 (1961).

37. J.P. Fackler Jr., F.A. Cotton, D.W. Barnum. Inorg. Chem. 2, 97 (1963).

38. J.P. Fackler Jr., F.A. Cotton. Inorg. Chem. 2, 103 (1963).

39. K. DeArmond, L.S. Forster. Spectrochemica Acta. 19, 1393 (1963).

40. T.S. Piper, R.L. Carlin. J. Chem. Phys. 36, 3330 (1962).

41. A.E. Martell, M. Calvin. Chemistry of Metal Chelate Compounds, Prentice-Hall (1952).

42. I. Robertson, M.R. Truter. J. Chem. Soc. (A), 310 (1967).

43. M. Courtois, L.S. Forster. J. Mol. Spect. 18, 396 (1965).

44. T.S. Piper, R.L. Belford. Mol. Phys. 5, 169, (1962).

45. J. Ferguson. J. Chem. Phys. 34, 611 (1961); 34, 1609 (1961); 34, 2206 (1961).

46. B.R. McGarvey. J. Phys. Chem. 60, 71 (1956).

47. A.H. Maki, B.R. McGarvey. J. Chem. Phys. 29, 35 (1958).

48. K. Nakamoto. Infrared Spectra of Inorganic and Coordination Compounds, John Wiley and Sons, Inc. New York.

49. D.R. Eaton. J. Am. Chem. Soc. 87, 3095 (1965).

50. F. Rohrscheid, R.E. Ernst, R.H. Holm. Inorg. Chem. 6, 1315 (1967).

51. R. Bralsford, P.V. Harris, and W.C. Price, Proc. Roy. Soc. (London) A258, 459 (1960).

52. R.D. Gillard, H.G. Silver and J.L. Wood. Spectrochimica Acta. 20, 63 (1964).

53. D.M. Adams. Metal-Ligand and Related Vibrations, Edward Arnold (Publishers) Ltd., London.

54. S. Pinchas, B.L. Silver and I. Laulicht, J. Chem. Phys. 46, 1506 (1967).

55. M. Mikami, I. Nakagawa and T. Shimanouchi. Spectrochemica Acta. 23A, 1037 (1967).

56. C. Djordjević. Spectrochemica Acta. 17, 448 (1961).

57. W.C. Fernelius and B.E. Bryant, Inorganic Syntheses, 5, 105, McGraw-Hill, New York.

58. J.P. McKaveney and H. Freiser. Analytical Chem. 30, 526 (1958).

59. D.A. Buckingham, R.C. Gorges and J.T. Henry. Aust. J. Chem., 20, 281 (1967).

60. M.F. Farona, D.C. Perry and H.A. Kuska. Inorganic Chem. 7, 2415 (1968).

61. J.P. Collman, R.A. Moss, H. Maltz and C.C. Heindel. J. Am. Chem. Soc., 83, 531 (1961).

62. P.R. Singh and Ram Sahai. Aust. J. Chem. 20, 639, (1967).

63. G.T. Morgan and A.E. Rawson. J. Soc. Chem. Ind. 462 (1965).

64. C.R. Hauser, F.W. Swamer, J.T. Adams. Organic Reactions, ed. Adams. John Wiley and Sons, Inc., New York.

65. C.G. MacDonald and J.S. Shannon, Aust. J. Chem. 19, 1545 (1966).

66. S. Sasaki, Y. Itagakki, T. Kwokawa, K. Nakanishi, and A. Kasahara. Bull. Chem. Soc. Japan, 40, 76 (1967).

67. F.W. McLafferty. Mass Spectrometry of Organic Ions. ed. F.W. McLafferty. Academic Press.

68. S.M. Schildcrout, R.G. Pearson and F.E. Stafford. J. Am. Chem. Soc. 90, 4006 (1968).

69. R.H. Holm and F.A. Cotton, J. Am. Chem. Soc. 80, 5658 (1958).

70. J.P. Fackler, Progress. Inorg. Chem. 7, 361 (1966).

71. J.L. Wood and M.M. Jones, Inorg. Chem. 3, 1553 (1964).

72. J.D. Hawthorne, M.J. Mays and R.N.F. Simpson. J. Organ. Chem. 12, 407 (1968).

73. M.J. Mays and R.N.F. Simpson. J. Chem. Soc., (A) 1936 (1967).

74. A.L. Clobes, M.L. Morris, R.D. Koob. Preprint.

75. R.E. Winters and R.W. Kiser, Inorg. Chem. 4, 157 (1965).

76. A. Streitweiser, Jr. "Molecular Orbital Theory", John Wiley and Sons, Inc. New York, 1961.

77. L.G. Van Uitert, W.C. Fernelius and B.E. Douglas, J. Am. Chem. Soc. 75, 457, 2736 (1953).

78. L.G. Van Uitert and W.C. Fernelius, J. Am. Chem. Soc., 75, 3862 (1953).

79. H.F. Holtzclaw, Jr., K.W.R. Johnson and F.W. Hengeveld, J. Am. Chem. Soc. 74, 3776 (1952).

80. H.F. Holtzclaw, Jr., A.H. Carlson and J.P. Collman, J. Am. Chem. Soc., 78, 1838 (1956).

81. E.R. Nightingale, Jr. and H.F. Holtzclaw, Jr., J. Am. Chem. Soc., 81, 3523 (1959).

82. R.L. Lintvedt, H.D. Russell and H.F. Holtzclaw, Jr. Inorg. Chem. 5, 1603 (1966).

83. P.R. Singh and R. Sahai, Aust. J. Chem. 20, 639, 649 (1967).

84. J.P. Collman, R.A. Moss, H. Maltz and C.C. Heindel, J. Am. Chem. Soc., 83, 531 (1961).

85. J.P. Collman and E.T. Kittleman, J. Am. Chem. Soc., 83, 3529 (1961).

86. R.H. Brook and H. Freiser, Inorg. Chem. 5, 2078 (1966).

87. J. Hine, "Physical Organic Chemistry", McGraw-Hill (1962).